TESTS ON PRESTRESSED CONCRETE BRIDGE BEAMS - FATIGUE TESTS OF THE BRIDGE BEAMS

by

Chetana Rao, Graduate Assistant
Gregory C. Frantz, Professor

JHR 95-245 Project 93-6

This research was sponsored by the Joint Highway Research Advisory Council of the University of Connecticut and the Connecticut Department of Transportation and was carried out in the Structural Research Laboratory of the University of Connecticut.

Technical Report Documentation Page

1. Report No. JHR 95-245	2. Government Accession No.	3. Recipient's Catalog No.
4. Title and Subtitle Test on Prestressed Concrete Bridge Beams- Fatigue Tests of The Bridge Beams		5. Report Date December 1995 6. Performing Organization Code
7. Author(s) Chetana Rao and Gregory C. Frantz		8. Performing Organization Report No. JHR 95-245
9. Performing Organization Name and Address University of Connecticut Department of Civil Engineering 261 Glenbrook Road, U-37 Storrs, CT 06269		10. Work Unit No. (TRAIS) 11. Contract or Grant No.
12. Sponsoring Agency Name and Address Connecticut Department of Transportation 280 West Street Rocky Hill, CT 06067-0207		13. Type of Report and Period Covered Final Report 14. Sponsoring Agency Code
15. Supplementary Notes		

16. Abstract

Two 27-year old precast prestressed concrete bridge beams were subjected to fatigue testing followed by loading to static capacity. The two box beams, 36 in. (914 mm) wide x 27 in. (686 mm) deep x 56 ft. (16.5 m) long, were removed from a deteriorated, simple span, multibeam bridge. The two beams showed some signs of distress due to water leaking through the longitudinal shear keys and due to corrosion of stirrups and strands. But, visually, they appeared to be in generally good condition. The two beams were precracked prior to fatigue loading and were subjected to over 1,500,000 cycles and 250,000 cycles with maximum bottom fiber stresses of $6\sqrt{f'_c}$ and $9\sqrt{f'_c}$, respectively. Periodic overloads were also applied during the fatigue testing.

Fatigue loading at the higher stress range had very adverse effects on the load-deflection response, flexural strength, crack widths and crack extensions. The beam loaded to a bottom tension stress level of $9\sqrt{f'_c}$ began failing after about 145,000 cycles. The beam loaded to the maximum permitted bottom tension stress level of $6\sqrt{f'_c}$ showed little or no deterioration in performance compared to the initial response after over 1.5 million cycles.

17. Key Words Beams, bridges (concrete), cracking, design concrete (prestressed), fatigue, maintenance, tests, prestressing, research, reinforcement, structural engineering	18. Distribution Statement No Restrictions

19. Security Classif. (of this report) Unclassified	20. Security Classif. (of this page) Unclassified	21. No. of Pages 147	22. Price

Form DOT F 1700.7 (8-72) Reproduction of completed page authorized

SI* (MODERN METRIC) CONVERSION FACTORS

APPROXIMATE CONVERSIONS TO SI UNITS

Symbol	When You Know	Multiply By	To Find	Symbol
		LENGTH		
in	inches	25.4	millimetres	mm
ft	feet	0.305	metres	m
yd	yards	0.914	metres	m
mi	miles	1.61	kilometres	km
		AREA		
in^2	square inches	645.2	millimetres squared	mm^2
ft^2	square feet	0.093	metres squared	m^2
yd^2	square yards	0.836	metres squared	m^2
ac	acres	0.405	hectares	ha
mi^2	square miles	2.59	kilometres squared	km^2
		VOLUME		
fl oz	fluid ounces	29.57	mililitres	mL
gal	gallons	3.785	Litres	L
ft^3	cubic feet	0.028	metres cubed	m^3
yd^3	cubic yards	0.765	metres cubed	m^3

NOTE: Volumes greator than 1000 L shall be shown in m^3.

Symbol	When You Know	Multiply By	To Find	Symbol
		MASS		
oz	ounces	28.35	grams	g
lb	pounds	0.454	kilograms	kg
T	short tons (2000 lb)	0.907	megagrams	Mg
		TEMPERATURE (exact)		
°F	Fahrenheit temperature	5(F-32)/9	Celcius temperature	°C

*SI is the symbol for the International System of Measurement

APPROXIMATE CONVERSIONS TO SI UNITS

Symbol	When You Know	Multiply By	To Find	Symbol
		LENGTH		
mm	millimetres	0.039	inches	in
m	metres	3.28	feet	ft
m	metres	1.09	yards	yd
km	kilometres	0.621	miles	mi
		AREA		
mm^2	millimetres squared	0.0016	square inches	in^2
m^2	metres squared	10.764	square feet	ft^2
ha	hectares	2.47	acres	ac
km^2	kilometres squared	0.386	square miles	mi^2
		VOLUME		
mL	millilitres	0.034	fluid ounces	fl oz
L	litres	0.264	gallons	gal
m^3	metres cubed	35.315	cubic feet	ft^3
m^3	metres cubed	1.308	cubic yards	yd^3
		MASS		
g	grams	0.035	ounces	oz
kg	kilograms	2.205	pounds	lb
Mg	megagrams	1.102	short tons (2000 lb)	T
		TEMPERATURE (exact)		
°C	Celcius temperature	1.8C + 32	Fahrenheit temperature	°F

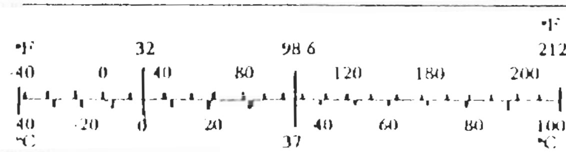

PREFACE

This is the final report on the JHRAC Project 93-6 entitled "Tests of Prestressed Concrete Bridge Beams - Fatigue Tests of the Bridge Beams". This work was sponsored by the Joint Highway Research Advisory Council of the University of Connecticut and the Connecticut Department of Transportation. This work was originally presented in the first author's thesis to the Graduate Faculty of the University of Connecticut in partial fulfillment of the requirements for the degree of Master of Science.

The support of the Connecticut Department of Transportation is gratefully acknowledged. The authors are very grateful to Blakeslee Prestress, Inc., of Branford, CT, for storing the bridge beams from the time of their removal from the bridge until the time they were tested at the University of Connecticut and for delivering and disposing of the beams.

ABSTRACT

Two precast prestressed concrete bridge beams were subjected to fatigue testing followed by loading to static capacity. The two box beams, 36 in. wide x 27 in. deep x 56 ft. long, were removed from a deteriorated, simple span, multibeam bridge after 27 years of service. Of the original thirteen beams in the bridge, four were very badly damaged and had to be destroyed in-place. Several of the remaining beams were saved for later testing. The two beams tested in this study showed some signs of distress due to water leaking through the longitudinal shear keys and due to corrosion of stirrups and strands. But, visually, they appeared to be in generally good condition. The two beams were precracked prior to fatigue loading and were subjected to over 1,500,000 cycles and 250,000 cycles with maximum bottom fiber stresses of $6\sqrt{f'_c}$ and $9\sqrt{f'_c}$, respectively. Periodic overloads were also applied during the fatigue testing.

The results of these tests support the following conclusions:

1. Fatigue need not be a concern as long as the beam remains uncracked.

2. A beam loaded to the maximum permitted bottom tension stress level of $6\sqrt{f'_c}$ showed little or no deterioration in performance compared to the initial response after over 1.5 million cycles.

3. A beam loaded to a bottom tension stress level of $9\sqrt{f'_c}$ began failing after about 145,000 cycles.

4. The maximum stress range in the tendons should be limited to 0.06 f_{pu}.

5. Fatigue loading at high stress ranges had very adverse effects on the crack widths and crack extension.

TABLE OF CONTENTS

CHAPTER 1

INTRODUCTION

1.1 GENERAL COMMENTS

The maintenance and repair of the transportation system in the state of Connecticut and indeed in the whole of the United States have become an increasingly important concern in the recent years. Studies have concluded that many existing bridges are below required strength due to high traffic loads, deterioration from insufficient maintenance and/or out-dated design and construction practices.

The major factors that have contributed to the present situation are:

1. The age of the structure
2. Inadequate maintenance
3. Increasing Load Spectra
4. Environmental contamination and Corrosion

Use of deicing salts has significantly increased the possibility of corrosion of reinforcement. Corrosion is a serious problem in some concrete structures built during the 1950s (28) when calcium chloride was commonly used as an admixture in cold climate. Reinforcement and prestressing steel placed in such concrete suffers corrosion 10-15 years from the time it was cast. The increase in size of the reinforcement as a result of corrosion generates bursting forces and has caused failure of prestressing strands and spalling in the concrete. Inadequate concrete covers over the reinforcement, the quality of the concrete used and the humidity conditions of the atmosphere would influence the degree of corrosion too. However, many bridge beams after being in use for many years have been judged to be in good condition based on results of load tests, material component evaluations and observations during dissection of the girder (34).

Evaluating the condition of an existing bridge is a difficult task because engineers do not have realistic methods to assess the in service strength of a bridge. Also, estimating the fatigue strength and the effects of long term loading is more complicated. Added to the usual problems of the complex structural analysis of the bridges, the material properties of concrete can be considerably different from those assumed in the original design and could even change with age. Under long-term loads, the prestressing force in the strands could also undergo losses that would be difficult to estimate accurately. Because of inadequate evaluation procedures some bridges are probably assigned low loading rates or are replaced or are strengthened unnecessarily when the existing bridges, even if deteriorated, do have sufficient capacity and simple repairs would be more appropriate. Information on the actual strengths of existing, deteriorating bridges could resort in savings in bridge repair costs.

This project completes the research started by JHRAC project 87-3, which studied the static flexural strength (33) and the chloride ion penetration (23) in 27-year old prestressed concrete bridge beams removed from the Walnut Street bridge in East-Hartford. This project examines the fatigue strength of the bridge beams.

1.2 BACKGROUND INFORMATION ON THE WALNUT STREET BRIDGE

This information is taken from Ref "Tests of Prestressed Concrete Bridge Beams", Shenoy, Chandrakanth V. and Frantz, Gregory C. (32,33)

"The Walnut Street bridge built in 1960 in East Hartford, CT, was replaced in early 1987. This 56 feet span simply supported multi beam bridge was made of thirteen rectangular prestressed concrete box beams. A photograph of the structure is shown in Figure 1.1. This is a very common type of a bridge in the United States. The condition of this bridge super structure was rated 4 on a scale of 0 (critical condition; bridge closed) to 9 (new condition) during an inspection by the Connecticut Department Of Transportation in November 1985.

Figure 1.2 shows the plan and cross-section views of the bridge. The prestressed concrete box beams were precast in a prestressing plant and transported to the bridge site where they were placed side by side on abutments to form the bridge deck. As shown in Figure 1.2, the exterior beams were six inches deeper than the interior beams. The exterior beams carried most of the sidewalk and the utility pipes were concealed in these beams. The interior beams were post-tensioned together laterally by passing prestressing strands at each end and mid-span through the diaphragms cast within the beams. Also, continuous longitudinal shear keys cast into the sides of the members were filled with high strength, non-shrinking mortar to provide lateral distribution of loads across the width of the bridge deck. A two inch thick asphaltic concrete topping was placed directly on the bridge deck to provide

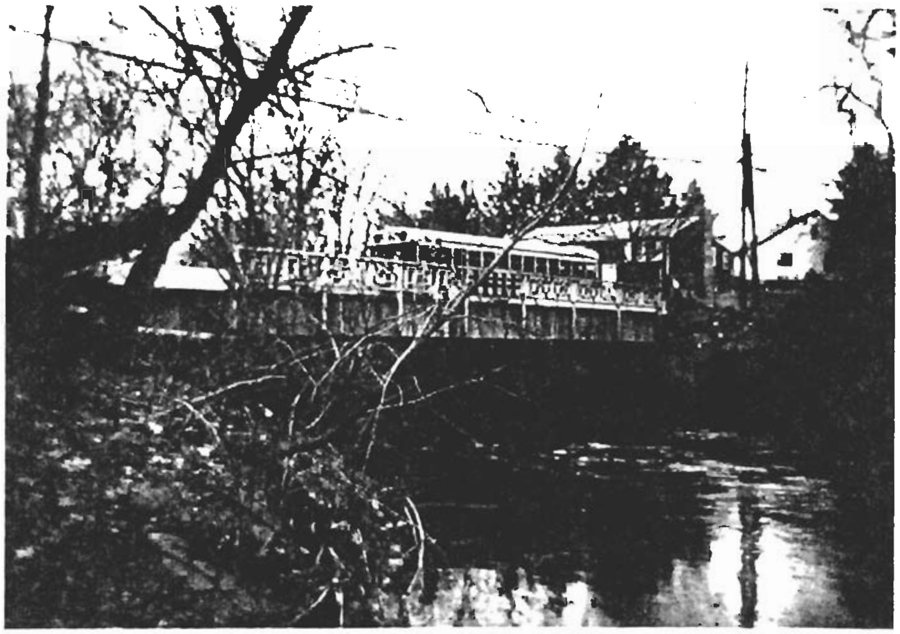

Figure 1.1 Elevation of the Walnut Street Bridge

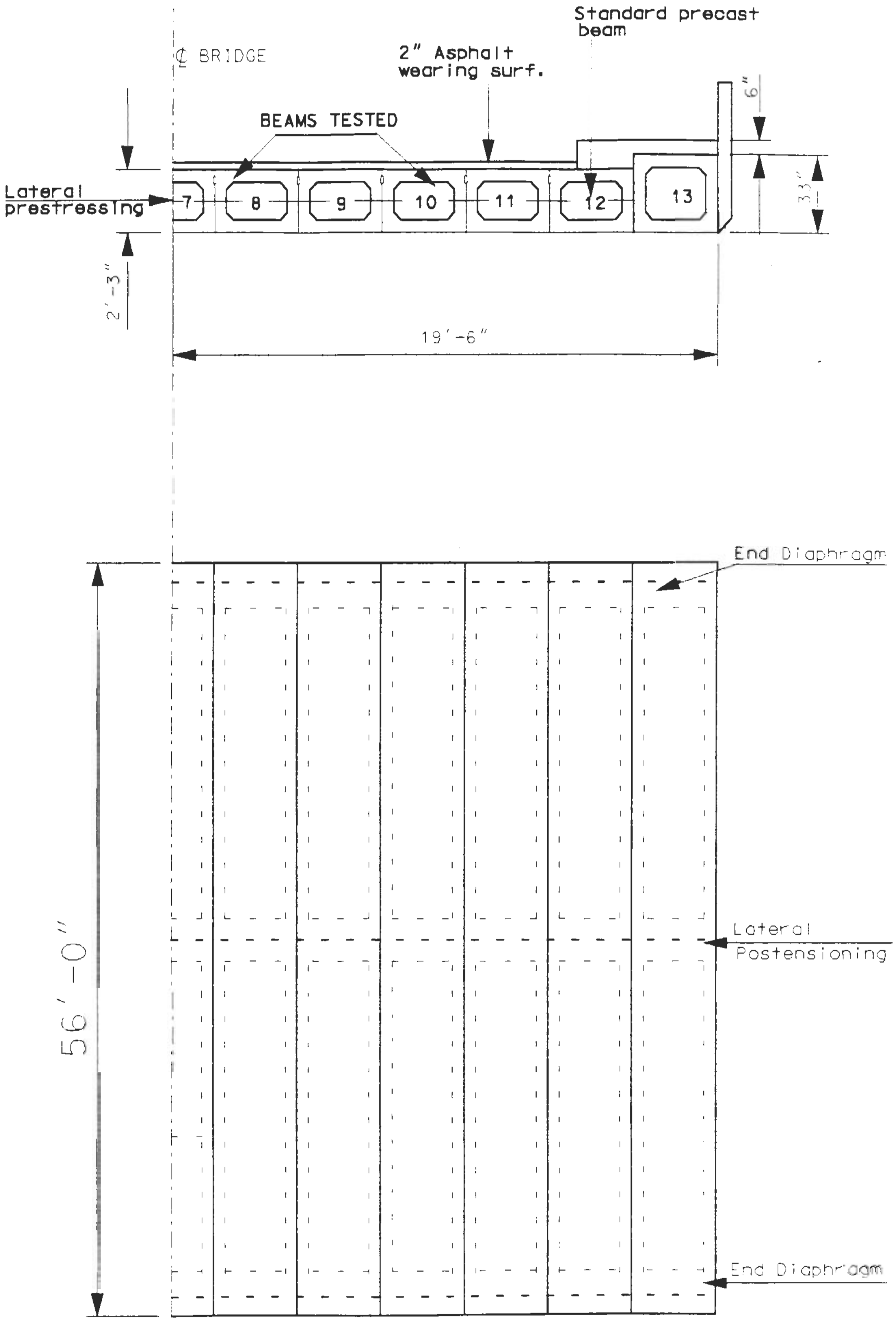

Figure 1.2 Arrangement of Adjacent Box Beam Bridge Components

the wearing surface. No special drainage provisions were made in the box beams.

Current construction practice places a waterproof membrane between the top of the beams and the asphaltic wearing surface to prevent penetration of the de-icing salts into the concrete. However, at the time of construction of the Walnut Street bridge no such waterproof membrane was used. As a result, large amounts of runoff water containing deicing salts were able to seep down to the beams and penetrate into the concrete cover. Some of the shear keys leaked causing deterioration of the concrete cover and corrosion of the prestressing strands in several beams. The most severe deterioration was observed in the second and third beams from each side at the curb line due to the slope of the asphalt wearing surface being towards the sidewalk beam. These four beams were severely deteriorated. This deterioration made a hole in one of the beams at the curbline (Figure 1.3). Typically, the leakage left whitish stains on the sides and bottom of the beams (Figure 1.4). Cracking was accompanied by spalling of the concrete cover and exposure of prestressing strands (Figure 1.5). Several strands were exposed and severely corroded with one strand ruptured and hanging down onto the river below (Figure 1.6).

Due to the observed deterioration and the unavailability of the original design plans and calculations, the town decided to replace the entire bridge rather than to attempt any repairs. When the Walnut bridge was replaced, nine of the structure's thirteen box beams were preserved. Four beams, the second and third beams from each edge were very badly deteriorated and had to be destroyed in-place prior to their removal." The others were retained for experimental and research purposes.

1.3 GENERAL DESCRIPTION OF THE TEST BEAMS

The two beams that were tested were Beam8 and Beam10. Both beams were apparently without any flexural cracking and they proved so during the tests as the load-deflection curves followed the predicted curve.

Beam8 was immediately adjacent to the beam in the center of the bridge and had very little staining from the rain water or salt deposits on the sides and the bottom. Also, it was likely that Beam8 was subjected to more severe loading owing to its position in the bridge and it was expected that it might be of lesser strength at this date. One noticeable damage in the beam was two large vertical cracks starting from the top of the beam and extending down both sides to almost 20 inches depth, at a distance of about 6 feet from the south end of the bridge. These cracks, it was suspected, were formed during the removal of the beam from the bridge or later during transportation or handling. This beam had a few rusty surface stains indicating some rusted stirrups or strands.

However, Beam10, being immediately next to Beams11 and 12 (the ones that had to be destroyed in place due to severe deterioration), showed evidence of rain water and deicer salts seeping down between the beams and had large patches of whitish stains with salt and calcium deposits. Two horizontal one foot long cracks at the level of the strands caused due to the rusting of the strands were noticed on the east side. This beam otherwise seemed to be in fairly good condition.

1.4 OBJECTIVES OF THE RESEARCH

A joint research program between the University of Connecticut and the Connecticut State Department of Transportation was set up to perform fatigue tests on the remaining two beams (as the others were used for tests on the static strengths and chloride ion penetration in Phase 1 and 2 of JHRAC Project 87-3). The Connecticut Department of Transportation supported the project with funding and provided structural steel for building the test setup.

The objectives of this study were:

1. To determine the remaining fatigue life of these two prestressed concrete box beams after being in service for over twenty-seven years.
2. To determine if the observed present condition of the beam can be related to the loss in fatigue strength , if any.
3. To verify the prestress losses determined in the previous phase of this project.
4. To determine the actual in-place material properties of the beam.
5. To observe and study the effects of cyclic loading on the stresses, the crack widths and their patterns, the deflections of the beam and on the slipping of the strands.

1.5 ORGANIZATION OF THE REPORT

Chapter II presents a discussion of fatigue in prestressed concrete and a review of the literature on similar tests performed with prestressed concrete bridge beams. Chapter III discusses the properties of the materials in the beams. Chapter IV discusses the theoretical analysis of the beam. Chapter V describes the test setup and the test procedure. Chapter VI presents the test results. Chapter VII concludes and summarizes the study.

Ms. Chetana Rao, Graduate Research Assistant, prepared this report as part of the requirements for the Master of Science degree (37).

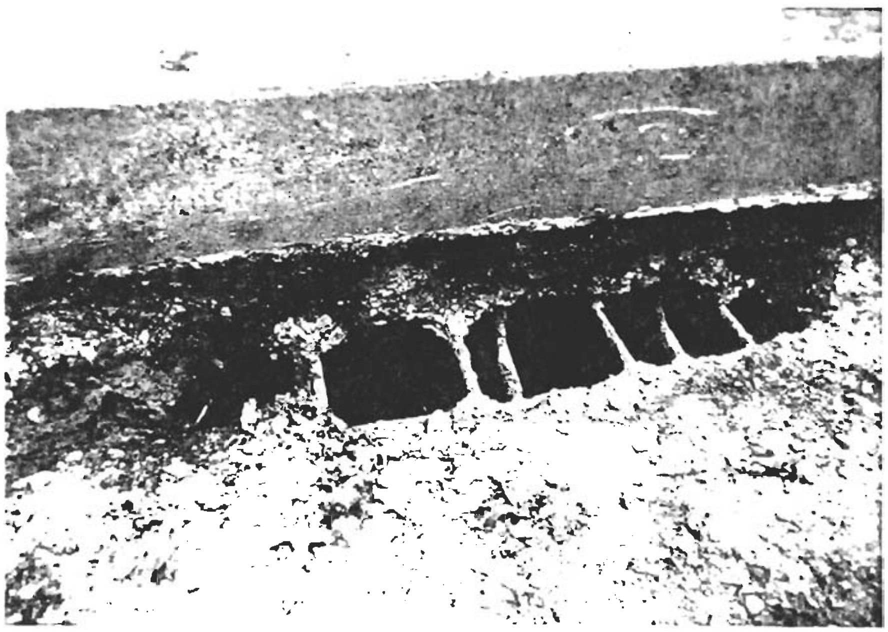

Figure 1.3 Hole in the Beam at the Curbline

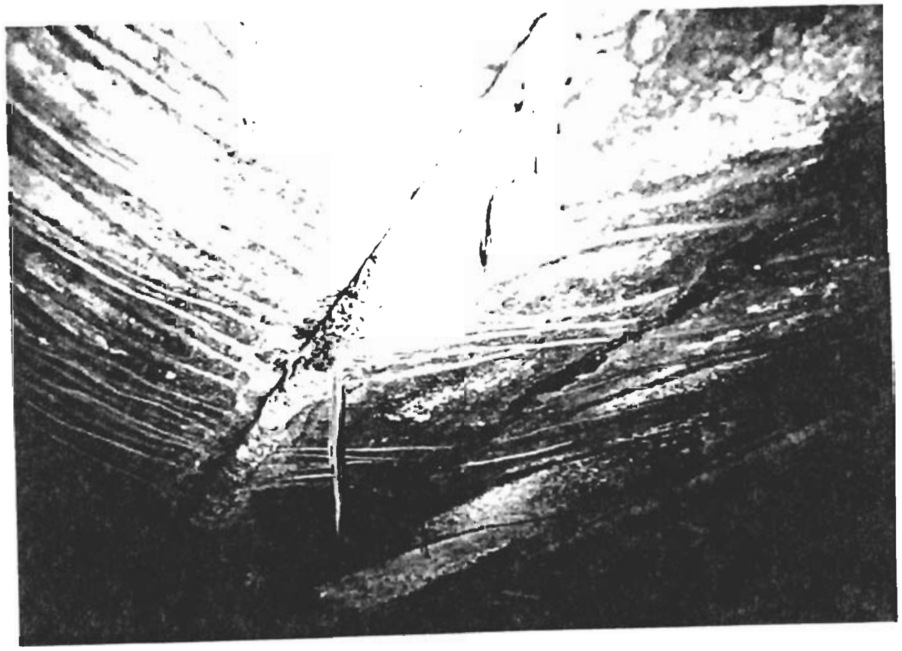

Figure 1.4. Whitish Stains at the Bottom of the Beam

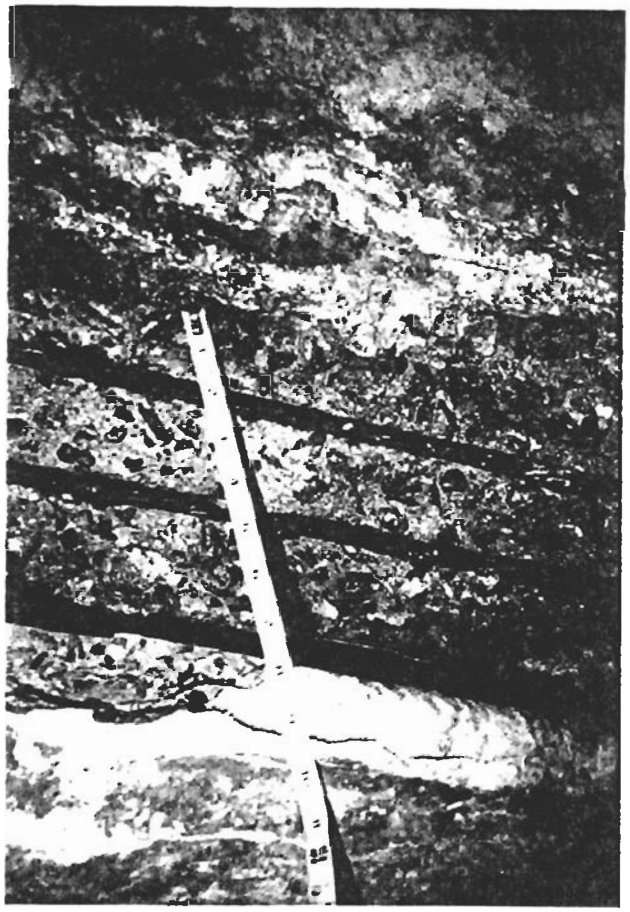

Figure 1.5. Spalling of Concrete Cover and Exposure of the Prestressing Strands at the Bottom of the Bridge

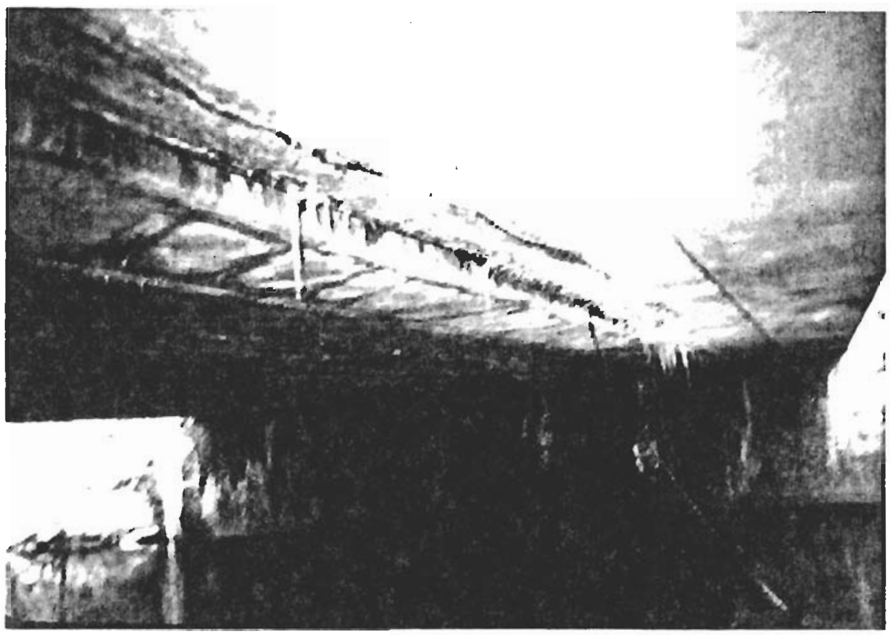

Figure 1.6. Deterioration of the Beams at the Bottom with One Ruptured Strand Hanging Down into the River

CHAPTER 2

FATIGUE IN PRESTRESSED CONCRETE

2.1 FATIGUE IN PRESTRESSED CONCRETE

Prestressing concrete is the concept of introducing sufficient precompression in the member so as to counteract tension in the member at service loads. Over the years, prestressed concrete bridges have become popular and extensive in use as they are being recognized for their efficient cross-sections, lightweight and ease in construction. AASHTO (8), Chapter 9 stipulates specifications for the design of prestressed concrete bridges in detail but specifies no particular limitations for fatigue considerations.

Structural members subjected to frequent reversals and variations in stresses require a sound fatigue resistance as there can be deterioration in their strength due to the effects of repeated loads. Fatigue is better resisted by prestressed concrete and partially prestressed concrete than by plain reinforced concrete. Despite the fact that there are no statistics in evidence of fatigue failure in prestressed concrete bridges, this aspect in design still cannot be ignored. Fatigue failure could occur in any of the following modes: (20)

Failure of concrete due to flexural compression.

Failure of concrete due to diagonal tension or shear.

Failure of strands due to tensile stress variations.

Failure of pretensioned beams due to loss of bond.

Failure of end anchorages of post-tensioned beams.

Most fatigue failures occur due to rupturing of the wires in the strands in the post-cracked stage of the concrete. While the concrete is uncracked, the concrete bears a large portion of the stress reversals and with the high limits of stress range capacity of concrete, fatigue life can be assumed to be infinite. Moreover, since the concrete is precompressed and reaches about zero stress in the bottom fiber due to loads from its own self weight, or is still in compression, the range of stresses it bears due to loading and unloading (live loads) is within limits. The changes in the level of stress in the strands is very small in prestressed members under the design live loads as high-strength steel is prestressed to high levels and the stress ranges are relatively low. It can hence be inferred that fatigue need not be a concern as long as the concrete has not cracked.

But with the moments exceeding the cracking moment (theoretically, that which causes a bottom fiber stress of $7.5\sqrt{f'_c}$), the neutral axis shifts upward leading to a higher rate of increase in steel stresses on applying additional loads. Once the structure is cracked and unloaded, the cracks close completely theoretically. Now, on reloading, the cracks reopen at a stage when the stress in the bottom fiber reaches zero which is theoretically the second cracking moment, which is usually about 50-60% of the original cracking moment. The stresses in the strands increase sharply from this stage on as the strands begin carrying most of the stresses and the compressive stresses in the concrete extreme fiber increase sharply to maintain equilibrium of forces and moments in the section. Fatigue now becomes a concern because the strands now see a larger stress range, specially if the range is between the precracked and cracked stages. In addition, fatigue loading causes further losses and the stress range for a specific load range increases with number of cycles. In prestressed bridges, this can be comparable to the ranges the strands withstand if the concrete is cracked (unintentionally) due to even one overloaded truck that causes moments exceeding the cracking moment.

Shear fatigue becomes critical after inclined cracks develop in prestressed concrete beams (10). Due to the high shear resisting capacity of prestressed concrete, shear reinforcement is minimal in these beams allowing the propagation of inclined cracks with less resistance and wider openings too. This results in a decrease in shear transferred through aggregate interlock and its consequences under fatigue conditions, though not under static conditions, can be a problem. There are certain loadings for which a prestressed beam will fail in shear under fatigue loading due to failure of stirrups although flexural failure would control behavior under static loading conditions. This aspect has not been dealt in this report as the tests did not produce any severe shear conditions.

Failure of the wires in the strands can be due to a combination of reasons. High concentrations of stresses exist in the strands in the vicinity where the concrete has cracked. There is a partial breakage of bond between the concrete and the steel near these cracks. Repeated loading can cause a complete loss of bond between the two materials. Under repeated loads, since the strands are under high strain levels, the wires of the strands rub against each other which can further cause them to rupture. Failure is found to usually start in the wires at the sections of maximum moment and often over separators and where the wires have a sharp bend. The secondary stresses that are developed in the strands as a result can be severe.

Fatigue has several deteriorating effects on the flexural behavior of a beam. There is a significant increase in deflections, residual deflections, crack widths and crack lengths (extensions) under service loads. It reduces prestress and bond properties, allowing the cracks to reopen earlier than expected. The stress levels in the strands increase as a result. Inclined diagonal tension cracks form under repetitive loading at appreciably smaller stresses than under static loading.

The fatigue life of a prestressed concrete beam can be estimated from constant stress fatigue tests assuming Miner's Hypothesis can be applied (9). The fatigue life of a beam is predicted directly from the fatigue life of the strands in air. The relation used is

$$\Sigma(n_i/N_I)=1$$

where n_i is the number of cycles applied resulting in a constant stress range and N_I is the predicted ideal fatigue life of those strands.

It would hence be of utmost use if there could be virtual guidelines for the design of highway bridges with due considerations for fatigue under flexure and shear. ACI Committee 215 report (1) suggests that the stress range in prestressed reinforcement that may be imposed on minimum stress levels up to 60 percent of the tensile strength shall not exceed $0.06f_{pu}$ based on cracked section analysis if the tensile stresses exceed $3\sqrt{f'_c}$ psi under a realistic estimate of service loads. In addition, recommendations have been made for prestressed members containing unbonded reinforcement with attention drawn to fatigue in anchorages, couplers and reinforcement susceptible to corrosion.

2.2 LITERATURE REVIEW

Reports of relevant experiments of prestressed concrete beams, particularly on fatigue testing were reviewed. Some of those that served as very useful references are discussed in this chapter.

Shenoy, C.V. and Frantz, G.C. tested two of the beams that were removed from the Walnut Street Bridge (32,33). The bridge was built in 1960 based on the 1957 AASHTO Specifications. These beams were structurally identical to the beams described in Chapter 5. One of the beams was from the center of the bridge and had a lower camber than the other one having been subjected to higher loads from both traffic lanes. The other, next to a badly deteriorated beam, showed signs of concrete cracking and spalling. The beams were 54 feet in length, 36 inches wide and 27 inches deep containing 22 straight strands of 7/16" diameter. The material properties were determined by removing concrete cores from the beams and testing them for stress-strain properties. After 27 years, the concrete had an average compressive strength of 7,100 psi and a modulus of elasticity of 4.1×10^6 psi. The concrete strength at 28 days was estimated to be 6000 psi and the modulus to be 3.8×10^6 psi. Six segments of strands were removed from the ends of the beam where strand stresses would have remained in the elastic range during the testing. Stress strain tests (31) determined the modulus of elasticity to be 25.3×10^6 psi and the breaking strength to be 263 ksi.

Static tests were conducted on the beams to study their performance after 27 years of service relative to what could be predicted. Loads were applied at third points for a simple span of 54 feet. Prestress losses of 18 Ksi were determined during the tests and were far less than the 37 Ksi predicted. The original design of the beam was more conservative than what would be required by the present AASHTO Specifications. It was designed to develop zero tension in the bottom fiber at 80 percent of the wheel load due to a HS-20 truck. The first cracks opened at a load almost two times the 1989 AASHTO service load. The measured load-deflection response of the beams closely followed the predicted pattern with elastic behavior prior to flexural cracking and rapid increase in the deflection after cracking. The beams were tested until the load-deflection curves flattened nearing ultimate capacity. The tests confirmed that the strain compatibility and moment-curvature methods display adequate accuracy in predicting deflections and stress levels. These beams were found to be capable of easily resisting factored static load levels based on 1989 AASHTO Specifications.

Murray and Frantz did chloride level tests on five of the prestressed concrete box beams from the 27-Year old Walnut street bridge (22,23). The beams tested were the middle beam, the three beams next to it and the exterior beam. The purpose of this research was to find a correlation between the chloride ion penetration in the concrete and the damage of the beams that necessitated the replacement of the bridge. This bridge, built during 1960, did not have a waterproofing membrane underneath the bituminous wearing surface. Samples were collected from drillings taken from top, sides and bottom locations of the beams as well as from cores taken from the top of the beams. They concluded that active corrosion was taking place in the beams. It was observed that the measured chloride levels could vary significantly from location to location on the beam. The concentration levels were as high as two to three times the corrosion threshold level. The results suggested that the penetration of chloride into a concrete structure is aided by water seepage into the concrete as the chloride levels in some locations were larger at deeper depths than at shallower depths. One of the beams had a high chloride concentration on the side face probably due to water seeping through the grouted shear keys. The exterior beams of the bridge carried the loads from a cast-in-place sidewalk. These beams had chloride concentrations above the corrosion threshold level to a depth of 8 inches below the top surface of the sidewalk. They recommended waterproofing membranes below all bituminous wearing surfaces to protect the structures from water seepage and chloride damage. This was especially important around the gutter area where water is likely to accumulate. Timely removal of snow was concluded as vital to avoid piling up of salt laden snow, the salt from which would eventually migrate into the structure leading to corrosion. This phenomena was evidenced by high chloride concentrations found in two top samples from beam1 inspite of a five inch thick sidewalk covering this beam through out the 27 years of its life. The Federal Highway Administration procedure was found to be an accurate method for chloride analysis.

Russell and Burns studied the static and fatigue behaviors of three new pretensioned composite bridge girders made with high strength concrete (30). On each of the three Texas Type-C girders, an unshored composite deck slab was cast. All the girders possessed identical section dimensions (I-sections), elastic properties, cracking resistance and ultimate strength but in two of the girders, eight of the 24 strands were debonded while the third girder had them draped and all the strands were fully bonded. The primary interests in this research were to study the behavior of pretensioned girders made with high strength concrete and to compare the behavior of pretensioned girders made with debonded strands to the behavior of girders made with draped strands. Horizontal and vertical mild shear reinforcement placed within the webs of the end regions of the girders prevented the propagation of web shear cracks and ensured integral strand anchorages. It was a known fact that web shear cracking propagated through the bottom flanges of pretensioned I-girders to cause bond failure of the pretensioned strands (36). The beams were precracked during the first static test to increase the stress ranges in the strands and the bond stresses that result from cyclic loading. During the fatigue testing web shear cracks were induced in two of the girders to observe the nature of effects that repeated loading would have on the propagation of these web shear cracks. The value of V_{cw} was lower for the beam that had the eight debonded strands and a bursting crack formed above the centerline of the support and extended toward the load point. During the ultimate testing of this beam, several other shear cracks formed but did not influence the behavior of the girder at that point. Instead, at higher loads, these shear cracks joined together to form a large horizontal shear crack at approximately the joint between the web and the lower flange. The two beams that had shear cracks were tested to over 225,000 cycles and the third beam was loaded to 696,158 cycles. Failure occurred due to a combination of effects including repeated loading, impact of debonding strands (reduces precompression) and reinforcement details. The girders performed very well and did not fail during the fatigue tests. At the end of the tests, each of the girders was tested statically to failure. Use of high strength concrete in prestressed concrete bridge girders was deemed safe. It was concluded that girders made with debonded strands can possess the same behavior and strength as girders made with draped strands and was recommended as an alternative to using draped strands.

K.E. Knudsen and W.J. Eney tested a new pretensioned concrete box beam(17), 38 feet long, 36 inches wide and 21 inches deep having 40 5/16" diameter 7 wire strands. The beam was subjected to 1,300,000 repetitions of an equivalent standard H20-S16 truck loading for which it was designed and a subsequent 100,000 cycles of 54 percent design overload. Seven intermediate static tests were also conducted with loads up to 100 percent design load and six more to 410 percent of the design load. The beam was only partially prestressed and at about 70 percent of the design load the bottom fiber concrete stresses changed to tensile stresses. The beam cracked during the first static test and the crack reopened during every load cycle of the fatigue tests. The beam behavior was very close to that predicted and confirmed the accuracy of the theoretical methods of analysis. The beam withstood the 1,300,000 cycles of loading with minor effects but the effects of 100,000 cycles of overloads were drastic. The deflections under design loads were close to the predicted span/800 but increased by 30 percent with overloads. Due to overloads, the concrete stresses increased by

25 percent but caused minor prestress losses. Methods for the prediction of steel stresses by assuming the steel to carry the total tension after the concrete has cracked were less accurate with increasing loads. It was concluded that fatigue was not a problem in their test beams that had prestress maintained solely by bond as no bond failure occurred. The beam failed during the ultimate load test due to crushing of concrete at a maximum moment of $(M_D + 4.2M_L)$ or $3.1(M_D + M_L)$. It was recommended that the cracking load be computed on the basis of zero bottom fiber stress. The test concluded that the beam was structurally satisfactory for use in a bridge at a severe location.

Leon, French, et al. investigated the reusability of four 20-year-old prestressed bridge girders and the effectiveness of techniques to repair impact damage (19). The research addressed the effectiveness of the means of restoring prestress in the girders resulting from the loss of strands as well as determining the prestress losses, the material properties and the deterioration due to chloride ion penetration from deicer salts (12). The bottom of the flanges and the sides of the beams exposed to the incoming traffic passing below the bridge had higher chloride ion concentrations than the side that was exposed to the departing traffic. Although the strands showed mild traces of rust, there did not appear to be any problems with corrosion in girders because of the superior quality of concrete and the depth of the cover. The beams were subjected to fatigue loadings up to the AASHTO HS-20 truck load limits. Repaired girders with additional post-tensioning were unable to regain their predamaged stiffness. The tests suggested that the original beams were in an excellent condition and could be reused provided they were removed carefully from the bridge.

Rabbat, Kaar et al. conducted fatigue tests of new pretensioned girders with blanketed and draped strands (29). Full-sized Type-II AASHTO PCI girders, 50 ft. long were tested. Two of the six girders had draped strands and the other four had straight strands with four strands blanketed at each end. Three of the girders were tested to 5 million cycles to produce a maximum stress of zero in the bottom fibers. These girders, when tested for their ultimate strength, failed at loads slightly above the theoretical ultimate load and showed no traces of distress due to fatigue. The other three girders were precracked and were tested for fatigue to produce a maximum stress of $6\sqrt{f'_c}$ psi in the bottom fiber. These girders experienced fatigue distress between 3.2 and 3.8 million cycles. It was concluded that specimens designed for zero bottom fiber tension had a fatigue life significantly superior to those designed for a maximum tensile stress of $6\sqrt{f'_c}$ psi. The test proved that blanketed strands could be used if adequate strand development length is provided. In the specimens that reached stress levels of $6\sqrt{f'_c}$, those with blanketed strands designed for a development length of l_d, the strands underwent slipping and a bond fatigue occurred. In specimens with blanketed strands having a development length of $2l_d$, very small slip in the strands were noticed. This suggested that for up to 3 million cycles, sufficient bond strength is retained if the longer development length is used. It was recommended that blanketing strands was a good alternative to draping them. Also, ties to confine the concrete in the stress transfer region of blanketing strands were found unnecessary.

Overman, Breen and Frank report on the fatigue behavior and strength of new pretensioned concrete girders (26) with unshored cast-in-place slabs. Eleven full scale pretensioned girder specimens were tested in the flexural fatigue portion of the project. The tests included determining the material properties and the prestress losses as well as collecting data on stresses, deflections and crack patterns. The tests were very extensive and almost all aspects covered in the above mentioned references of this chapter were examined. The experimental parameters that varied were: maximum load levels for nominal concrete tensile stresses based on uncracked gross section calculations; girder strand stress ranges; cross sections (which included AASHTO PCI Type II girders and Texas Type C girders); strand patterns (draped and straight); provision of passive reinforcing steel in the precompressed tension zone; distribution and confinement of passive reinforcement; degree of precracking of sections and the presence or absence of occasional modest overloads during static tests. It was concluded that even a small number of cycles of modest overloads can cause high stress ranges and sharply reduce fatigue life. An important conclusion was in regard to relating the design of pretensioned concrete girders to the general AASHTO fatigue provisions. It was found adequate to design the girders for a stress range similar to AASHTO structural steel Category B values for redundant load path structures. It was inferred that use of well distributed passive reinforcing steel gave the advantage of rendering good ductility, reducing prestress losses and thus restricting high stress ranges. They also inferred that adopting $6\sqrt{f'_c}$ as the maximum tensile stress in the fiber was not acceptable without being supplemented by a well distributed confined reinforcement. It was recommended that a maximum tensile strength of $3\sqrt{f'_c}$ would be sufficiently conservative to prevent damages due to fatigue.

CHAPTER 3

MATERIAL PROPERTIES

3.1 INTRODUCTION

In order to be able to predict the load-deflection and moment-curvature of the beam, it was necessary to know the stress-strain behaviors of both the concrete and steel. Initial estimates of responses for different load stages were made referring to the material properties as measured in the earlier project, JHRAC 87-3(32,33). However, at the end of the fatigue tests on both the beams, 4 and 7 cores were drilled out from Beam10 and Beam8 respectively. The actual compressive strengths were determined from testing these core samples. The results from strand stress strain tests conducted by Florida Wire & Cable (a manufacturer of prestressing strands) and reported in Table 3.3 were used where the modulus of elasticity of the strands was needed.

3.2 CONCRETE PROPERTIES

3.2.1 Specifications for Testing of Specimens

The in-place compressive strength of the concrete was determined by testing the cores according to ASTM standards. The procedures for obtaining drilled core specimens are standardized in ASTM method for obtaining and testing drilled cores and sawed beams of concrete(5). This method requires the diameter of the specimens to be at least twice the maximum nominal size of the coarse aggregate in the core sample and preferably three times the nominal maximum size of the coarse aggregate (4,6). The aggregate in this beam was approximately 3/4"-1" size.

This method also requires the length of the capped specimens to be as nearly as practicable twice its diameter. Specimens should avoid embedded reinforcement if possible or the ends should be trimmed to eliminate the reinforcement. The test method also provides a table of correction factors for cores with L/D (length/diameter) ratios from 1.0 to 2.0. The web of the box girder was only 5 inches thick and hence the height of the cores drilled out were limited to a height of approximately 5 inches with Beam10. But, surprisingly, some of the cores from Beam8 were almost 6 inches in length from one side and 4 inches from the opposite side indicating a differential or non-uniform thickness in the web. This was perhaps due to the movement of the inner cardboard mold during fabrication.

3.2.2 Test Procedures

Stirrup locations were determined out on the sides of the beam using a rebar detector. The specimen cores were drilled using an approximately 2.75" diameter bit, mounted horizontally against the side of the beam. Four cores were removed from Beam10, one from each corner, at about mid depth. They were capped with sulphur mortar and soaked in lime water solution for 48 hours. Similarly, seven cores were removed from Beam8 and capped with sulphur mortar. One of the cores had a rebar running through it. Two were tested dry and the other five, one of which had a rebar, were tested after soaking in lime water for 48 hours. The lengths and diameters of the capped specimens were measured using a vernier

TABLE 3.1 COMPRESSIVE STRENGTH OF CORES FROM BEAM# 10

CORE #	*L/D*	*Measured Compressive Strength*	*Correction factor for l/d*	*Corrected Compressive Strength (psi)*
1	1.78	6600	1.0	6600
2	1.618	7800	0.97	7560
3	1.377	6540	0.95	6180
4	1.645	7510	0.97	7300

TABLE 3.2 COMPRESSIVE STRENGTHS OF CORES FROM BEAM#8

CORE #	*L/D*	*Measured Compressive Strength (psi)*	*Correction factor for l/d*	*Correction factor for Rebar*	*Corrected Compressive Strength (Psi)*
5	1.344	7580	0.94	-	7140
6	1.376	6310	0.95	-	5960
7	2.01	6360	-	-	6360
8	2.01	6320	-	-	6320
9	2.01	6070	-	1.04	6310

calipers to an accuracy of 0.001". These measurements were used to calculate the l/d ratios. They were then tested till failure at a constant stress rate of 35 psi per second in a compression testing machine.

3.2.3 Results and Discussion

This normal weight concrete had a unit weight of 152 pounds per cubic foot. Correction factors from the ASTM specifications were applied to correct the concrete strength for l/d ratios different from 2.0. Since one of the cores from Beam8 (core # 9) had a rebar running through it perpendicular to the direction of the compressive load, a correction factor was applied to account for it. The influence of these reinforcing bits on the compressive tests of concrete has been reported (14) to usually reduce the strength by 4 percent and hence its strength was increased by 4 percent. Table 3.1 and 3.2 give the results obtained when the cores were tested wet. The modulus of elasticity of concrete E_c was determined using Equation 5.1 of the ACI High Strength Concrete Committee 363 (3) and using the ACI Building Code Section 8.5.1 (2). These equations are

$$E_c = 4000\sqrt{f'_c} + 1.0 \times 10^6 \qquad [5.1]$$

$$E_c = w_c^{3/2}\, 33\sqrt{f'_c} \qquad [8.5.1]$$

The average compressive strength of the cores tested wet was 6640 psi and the modulus of elasticity, E_c was 4.2×10^6 psi based on Equation 5.1 of the ACI High Strength Concrete Committee 363 Report and was 4.8×10^6 based on ACI Building Code Section

8.5.1. This value of f'_c and E_c of 4.8×10^6 psi were used to predict the theoretical load-deflection and moment curvature behavior. The compressive strength of the two cores tested dry was 9000 psi but these results were not used for calculation purposes. The measured average f'_c and E_c were 7100 psi and 4.2×10^6 psi in the previous project (30), tallied closely.

3.3 PRESTRESSING STEEL PROPERTIES

It was known previously that the prestressing strands used in the beam were uncoated, 7/16" diameter, 250 ksi, seven wire strands. For theoretical calculations, results from the tests conducted by Florida Wire & Cable Company were used. They conducted tests on three samples taken out of Beam # 4 as a part of the previous project, JHRAC 87-3, "Tests on Prestressed Concrete Bridge Beams" (32,33). Specially designed equipment for testing 7-wire strands was used. A mechanical extensometer determined the strain readings. The tests were conducted in accordance with ASTM A-416. The results are tabulated in Table 3.3 and Figure 3.1 shows the complete stress strain behavior of the steel. Also, these results of the Florida Wire & Cable Co. correlated well with the tests done by the investigators of the previous project (31). The average actual modulus of elasticity was 24.86×10^6 psi.

TABLE 3.3 TEST RESULTS FROM FLORIDA WIRE & CABLE COMPANY

SAMPLE	f_{pu} *(Ksi)*	*Ultimate Breaking Load (Ksi)*	*Load @ 1% Extension*	*Ultimate Elongation*	*Area (in²)*		*Modulus Of Elasticity x10⁶*	
					Actual	*Nominal*	*Actual*	*Nominal*
1	255.8	28550	24400	5.73%	0.1116	0.108	24.8	25.6
2	255.1	28160	23800	6.51%	0.1104	0.108	24.9	25.5
3	260.3	28500	24100	6.25%	0.1095	0.108	24.9	25.3

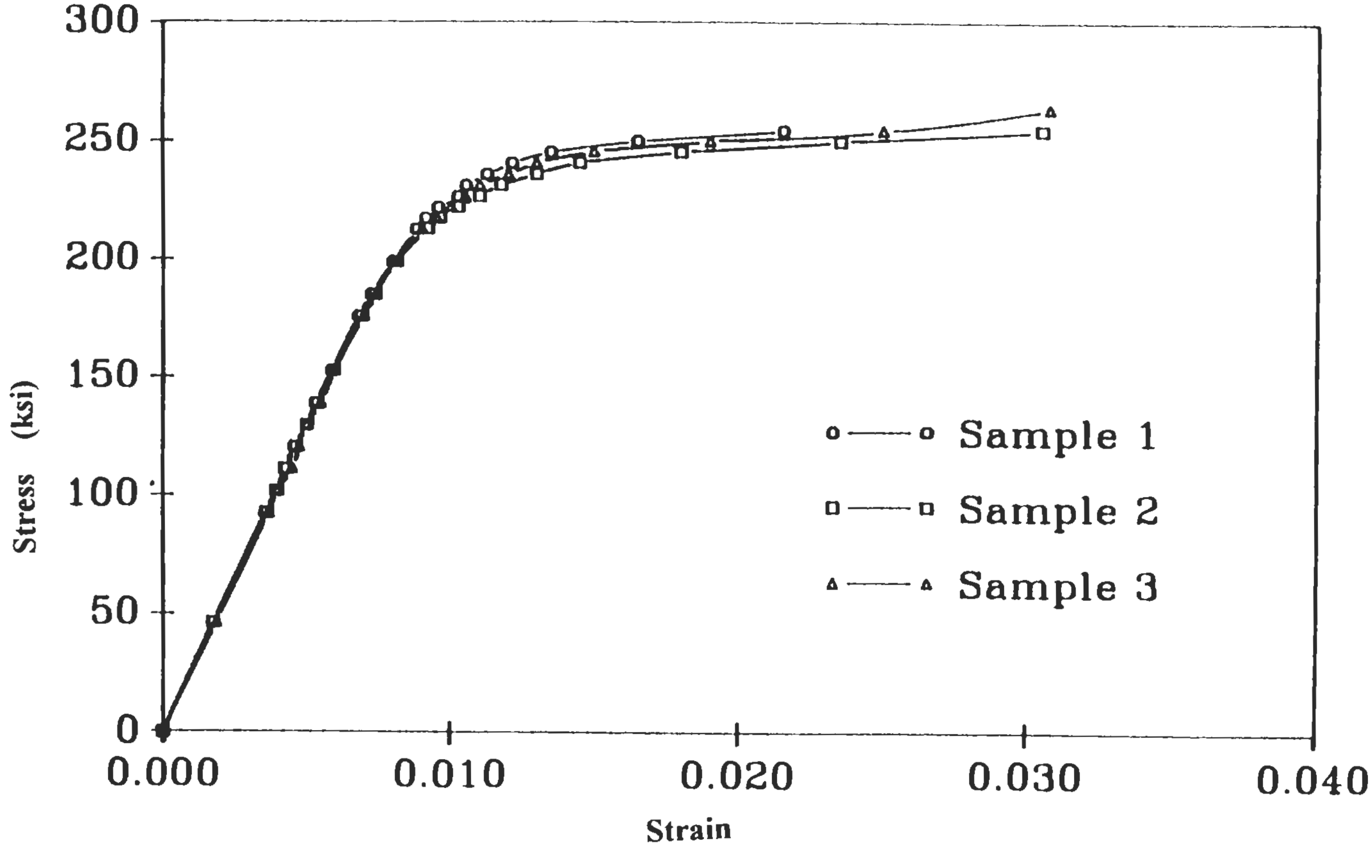

Fig 3.1. COMEPLETE STRESS STRAIN CURVE FOR THREE 7/16th INCH DIA STRANDS: STRANDS TESTED BY FLORIDA-WIRE & CABLE COMPANY

CHAPTER 4

THEORETICAL ANALYSIS

4.1 DESIGN OF THE WALNUT STREET BRIDGE

The Walnut street bridge was a prestressed concrete box beam bridge built during 1960 and based on the then used AASHO 1957 Specifications for Highway Bridges (7). This was a period when many such bridges were built all over the United States. The beams were made in precasting yards and transported to the bridge site, where they were erected side by side on cast in place piers. In addition to the 1957 AASHO specifications, the "Criteria for Prestressed Concrete Bridges" of the Bureau of Public Roads (13) and the "Tentative Recommendations for Prestressed Concrete" of the ACI-ASCE Joint Committee 323 (35) were referred to in reviewing this bridge design. The design calculations and drawings were not available when the research project was undertaken. But during phase 1 of this project (31,32,33) design details and required information were assimilated from similar bridges constructed during that period. The theoretical analysis and planning for this experiment were made based on this information.

4.2 DESCRIPTION OF THE BRIDGE BEAMS

As stated in Chapter 1, the beams tested were two interior beams of the 13 beams of the bridge. The cross section and theoretical section properties of a typical interior beam and are shown in Figure 4.1. The cross-sections of the interior beams conform to the BI-36 type of

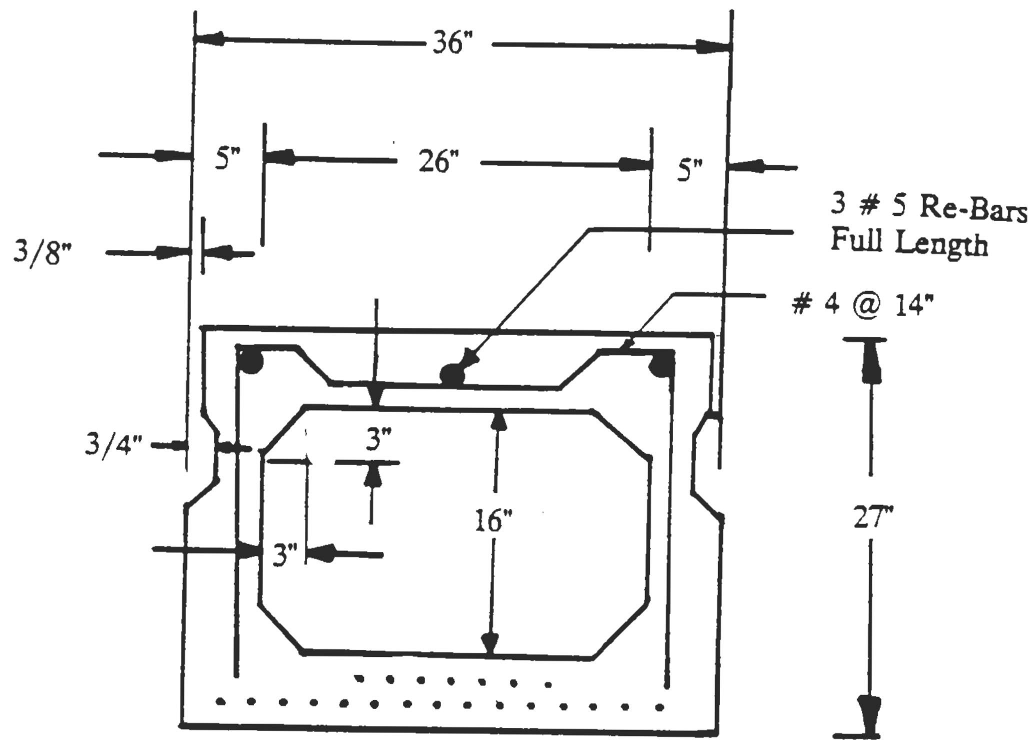

Area of Concrete Cross-Section	Ac	=	560.5 sq. in
Moment of Inertia of Concrete	I_g	=	50,334 in ^{4}
Distance from bottom fiber to c.g. of the section	C_b	=	13.35 in.
Unit weight of concrete	W_t	=	584 lb/ft
Area of Prestressing steel	A_{ps}	=	2.38 in^2
Eccentricity of prestressing steel	e	=	10.71 in

Figure 4.1 Cross-Section and Sectional Properties of the Interior Box-Beam

the AASHTO-PCI standards. The beams were 56 feet long box beams and were simply supported with an effective span of 54 feet and a span to depth ratio of 24. They were 36 inches wide and 27 inches deep. Voids were created in the beams by placing rectangular water resistant cardboard tubes in the forms. The cardboard tubes were left in the finished beams. Prestressing was accomplished by 22 strands of 7/16 inch diameter straight strands distributed in 2 layers. Shear reinforcement was adequately provided by #4 stirrups at 14 inch spacing. Three #5 rebars placed on the top supported the stirrups. The beams were post-tensioned transversely at the ends and the center and had solid cross sections at these regions. For lateral distribution of loads across the width of the bridge, the beams were grouted together at keyways cast into the sides of the beams. .

These beams were not provided with sufficient anchorage zone reinforcement in the ends due to no such requirements at the time of their design. The beams as a result had visible thin horizontal splitting cracks in the end zones. These cracks were neither long nor more than 0.001 inches wide. They were not affected by the loading sequences during the experiment either.

4.3 DESIGN LOADS AND SPECIFICATIONS

The percentage of prestressing steel (ρ) required for the ultimate moment capacity of the section was lower than the maximum required for a balanced strain condition (ρ_b). The beams were hence underreinforced and were expected to fail by the "yielding" of the prestressing strands under static loads.

The self weight of the beam, the weight of the center diaphragm and the 2 inch asphalt wearing surface were the dead loads considered for the design of these bridge beams. The superimposed dead load included loads due to the guard rail, parapet and sidewalk. Since the exterior beams were not post-tensioned laterally with the interior beams, the exterior beams carried most of the superimposed dead load. The load from the sidewalk portion on the first interior beam was uniformly distributed to all the interior beams and was accounted for the superimposed dead load for the interior beams. AASHO HS-20 wheel loads and AASHO(7) impact factors were used for live load design forces and moments. The maximum live load based on the concept of moving loads was determined from Appendix A of the AASHTO specification. Also, the distribution factor for the transverse distribution of live loads to each beam was assumed to be S/6 times the live load, where S is the beam spacing, 3 feet for this bridge. As per the 1957 AASHO, beams were designed to carry a live load of four fifths (80%) of the HS20-44 wheel load with zero tensile stresses in the bottom fiber after all prestress losses. The current AASHTO specification (8) uses a different expression to determine the live load distribution factor as compared to the 1957 AASHO specifications.

The load factors for the ultimate flexural capacity of a section, as per the 1957 specifications, were 1.5 for dead loads and 2.5 for live loads. This required ultimate capacity and the service load design condition determined the amount of prestressing steel, prestressing force and eccentricity of the tendons. The amount of prestressing steel necessary to meet these conditions resulted in members having an ultimate flexural capacity about 24%

greater than that required to meet current AASHTO specifications (8). The flexural design calculations for the box beams for the 1957 AASHO specifications are shown in Appendix 'A' of Reference 33. The design based on the current 1992 AASHTO specifications is shown in Appendix 'A' of this report .

The shear reinforcement provided was #4 stirrups at 14 inch spacing within the maximum allowable spacing as per the 1957 AASHTO Specification of 0.75d = 20 inches. This was determined by applying HS-20 truck loading to the full lane longitudinally to obtain maximum lane shear at the span quarter point to be distributed to an individual beam with appropriate live load and impact factors as per the 1957 AASHTO requirements. This shear reinforcement provided sufficient shear capacity so that the beam could not have failed under shear. Shear analysis was also done in accordance with the provisions of section 11.4 of the Building Code Requirements for Reinforced Concrete (ACI 318-83). At any section the nominal shear strength (ϕV_n) was far greater than the factored shear force.

4.4 FATIGUE IN WALNUT STREET BRIDGE

A survey conducted by the ConnDOT for the Walnut Street Bridge reported that the Annual Average Daily Traffic (AADT) is 5500 vehicles per day. The ConnDOT assumes 5% of this as equivalent to the the Average Daily Truck Traffic (ADTT). So in a bridge of this traffic capacity on this type of a road, a longitudinal load carrying member would be designed to resist 500,000 cycles for truck loading. It is not known if these factors were considered during the time of the design of the bridge. Considerations might have not been the same, as the traffic statistics has changed tremendously over the years. But it would be sufficient to design a bridge of this type today to withstand a fatigue load of 500,000 cycles.

4.5 THEORETICAL ANALYSES

4.5.1 Moment-Curvature Relationship

The theoretical moment curvature relationship represented as an M-ϕ curve depends on the effective prestress in the strands. Prestress losses were not theoretically evaluated during this project. However, the actual effective prestress was determined experimentally during the tests and the results closely matched the results established by the previous researchers. An effective prestress of 153 ksi determined in the previous project (31,32,33) was used for the two beams tested in this project. Experimental estimation of the effective prestress is discussed later.

4.5.1.1 Determination of the M-ϕ Curve

The moments and the corresponding curvatures were found by analyzing different stages of loading. The M-ϕ curve has two distinct regions, the initial linear portion representing the elastic range and the non-linear portion for the section in the inelastic range. The concept used was strain-compatibility (21). It is assumed that the changes in strain in steel and concrete are equal and that the variation of strain along the depth of the section is linear. The curvature is calculated as the strain per unit depth of the section. The first stage was the fictitious stage of only the prestressing force acting on the section neglecting the self-weight of the beam. The curvature in this stage is negative (has a camber) as the section is largely under compression. The consequent stages considered in order were: with the self-weight acting, when the stress in the bottom fiber reaches zero, when the strain at the level of steel is zero and then at the cracking stage. This stage demarcates the elastic behavior from the inelastic behavior.

For the curve in the inelastic region, the coordinates were determined for points where the extreme fiber strain in the concrete in compression zone was 0.0002, 0.0003, 0.001, 0.002 and 0.003 in/in was assumed to be the strain in the concrete at ultimate. The failure was predicted for flexure assuming the section has sufficient shear capacity. The basic principle was to equate the total compressive force to the total tension in the section. Stress - strain curve for the prestressing steel is shown in Figure 3.1. A parabolic concrete stress-strain curve based on studies by Hognestad et al (16) was used. The secant modulus of elasticity for the curve tallies with the ACI code value for E_c. This method gives the total compressive force and the distance of the center of gravity of the compressive force from the neutral axis. The position of the neutral axis gives the strain distribution along the depth of the member and in turn gives the curvature. Summing moments about the line of action of the tensile forces gives the total moment in the section.

A computer program, RESPONSE (11), capable of predicting the response of prestressed concrete sections subjected to any combination of axial load, moment and shear was also used to predict the moment curvature relationship. Results from this program were compared with the results of the theoretical analysis by hand calculations. The moment-curvature responses are plotted in Figure 4.2. The analysis from the program required input of the constants of the Ramberg-Osgood function for the stress-strain relation of the prestressing strands and there could have been some error in determining these constants. For the calculation of load vs deflections, the m-Φ curve by hand calculations was used.

4.5.2 Load-Deflection

4.5.2.1 Load Deflection in Prestressed Concrete

The deflection characteristics of a prestressed concrete beam is dependent upon the effective prestress in the beam which determines the cracking moment of the section. The load-deflection response is linear so long as the concrete is uncracked. Under cracked conditions, because of varying amounts and extent of cracking, the moment of inertia varies. With the cracking of concrete (at a moment = M_{cr}) the neutral axis moves upward and the moment of inertia of the cracked section is greatly reduced. This in turn causes larger deflections in the beam and the load-deflection response is no longer linear. Prestressed concrete beams are usually designed to retain a small camber under their self weight. Under full live load they may be allowed to develop tension to a limited extent in their bottom fiber. A typical load deflection curve for a single cycle of loading in a prestressed concrete beam is shown in Figure 4.3. Once the concrete is cracked, on reloading, the cracks reopen when the stress in the bottom fiber reach zero, as opposed to $7.5\sqrt{f'_c}$ when the cracks originally formed. The load-deflection response of the beam becomes non-linear from this stage on.

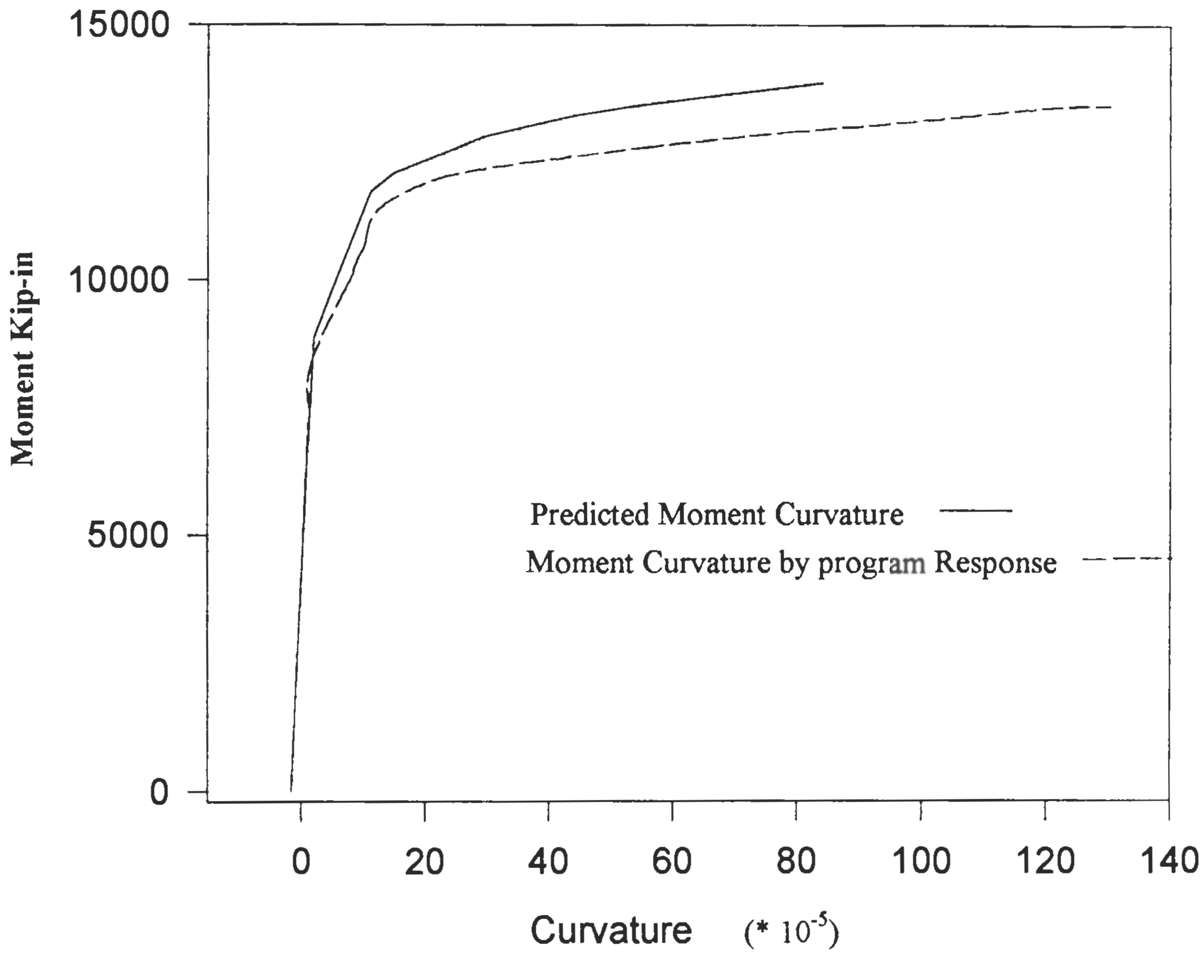

Figure 4.2 Moment-Curvature variation for the beam

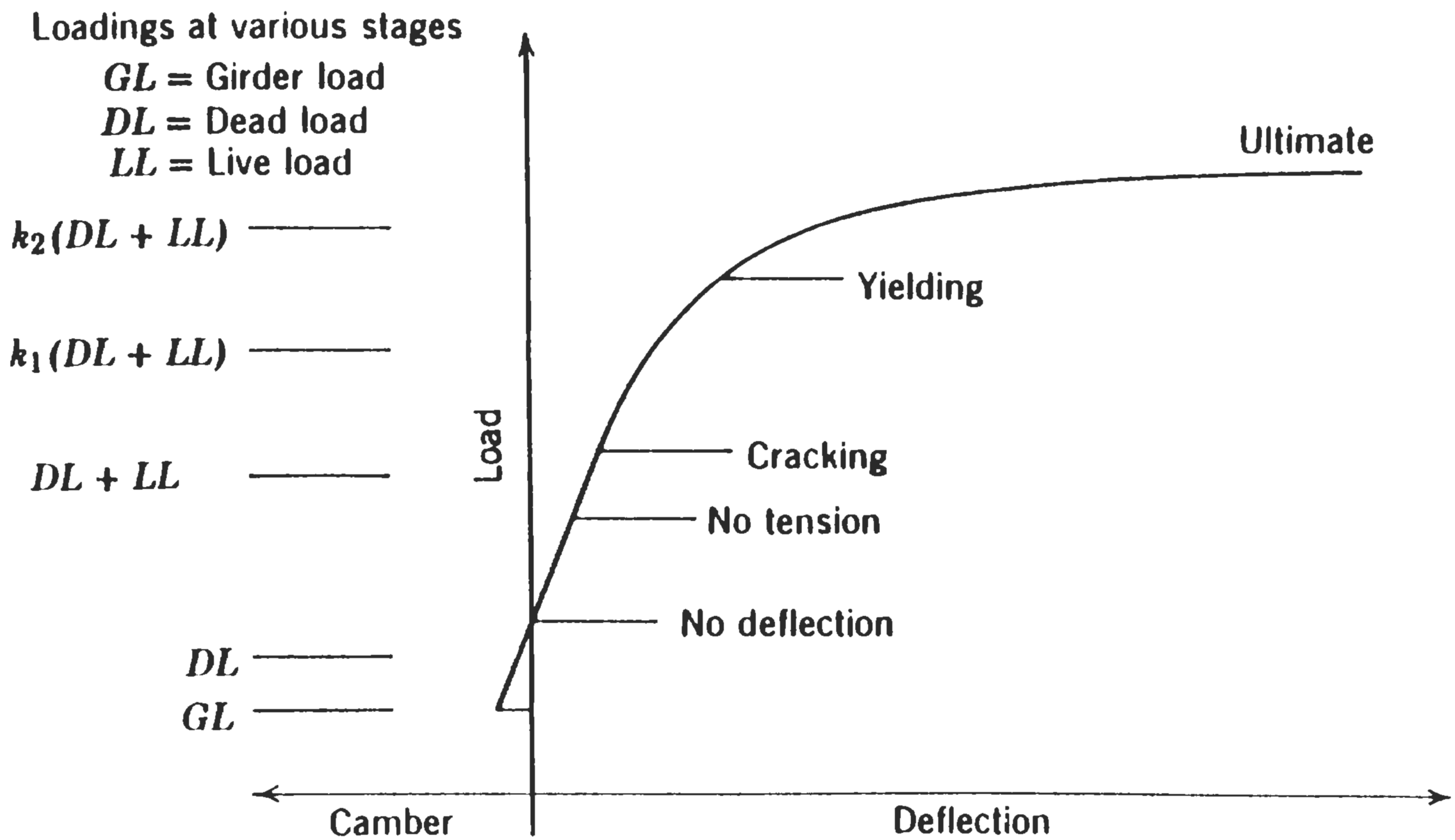

Figure 4.3 Life History of a Prestressed Concrete Member Under Flexure

4.5.2.2 Deflections under fatigue

Cyclic loading has additional effects on the deflections depending on the range of loads. There is a certain stress limit, defined as the shakedown limit (18), below which repeated loading cycles do not affect the strength or the strain capacity of the material. If the shakedown limit is not reached in the concrete and the steel stress is below the yield stress, the reloading curve after attaining the magnitude of the repeated load will follow the single cycle load-deflection curve. If the shakedown limit is exceeded, on increasing the load cycles, the rate of increase in deflection increases. Residual deflection becomes higher. The total recovery is a function of the cyclic load.

Prestressed concrete load-deflection characteristics over time are difficult to predict owing to lack of accuracy in predicting the elastic modulus of concrete and the prestress losses that occur due to creep and shrinkage. It was predicted that the beam will have a camber between 0.13 inches (condition of live load acting at all times) and 1.16 inches (condition of no live load acting at any time) after all losses. The measured camber for Beam 10 was 1.025 inches, within the predicted range.

4.5.2.3 Determining the Load-Deflection curve

Load-deflection trends in a beam are very similar to the moment-curvature trends. The calculations were based for the loading condition as in the actual experimental setup, with the total load distributed into two equal loads placed 11 feet apart symmetric about the center line of the beam. Deflections of the beam for different load stages were calculated using the moment-area method. M/EI is the curvature, ϕ, of the beam. From the moment diagrams, corresponding ϕ diagrams were drawn by substituting the values of ϕ from the M-ϕ curve. End slopes and centerline deflections were determined for a particular load stage, such as the load for cracking moment, service load moment etc. Figure 4.4 shows the predicted load-deflection curves for the beam and the load-deflection curve for Beam10 and Beam8 during their first static tests. Figure 4.5 shows the load-deflection curves for the two beams in their precracked and cracked stages.

4.5.3 Stresses

4.5.3.1 Stresses in Prestressed Concrete Beams

The stress variation in a prestressed concrete beam is very similar to the load-deflection behavior with distinct linear and non-linear portions marking the precracked and cracked stages respectively for the section. Till the cracking of concrete, loads applied cause decompression in concrete and subsequently induce identical tensile strain stresses in the concrete and the prestressing strands. The only increase in the stress levels of the tendons is the increase due to the increased tensile strains in concrete. The stress-strain and the load vs. stress behavior is linear till the cracking of concrete. With the cracking of concrete, stresses in the strands increase sharply as a result. The stress response becomes non-linear from this stage on.

4.5.3.2 Stresses under fatigue

Again, the stress variation in the strands under cyclic loading is very similar to the load-

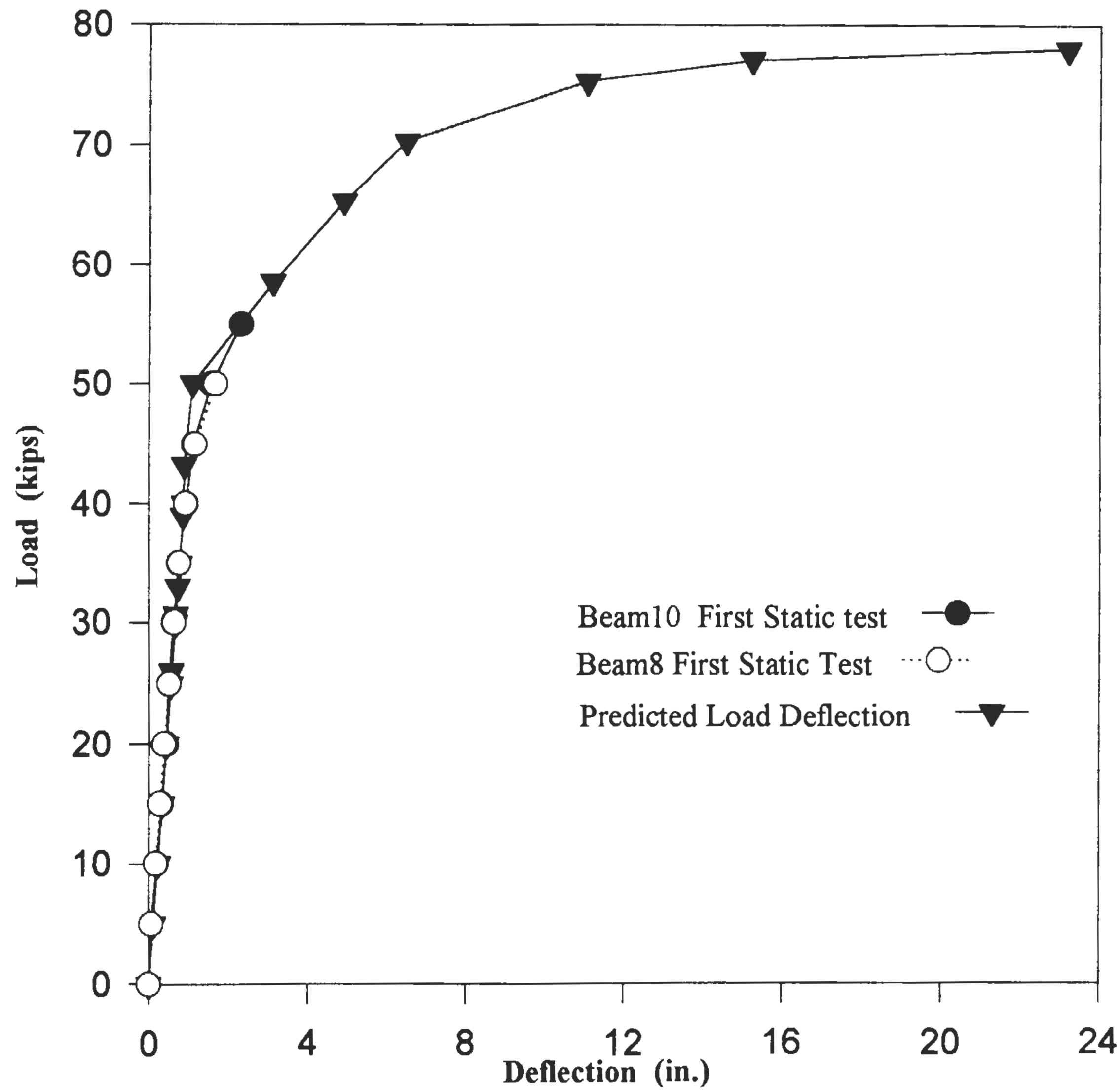

Figure 4.4 Load-Deflection Relationship at the centerline of the Beams

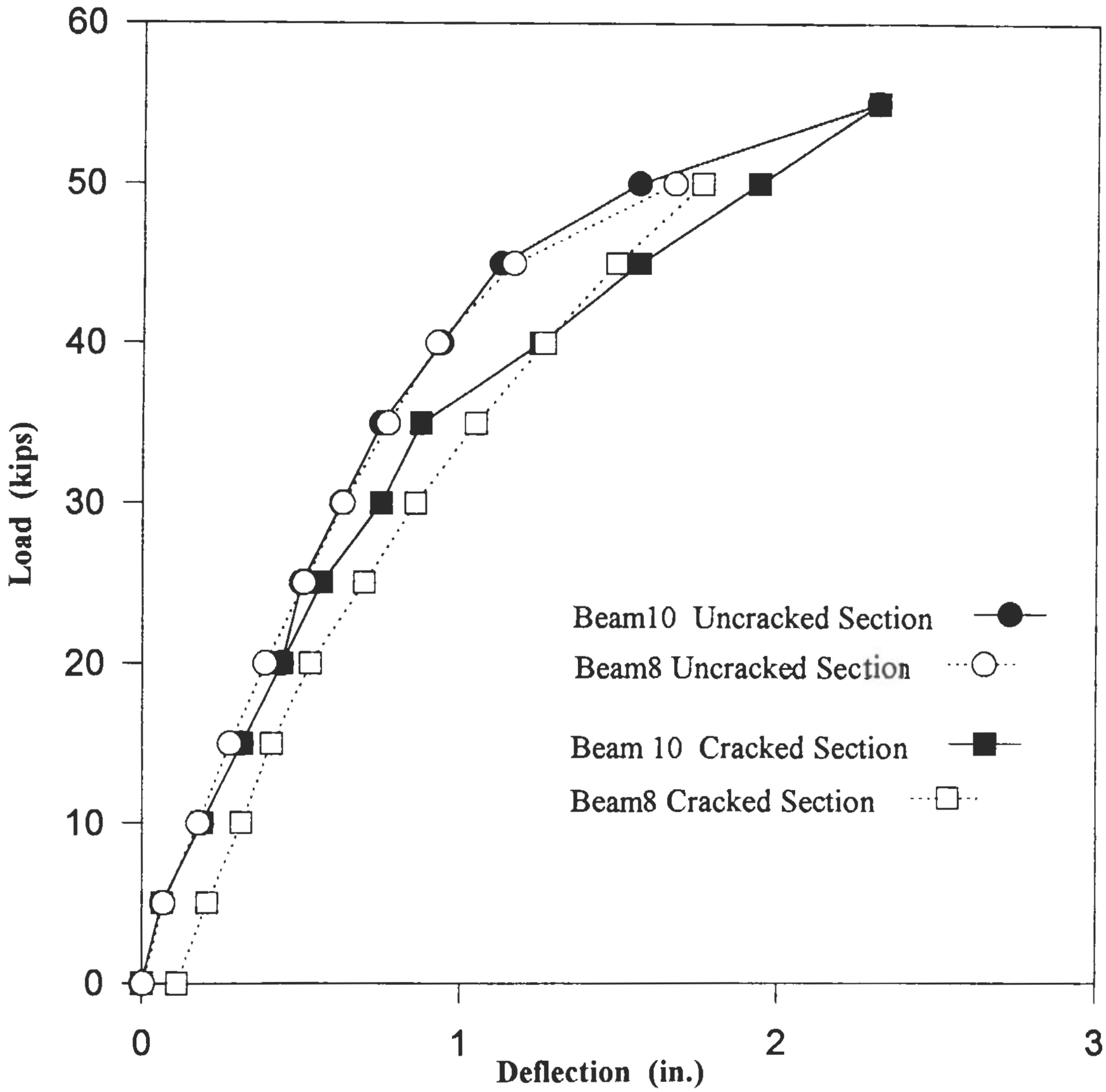

Figure 4.5 Load-Deflections of Beams with and without cracks

deflection behavior under fatigue. The stress ranges that the strands are subjected to determine the intensity of the effects. In general, the stress levels under a certain load will increase as the number of cycles of loading increases. S-N curves for the beams shown in Chapter 6 illustrate the stress variations under repeated loading.

4.5.3.3 Theoretical determination of stresses

Stresses for the strands within the elastic limits were calculated from the strain levels of the concrete at the level of the tendons and using the elastic modulus as determined by the tests from Florida Wire & Cable Co. Beyond the cracking stage a transformed section analysis was performed. For cracked prestressed concrete, the neutral axis location and effective section properties depend on the cross-section and the material properties as well as on the effective axial prestressing force and the loading. The effective prestressing force will have to be either determined or assumed with close accuracy if the information is available for this analysis. An effective prestress of 153 ksi was used as was in all other calculations. A fictitious load stage corresponding to complete decompression of concrete along the entire depth of the section was considered and the fictitious external force pulling the tendon at this stage was determined. The effect of this force is counteracted by an equal and opposite force 'F'. The effect of this force and the total moment acting on the section was represented as a resultant force 'R' (R=F) applied at an eccentricity above the cracked concrete centroid. The stress in the strand was then determined on principles of statics similar to a reinforced concrete section subjected to an eccentric compressive force (25). The Stress levels at different load stages determined for the beams is shown in the load vs. stress curve in Figure 4.6.

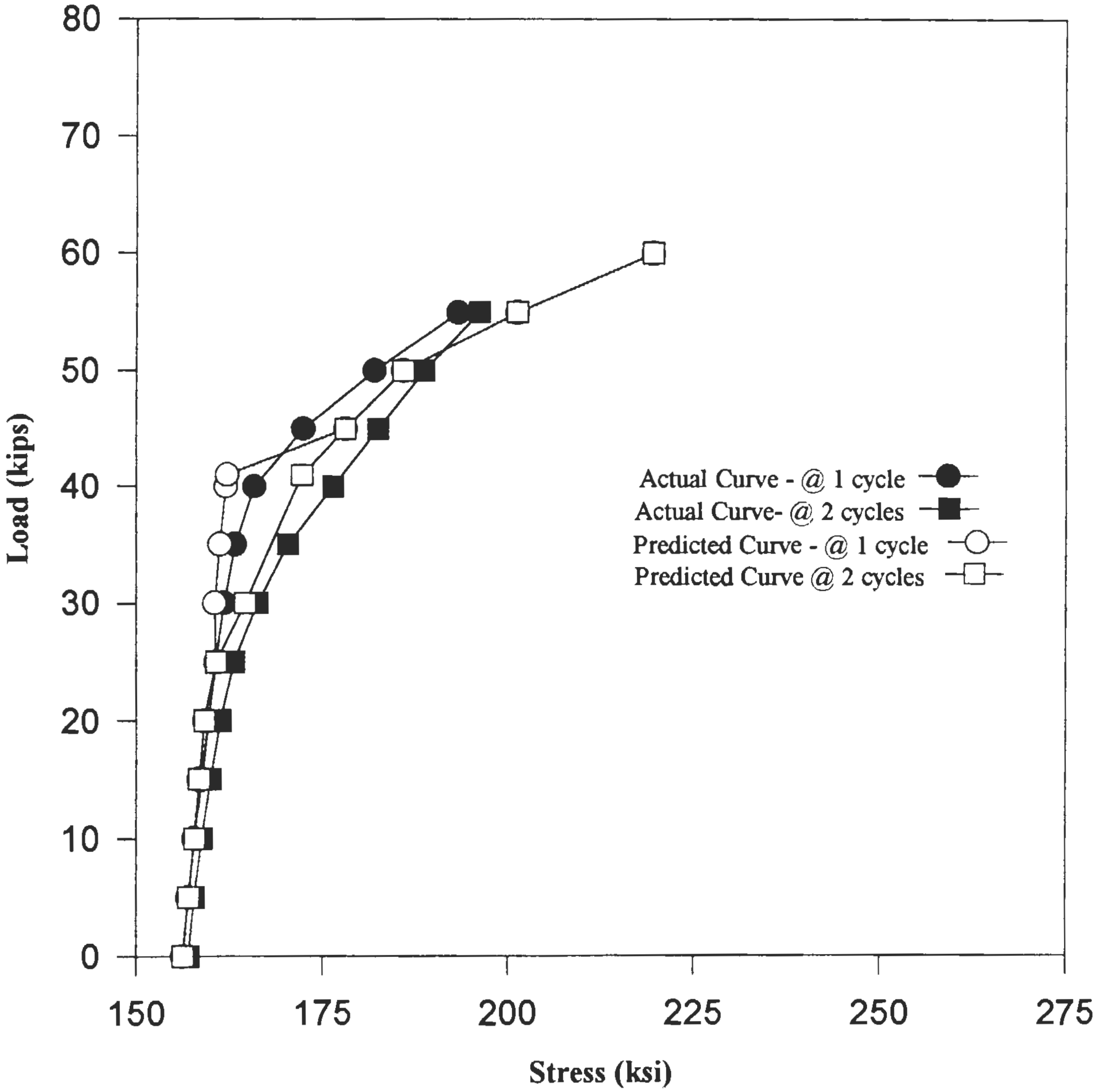

Figure 4.6 Predicted and Actual Stresses in Beams

CHAPTER 5

EXPERIMENTAL SETUP AND TEST PROCEDURE

5.1 OUTLINE

The beams, while in the Walnut Street Bridge, were simply supported at both ends. They were placed side by side and post-tensioned laterally at the center and at both ends. The experimental setup was designed so that the basic function of the beam in the bridge could be simulated as much as possible. The beam was 56 feet long, with a test span of 54 feet and an overhang of 1 foot at each end. The beam was set on roller supports that could allow it to rotate and slide longitudinally. The beams were supported on large concrete blocks. These blocks were cast 6'x4'x2'-3" in size and were sufficiently reinforced for both flexure and shear.

It was impractical to provide a three point loading as from one line of wheel loads for the standard AASHTO HS20-44 loading. An equivalent two point loading was provided instead. A 12 feet long triple I-Section steel beam that could be loaded at its midpoint was set in the center of the prestressed concrete beam. The prestressed concrete beam was subjected to a two point load 11 feet apart and equidistant from its center. Load from the steel beam was applied to the prestressed concrete box beam on four points over each web of the box section. The experimental set up is shown in Fig. 5.1A and 5.1B.

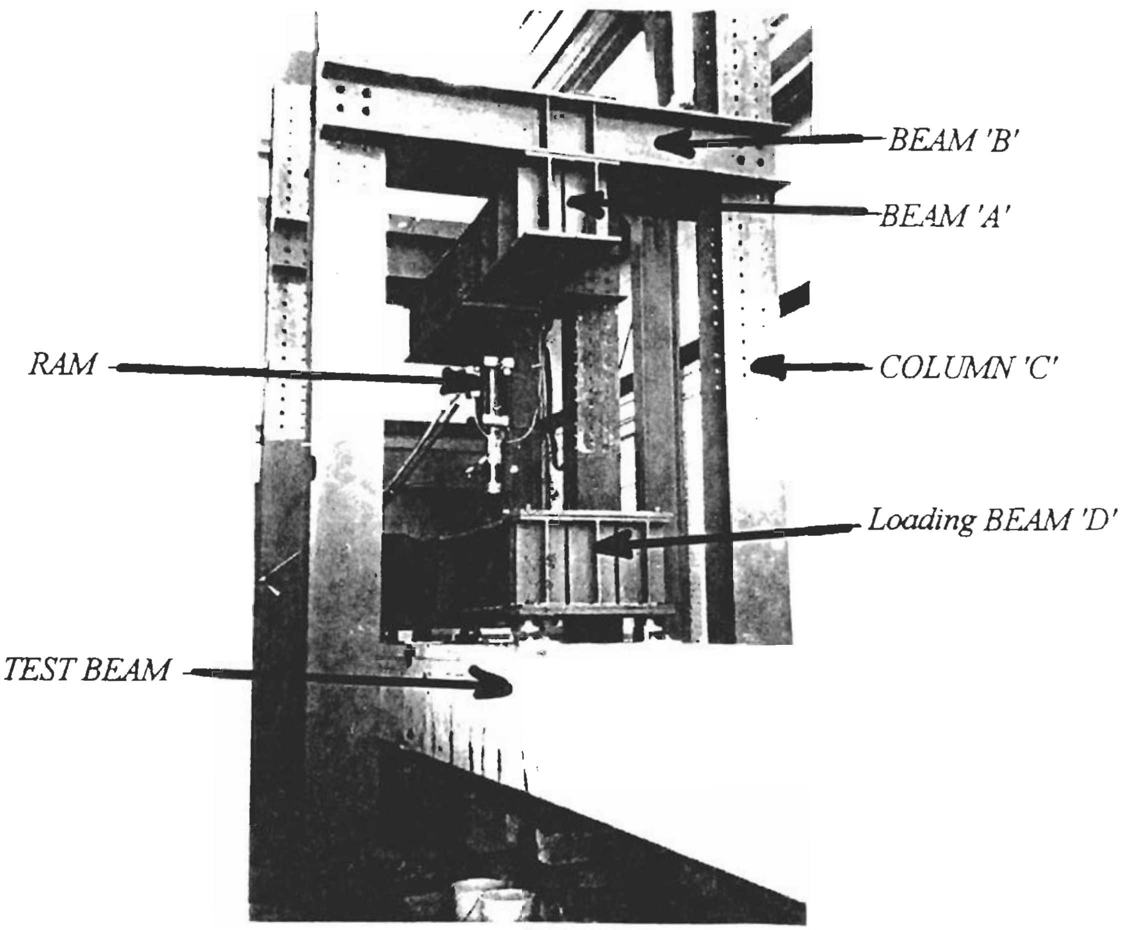

Figure 5.1A View of the Test Setup

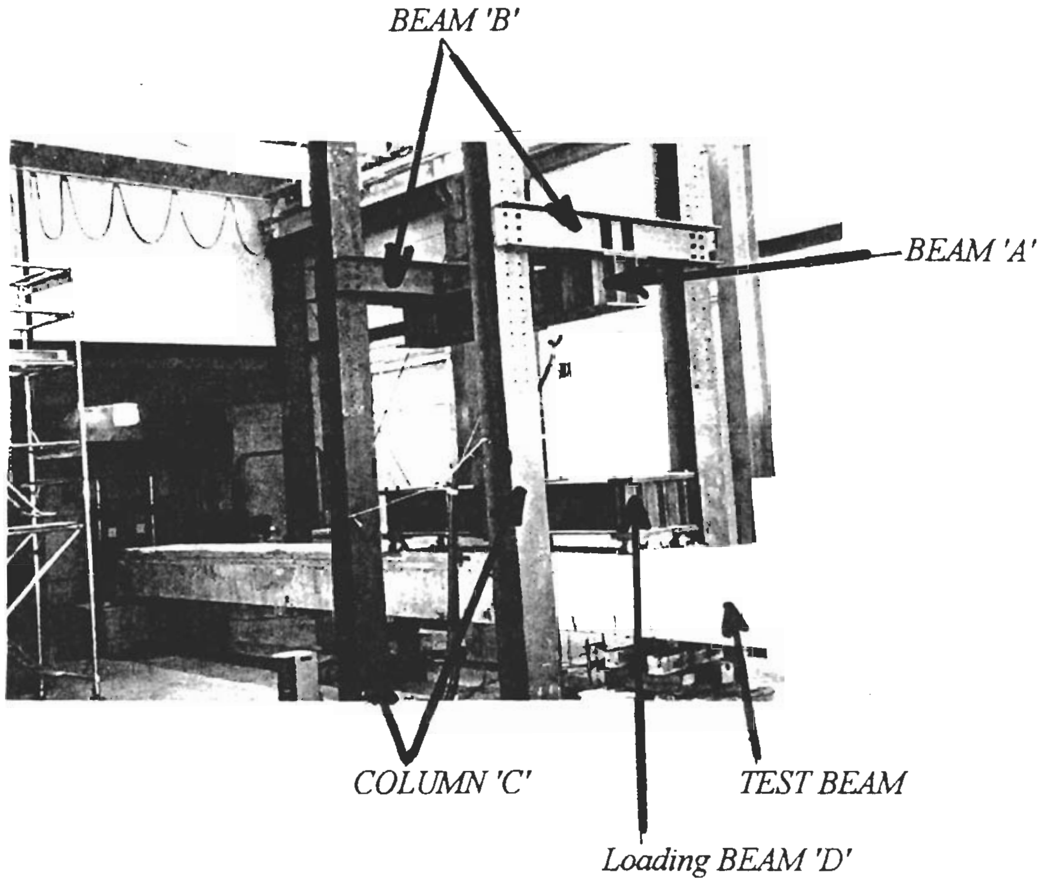

Figure 5.1B The Test Frame

5.2 THE REACTION FRAME

5.2.1 Strong Floor

The strong floor in the Structures laboratory of the Civil Engineering Department of University Of Connecticut, Storrs, CT made possible the testing of the beams. The floor is a 4 feet thick concrete slab with heavy reinforcement running in both directions. It spans 65 feet longitudinally and 40 feet laterally. The floor has multiple groups of four 1-1/2" inch diameter holes in an 8" x 8" pattern. Such groups of four holes are spaced at 4 feet center to center in both perpendicular directions. At the bottom of the slab at each hole is a steel plate and a nut into which a threaded rod can be screwed. Threaded rods of 1.125 inches diameter are used to bolt structures down to the floor. These rods are also threaded on the top end and a nut applied can tighten from the upper end. The floor is capable of resisting up to 120 kips in either tension or compression at each four hole group.

5.2.2 Test Frame

5.2.2.1 Loads and Factors

The test frame was designed to support the reaction forces from the ram as well as hold the ram in position. The frame was designed for moment-resistant connections. The ram had a capacity of 110 Kips. The frame was very conservatively designed to resist up to 110 Kips of ram load under a fatigue range between 0 and 110 Kips and with a factor of safety of 3.0. However, during the course of testing these beams, the maximum loads reached were not more than 50 Kips for static tests, 74 Kips for static ultimate tests and when cycling under fatigue loads, the maximum range was 30 Kips (i.e. 20 to 50 Kips). The structure had at least a factor of safety of 6 for regular static tests there by ensuring a very safe test. The frame design was intended to be sufficient for future tests too and to be safe enough to resist the maximum load and ranges that the ram could apply.

5.2.2.2 Description of the Test Frame

The steel sections for the design and fabrication of the test frame were either HP14x102 or W18x97 and were provided to us by the ConnDOT. The view of the frame is in Figure 5.1B. The four columns 'C' and the four beams 'B' were HP sections and the beams A and D between which the ram was bolted (the steel beams running parallel to the length of the concrete beam) were W-sections. Beam 'A' was a double W-section, two W-sections with full penetration welds longitudinally between their flanges. Beam 'D' was a similar triple W section. All the bolts for the beam-to-column connections were 7/8" diameter, grade A490 designed for friction connections. The welds were E70; stiffeners and base plates had 5/16" fillet welds.

The columns were 20 feet tall and were welded with 5/16" fillet welds to base plates of size 1-1/2" x 18" x 18". These base plates had 1-1/4" diameter holes for the 1-1/8" diameter anchor rods which were used to bolt the columns to the strong floor allowing the base plates to resist a tension or compression of at least 120 Kips. The columns also had holes centered on the flanges @ 4" center to center longitudinally for the beam-to-column connection. The four columns were erected in an 8ft. x 8ft. pattern.

Stiffeners were provided in all beams in regions where concentrated forces were resisted. These stiffeners were cut to fit flush between the flanges and were welded all around.

5.3 SUPPORTS

5.3.1 Supports for the Prestressed Concrete Beam

The concrete beam was set on two end supports made to simulate simply supported conditions which could allow rotation and horizontal movement at the ends. The beam was supported on 2" diameter rollers at both ends. Steel plates 8" x 36" x 1/2" were placed at the top and bottom of the roller to distribute the load. The roller was welded to the top steel plate and was seated on 1/2" diameter keeper pins that allowed the rod to simply rotate when the beam was loaded. The top plate was grouted to the bottom of the concrete beam. Teflon coated bearing plates were used beneath the bottom steel plates to allow for any sliding of the plate that was supporting the roller. This teflon coated plate was welded to another plate (with stoppers) which was grouted to the concrete block. Details of the supports are shown in Figure 5.2. Three braces were provided at each end of the beam restraining the beam from excessive longitudinal and transverse movement.

5.3.2 Supports for the Loading Steel Beam

Since the bridge girder was a box-beam, loads were applied directly above the webs . The steel load distribution beam was set on four supports, one at each corner (Figure 5.3A,5.3B). The supports were similar to pot bearings found in bridges. A steel plate 1/2" x 6" x 8" was

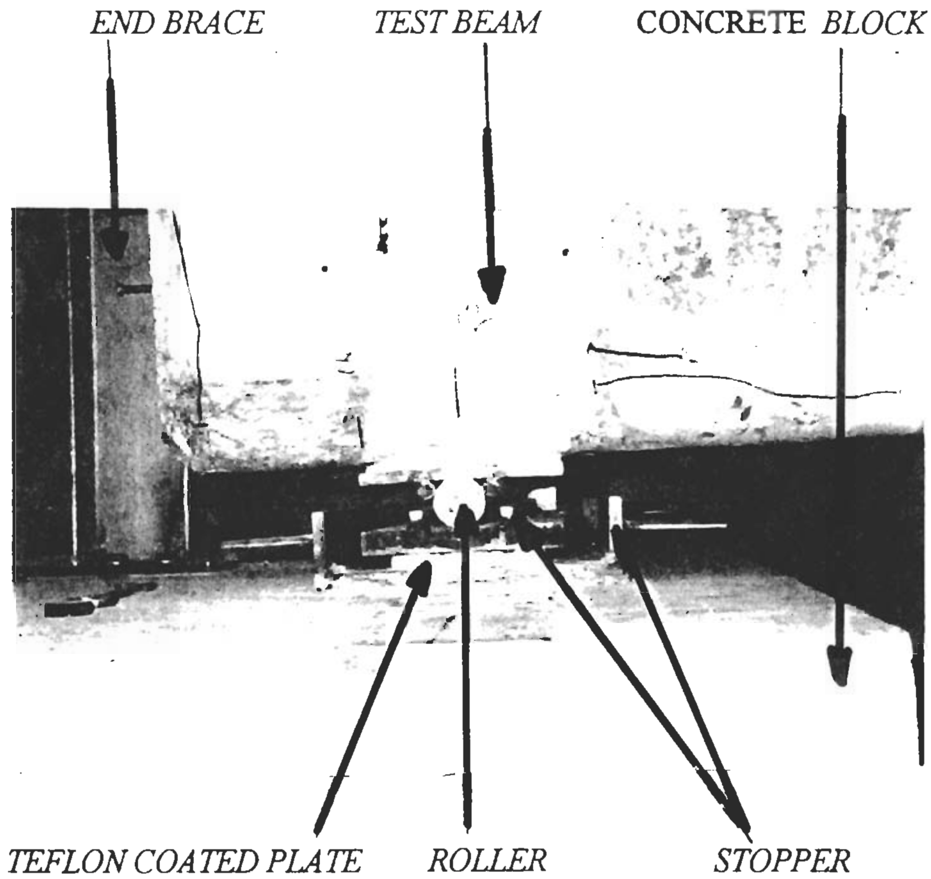

Figure 5.2 Supports Underneath the Concrete Beam

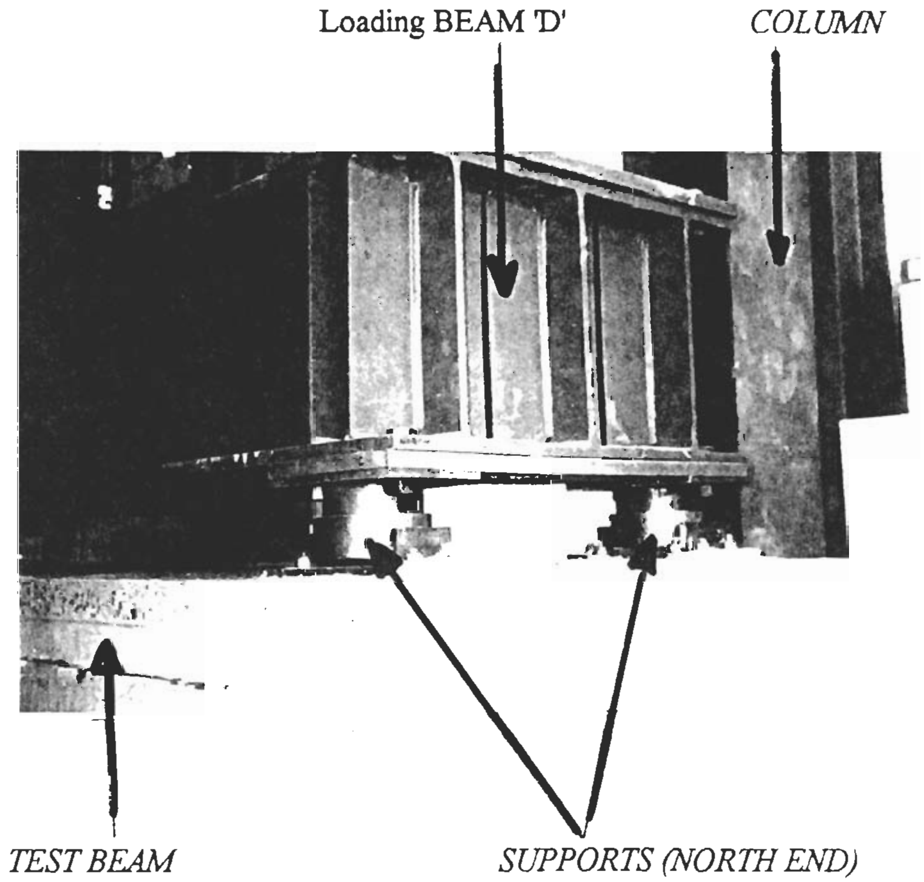

Figure 5.3A Supports Beneath the Steel Beam

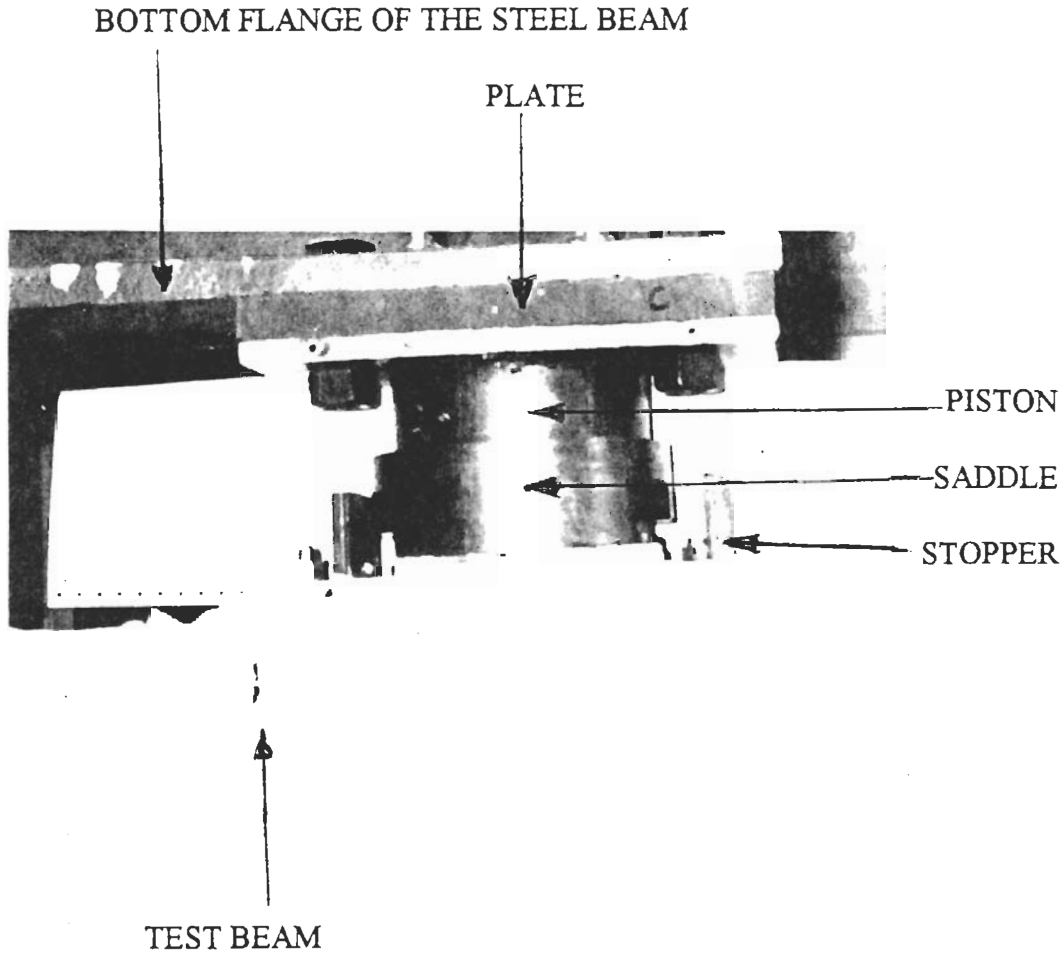

Figure 5.3B Details of a Support Underneath the Steel Beam

bolted to the bottom flange of the steel beam and a 6" diameter piston was welded centered on the plate. The solid steel piston sat on an elastomeric bearing pad inside of a saddle. These pads allowed rotation as well as protected the steel from rubbing on each other. They were replaced whenever needed. The bottom of this saddle was shaped to sit on a teflon coated plate so that this whole unit could slide on the teflon plate longitudinally. The teflon plate was welded to another plate 1/2" x 6" x 8", bolted to the top of the concrete beam. Suitable stopper plates were provided on this support on both sides that restricted longitudinal movement of 1/2" or less.

5.4 LOADING SYSTEM

The load was supplied by a 110 Kip MTS hydraulic ram assembly which consisted of the swivel bases, the actuator and the loadcell. The actuator could extend within a range of 0" to 10". The hydraulic ram was powered by a 60 HP pump which could supply oil at the rate of 30 gallons/minute at a pressure of 3000 psi to a manifold . A cooling system installed with the pump system maintained an oil temperature level not to exceed 105 degrees Fahrenheit by supplying cooling water at the rate of 10-15 gallons/minute as needed. This rate of supply was determined by the automatic opening and shutting of a valve in the pump depending on the temperature the oil reached.

The loading system was controlled through the MTS computer. A second computer operating the TESTSTAR software (on the OS/2 operating system), supplied by MTS, controlled the MTS computer. This whole unit operated the ram through controlled electronic signals generated by the MTS computer. In addition to controlling the ram through the computer generated 'Segment Generator', basic operations such as *'Start'*, *'Stop'*, *'Load'*, *'Unload'* could be controlled manually through a 'Pod'.

The TestStar software consists of several programs each of which runs for a specific purpose. Those that are of relevance to the experiment are briefly discussed below.

1. The **TestStar** application is the main program that sets up a test and controls the digital controller. A picture of a typical TestStar window is shown in Figure (5.4). Configuration files are created in this program. A configuration file contains information about every selection made in every TestStar window. This file saves every parameter setting for a specific test, ensuring the servo loop has known parameters assigned. Different tunings of the system and different detector actions and limits were used for static and dynamic tests.

2. **Testware-SX (TWSX)** is an optional, flexible, general-purpose program that combines processes that can produce a test command, acquire test data and can interface with external devices. All the fatigue tests were programmed on TWSX with data files linked to them. Static tests were controlled through the pod.

3. The **Sensor Calibration** program creates or imports sensor calibration data. This program keeps a database of the calibrated sensors.

Main TestStar Window

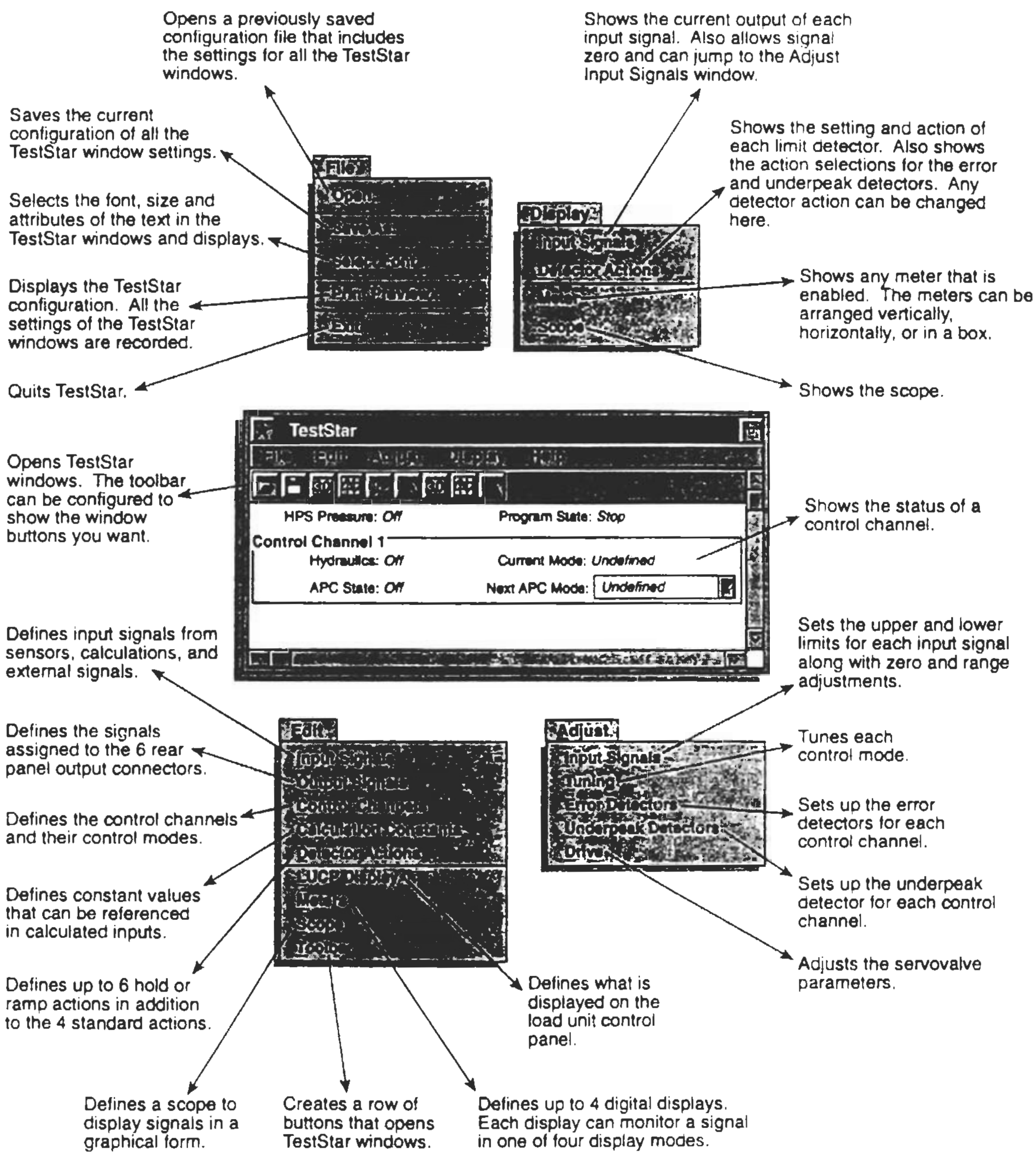

Figure 5.4 TestStar Menu and Options

5.4.1 Tuning of the MTS system

The tuning for the loading system was set initially to function for the load-deflection response of the beam with an uncracked cross-section. The system tuning was later changed to allow for the less stiff beam. The same tuning was also used for the dynamic tests. Appendix B and Appendix C show the configuration for the static and dynamic tests respectively.

5.5 INSTRUMENTATION

5.5.1 Data Acquisition Unit

An analog to digital converter called the UPM 100, a multipoint measuring unit, manufactured by Hottinger Baldwin Messtechnik, was used to make electrical measurements of strain, deflection and load. This system was capable of detecting, processing and editing signals of up to 20 channels simultaneously with the two module boards that were installed for this test. The selector module used for this test was UMH 3251. All strain gage bridge circuits were connected to a terminal board which was connected to the unit. The channels are scanned one after another. Each channel reading is actually the average of several rapid readings. The unit allows for all individual data stored for this channel. Further, the unit executes an absolute calibration at fixed time intervals during which zero point and sensitivity settings of the analog components are checked, and the corrected values are stored.

5.5.1(a) Operation

The channels are activated by means of selector modules available for different types of transducers and connections. AC or DC voltages of desired frequencies are chosen. The bridge excitation voltage is only applied to the selected channel. The measuring signal is amplified, digitized and admitted to the internal microcomputer for further processing. Controlled by a program the microcomputer switches a zero signal and then a calibration signal to the amplifier input at 5-minute intervals. The calibration characteristic found that way interrelates the measured values. Thus an automatic, numeric calibration of the instrument is obtained and potential alterations to zero point and sensitivity settings do not affect measurements. The measured values are calculated by the micro computer according to the scale and gage factors for the units set.

The standard RS-232-C interface permitted connection of the UPM100 to a computer and all device settings and control functions relevant for measurement were performed through the computer terminal. A software program called "Beam 3.1" was used to make all settings to be specified for the operation of the unit. This software also gave the advantage of being able to reduce the data as desired later during the analysis and make graphic representations.

5.5.1 (b) Configuration of the Data Acquisition unit for the experiments

The data system measured the stroke and load of the ram, the strains in the strain gages bonded to the strands and the deflections from the LVDT. The sample time, integration time and total time for the measurements were determined so as to record measurements at the maximum possible rate for dynamic tests and maximum possible accuracy for static tests. A sample configuration file is shown in Appendix D. The channels were all tared at the beginning of the test with zero ram load and the self weight of the prestressed concrete beam and the weight of the steel beam acting on it. Any taring done at later days were adjusted with the taring done on the first day.

5.5.2 Strain Measurements

Electrical strain gages were used to measure the strain within the constant moment region of the beam. Concrete cover in the center span at the bottom of the beam was removed for installing strain gages on the strands. The approximate location of the strands was marked in about a one square foot area and the concrete cover was removed using a pneumatic chipping tool. Five strands were exposed for about one foot length. Care was taken to avoid nicking of the strands while using the chipping tool. The surface of the strand was cleaned first using a sand paper and then thoroughly with acetone. Further on, a metal conditioner was used followed by a neutralizer to remove any acidic deposits from the metal conditioner. SR-4 electrical resistance gages of 3.18mm gage length were bonded on a wire of each strand using epoxy. They were then covered by silicone rubber barriers to avoid any damage. Two gages were installed on a sample prestressing strand for temperature compensation gages.

Strain gages were connected to the UPM 100 with quarter bridge circuits which could measure strains in 10 channels per board with one common temperature compensation gage serving as the internal completion resistor. The bridge factor was hence 1 for all the gages. The strain gages had a gage factor of 1.98 for Beam10 and 2.06 for Beam8 with a resistance of 120 ohms. The strains were measured in μm/m.

5.5.3 Load Measurements

The magnitude of the loads applied by the ram could be visually read from either the computer monitor or the pod. This was however not convenient for dynamic measurements. Therefore, electrical signals from the loadcell were measured and recorded by the data acquisition unit. The signal output from the loadcell was of DC voltage and was connected to the UPM 100 as a full bridge configuration circuit. The channel was calibrated with a suitable gage factor of 3.96 to read load data proportional to the applied load to an accuracy of 10 pounds. The ram load was measured as a change in resistance relative to the change in voltage output from the loadcell. The bridge factor used for this channels was 4. This channel was used with an amplifier of DC 5V.

5.5.4 Deflection Measurements

The stroke from the ram could be read from the pod or the computer monitor as well as recorded by the data acquisition unit. The ram stroke was measured with a full bridge circuit on the UPM100 as this involved measuring the change in resistance relative to the change in voltage output from the ram LVDT. The bridge factor used for this channel was 4. The channel was calibrated with an appropriate gage factors 1.98 to measure up to a convenient accuracy of 0.001 inches. This channel was used with a DC 5V amplifier.

There was also an LVDT installed at the center of the beam to measure the mid span deflections. The LVDT was connected to the UPM 100 as an inductive half bridge circuit. The actuator stroke and the midspan LVDT measurement tallied with an accuracy of 0.05".

The LVDT took measurements in millimeters and was calibrated with a gage factor of 159.432. The deflections were measured to an accuracy of approximately 0.001 inches.

Measurements were also taken by measuring the vertical height from the floor to a mark made on the side of the beam at midspan. These measurements were taken at the beginning and end of every static test series. These measurements had an accuracy of ±1/16". These measurements could also give an estimate of the residual deflection that resulted after the completion of a certain number of cycles.

A pointer at a fixed height, pointing to a scale fixed vertically on the side of the beam was used to read deflections at every static load stage. These measurements had an accuracy of ±1/16" but could have included some visual errors. This measurement was used only as a check on the LVDT reading.

5.5.5 Crack Measurements

After each load increment, the beam was carefully checked for new and extending cracks, which were marked using magic markers on both faces of the beam. Crack widths were recorded for several cracks at different load stages with a 50 power hand microscope with an accuracy of 0.001".

5.5.6 Slip Readings

Ends of strands were exposed at one end of the beam. Dial gages accurate to 0.001" were attached to the beam end and their plungers made contact with the ends of the strands. The purpose of the dial gages was to record any movement in the gages that would indicate slip of the strands. These measurements were taken regularly during the test.

Since this was the first time the Structures laboratory of the University was being used, a lot of time was spent in the set up for the experiment and bring everything to function properly. It turned out to be the most challenging part of the entire project.

5.6 EXPERIMENT

5.6.1 Simulated Service Load

The bridge was designed for the HS-20 truck load and impact, the most severe loading for highway bridges as per the 1957 AASHO codes. This is the live load of maximum intensity for simple spans up to 140 feet. Spans longer than this experience critical conditions under lane loading. To study the behavior of the beam under varying moments (and loads), under both static and fatigue conditions, loads were applied to the beam at two points, 11 feet apart and symmetric about the centerline of the beam (Figure 5.5). This simulated an equivalent HS-20 truck loading in terms of causing moments in the beam equal to that caused by the actual truck loading. For example, a ram load of 20.75 kips, distributed into two 10.4 kips loads would simulate the current 1992 AASHTO truck loading, producing an identical maximum moment. This has been figuratively explained in Figure 5.6. The simulations of the front axle (wheels) was not considered because the effects on the results would have been negligible.

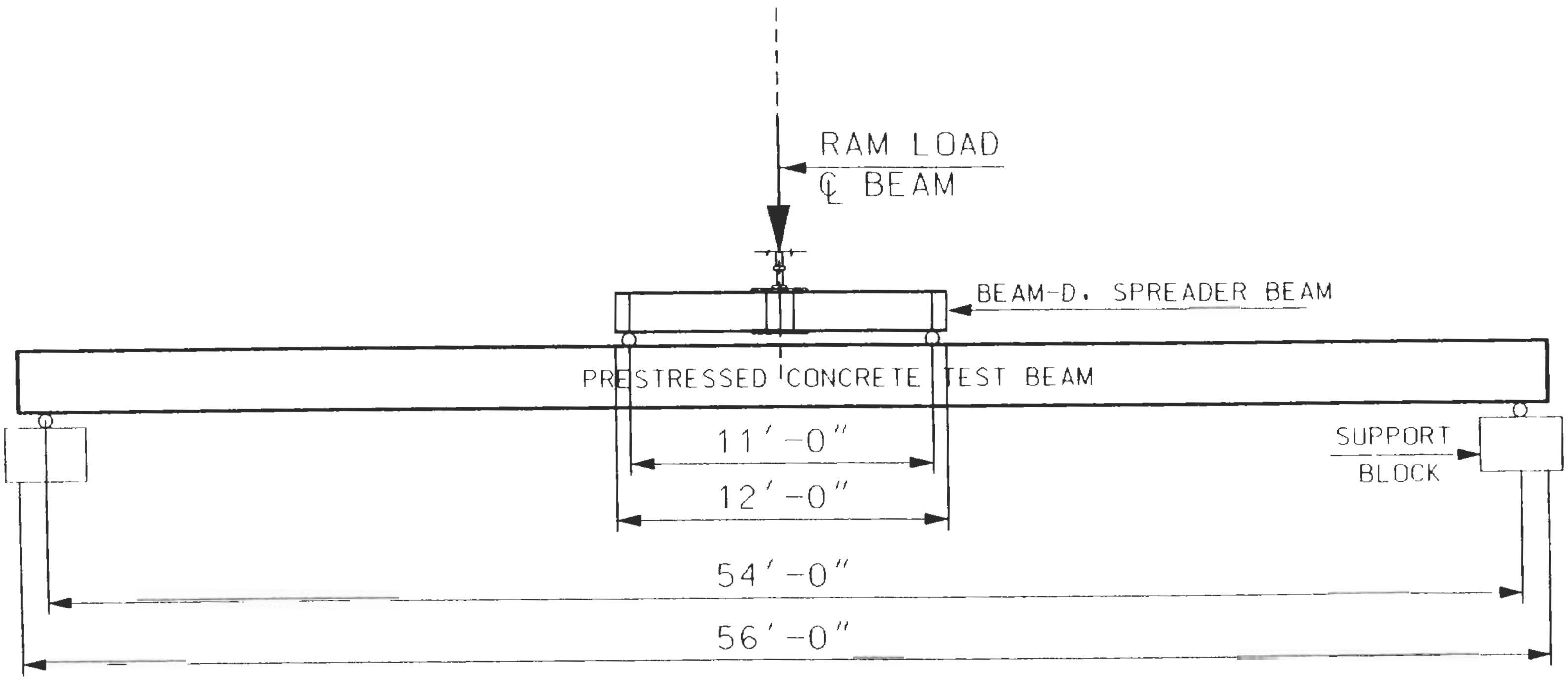

Figure 5.5 Loading for the Test

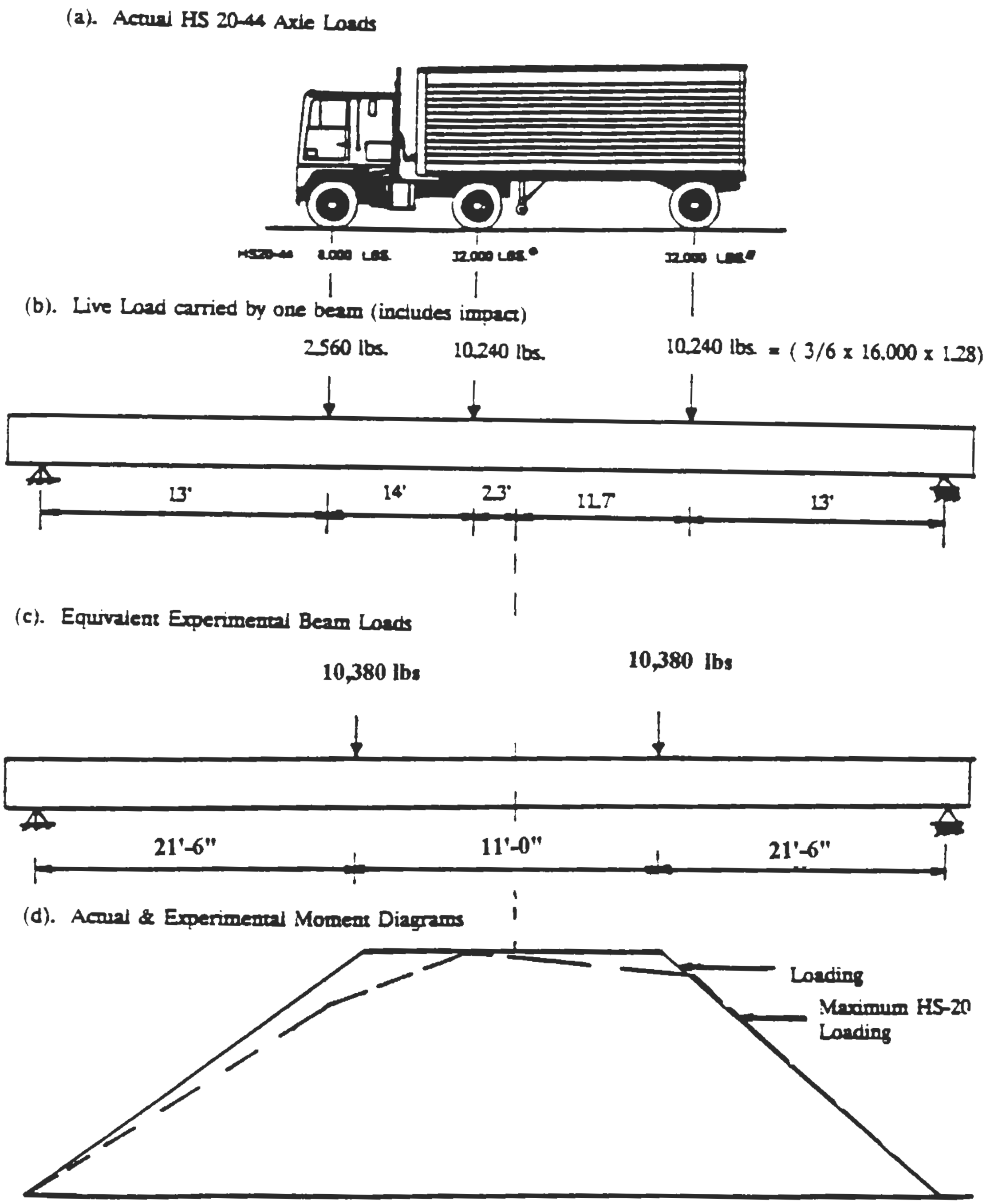

Figure 5.6 Equivalent HS-20 Loads

Due to the more conservative design methods of the 1957 AASHO specifications, these beams have excess capacity based on the 1992 specifications. Therefore, the following concepts were used to set the Dead Load and Live Load levels from the tests. The current 1992 AASHTO specifications allow a bottom fiber stress of $6\sqrt{f'_c}$ psi at maximum design loads. This would be the most severe service load condition that the beam would be expected to see. The beam with its self-weight and the load of the steel beam (Beam D) required an additional 41 kips of ram load to produce a bottom fiber stress of $6\sqrt{f'_c}$ at a moment of 709 kip-ft. The ultimate moment capacity of the beam, 1117 kip-ft, based on the beam section properties was used as the maximum strength at factored loads. These two conditions were used to calculate the live load and dead load moments the beam will be subjected to.

$$M_D + M_{LL+I} = 709 \text{ k-ft} \qquad \ldots\ldots \text{ based on } f_b = 6\sqrt{f'_c}$$

$$1.3(M_D + 1.67M_{LL+I}) = 1117 \text{ k-ft} \qquad \ldots\ldots \text{ based on } M_u = \Phi M_n$$

These simultaneous equations were solved to arrive at a ram load of approximately 20 kips to cause dead load moment, M_D. The ram load that caused a service load moment of $M_D + M_{LL+I}$ was 41 kips.

5.6.2 Experimental Determination of Effective Prestress

The stage of reopening of the cracks when the beam was reloaded after flexural cracking determined the effective prestress. This load stage can be identified as that which carries zero stress in the bottom fiber. The effective prestress in the member can then be calculated using statics. During the first static test for both the beams, after the beam was cracked, the beam was unloaded until the cracks completely closed. It was then reloaded at a slow rate during which the reopening of a prominent crack was observed using the microscope. The load causing the cracks to open to .001 inches was assumed as the load causing zero bottom fiber stress. The reading was taken thrice by each of the three observers.

5.7 SEQUENCE OF LOADS

Initially, a static test was done for both beams with loading beyond their cracking moment. A second static test was done next to observe the effects of a cracked section and the changes it would cause to the response of the beam. The beams were then tested under cyclic loading with intermediate static tests. Deflections, strains, crack widths etc. were monitored at different load stages for comparisons and to study the effects of repeated loads. Beam10 was tested first and Beam8 next. Their tests are discussed in detail in 5.7.1 and 5.7.2 and summarized in Tables 5.1 and 5.2.

5.7.1 Beam10

5.7.1.1 Static Testing

The beam was loaded statically up to a load of 55 kips at increments of approximately 5 kips. The ram was controlled with the pod and the loading was done using the *'stroke control'* mode allowing a uniform rate of increase of stroke. Using this mode rendered the convenience of maintaining a constant stroke while the loading was stopped at different load stages for recording data. Since the beam was expected to crack at 44 kips, the beam was inspected carefully for flexural cracks for ram loads from 35 kips and the loads were applied at smaller

TABLE 5.1 LOAD SEQUENCE FOR BEAM10

TEST ID	*LOAD CYCLES N*	*Load Range kips*
A	1	0-55 (S)
B	2	0-55 (S)
C	104003	20-41 (F)
D	104004	0-50 (S)
E	204004	20-41 (F)
F	204005	0-50 (S)
G	306005	20-41 (F)
H	306006	0-50 (S)
I	406006	20-41 (F)
J to T	909014	sequence repeated
U	1109014	20-41 (F)
V	1109015	0-50 (S)
W	1309015	20-41 (F)
X	1309016	0-50 (S)
Y	1509016	20-41 (F)
Z	1509017	0-73.8 (S)

Static tests are identified with an (S)
Fatigue tests are identified with an (F)

TABLE 5.2 LOAD SEQUENCE FOR BEAM8

TEST ID	***LOAD CYCLES N***	***Load Range kips***
AA	1	0-50 (S)
BB	2	0-50 (S)
C C	19252	20-50 (F)
DD	19253	0-50 (S)
EE	73903	20-50 (F)
FF	73904	0-50 (S)
GG	145098	20-50 (F)
HH	145099	0-50 (S)
II	250636	20-50 (F)
JJ	250637	0-50 (S)
KK	264188	20-50 (F)
LL	264189	0-55.69 (S)

Static tests are identified with an (S)
Fatigue tests are identified with an (F)

increments. The first flexural cracks were observed at approximately the predicted cracking load. A maximum load level of 55 kips was chosen for the last stage of loading as the stress level of 201 ksi in the strand at this load level as determined assuming a fully cracked section was below the yield strength of the strand. This load also was marked as being approximately 70% of its ultimate capacity. After loading up to 55 kips, the beam was unloaded in two stages and the immediate residual deflection was recorded. During later static tests (after cycles of fatigue loading), the maximum static load applied was only 50 kips. Static tests were done at the end of every 100,00 cycles initially but since there were very little effects observed, they were done thereafter at every 200,000 cycles.

5.7.1.2 Fatigue Testing

The beam was subjected to a total of over 1.5 million cycles between 20 kips and 41 kips, 41 kips being the load that causes a bottom fiber stress of $6\sqrt{f'_c}$ in the beam. This load level was chosen as the maximum that the beam in the bridge would be expected to carry. The lower limit of 20 kips was approximately the dead load and was approximately 50% of the service live load. The amplitude of loading (the range of loads), 21 kips was about 26.6% of the ultimate capacity or P_{ult}. The theoretical stress range in the strand assuming a complete cracked section, was expected to be close to 15 ksi or $0.06f_{pu}$, the limit stipulated by the ACI 215 committee report (1). Loads were cycled at the rate of one cycle per second (i.e. 1Hz) and the range of deflection was almost 1 inch. These results are summarized in Chapter 6.

The Teststar program was used to load the beam in a particular sequence. The operation was controlled by the *'load control'* mode. The beam was first loaded to the mean load level of the cyclic load range (35.5 kips in this case) at the rate of 5 kips per second. The cycling was then started at a frequency of 1 Hz. The test program was programmed to cycle for the required number of cycles (100,000 or 200,000 cycles). Cyclic loading terminated at the mean load level which subsequently unloaded to zero load. Figure 5.7 shows the loading sequence for beam 10. A test file for fatigue loading on Beam10 is shown in Appendix E.

5.7.1.3 Ultimate Test

The ultimate test was done at the end of over 1,500,000 cycles of loading at a constant load range of 21 kips between 20 kips and 41 kips of ram load. The loading was at approximate increments of 5 kips like all other static tests up to a load level of 65 kips and at 3 kips beyond that. The deflection was almost 4.6 inches and the ram stroke was 2.122 inches at this stage. During the later load increments, the measurements were recorded during the load increments to identify the exact load and stroke at which failure occurred. The beam was loaded till the deflection was 7.375" and the load at this stage was 73.8 kips. Our test equipment limited the maximum attainable deflection to 7.5 inches. This stage was very close to the stage for ultimate loads and the load-deflection curve had flattened. The supports for the concrete beam and the steel beam were observed closely during the entire experiment. The supports slid 1/2 inch at both ends at the final load stage relative to their position at the beginning of the test.

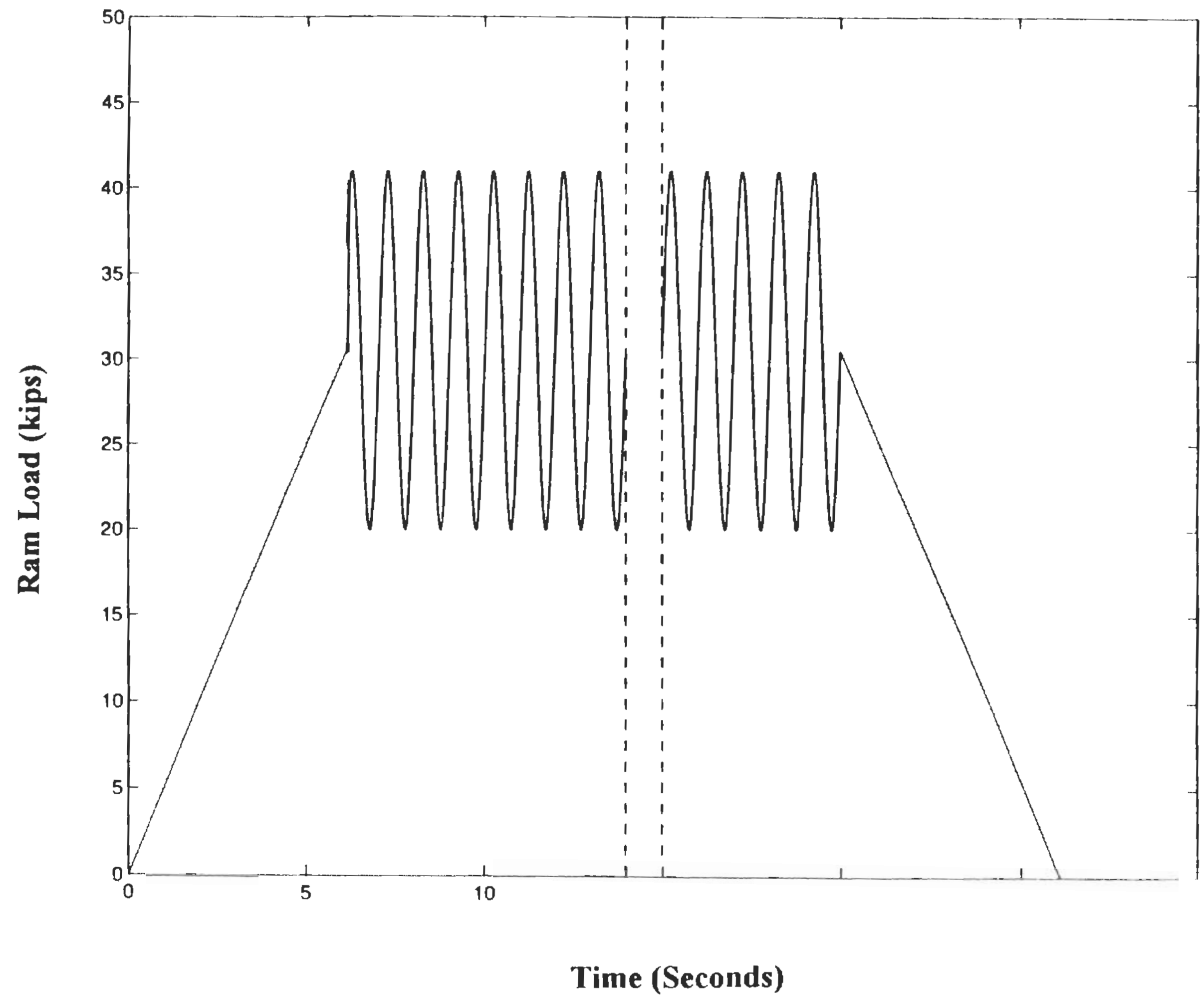

Figure 5.7 Fatigue Load Sequence for Beam 10

5.7.2 Beam 8

5.7.2.1 Static Testing

The static tests were identical to those performed for Beam10. However, the maximum load applied was 50 kips through out the tests. Intermediate static tests were not necessarily performed at the end a specific number of cycles. Instead, they were performed when a noticeable change in the behavior of the beam was observed under fatigue loading.

5.7.2.2 Fatigue Testing

Since Beam10 performed very well under severe conditions of fatigue loading, it was intended that Beam8 be loaded with larger loads. Ram loads were between 20 kips and 50 kips. 50 kips was the load causing maximum bottom fiber stresses of $9\sqrt{f'_c}$. The amplitude of loading, 30 kips was almost 38% of the ultimate capacity, P_{ult}. The expected stress range was 32 ksi, almost $0.12f_{pu}$ based on a complete cracked section analysis. The stress range at the beginning of the test was slightly lower than the predicted value. The frequency of loading was 0.66 Hz with a time period of 1.5 seconds. This beam was loaded to over 264,000 cycles. The fatigue load sequence for Beam8 is shown in Figure 5.8. A typical data file for Beam8 is shown in Appendix F.

5.7.2.3 Ultimate Test

The beam had experienced fracture in some of the wires of the strands before the ultimate test was performed for Beam8. It was therefore expected that it would not withstand the theoretical ultimate moment loads. At a load of 50 kips the beam deflected almost 3.3 inches.

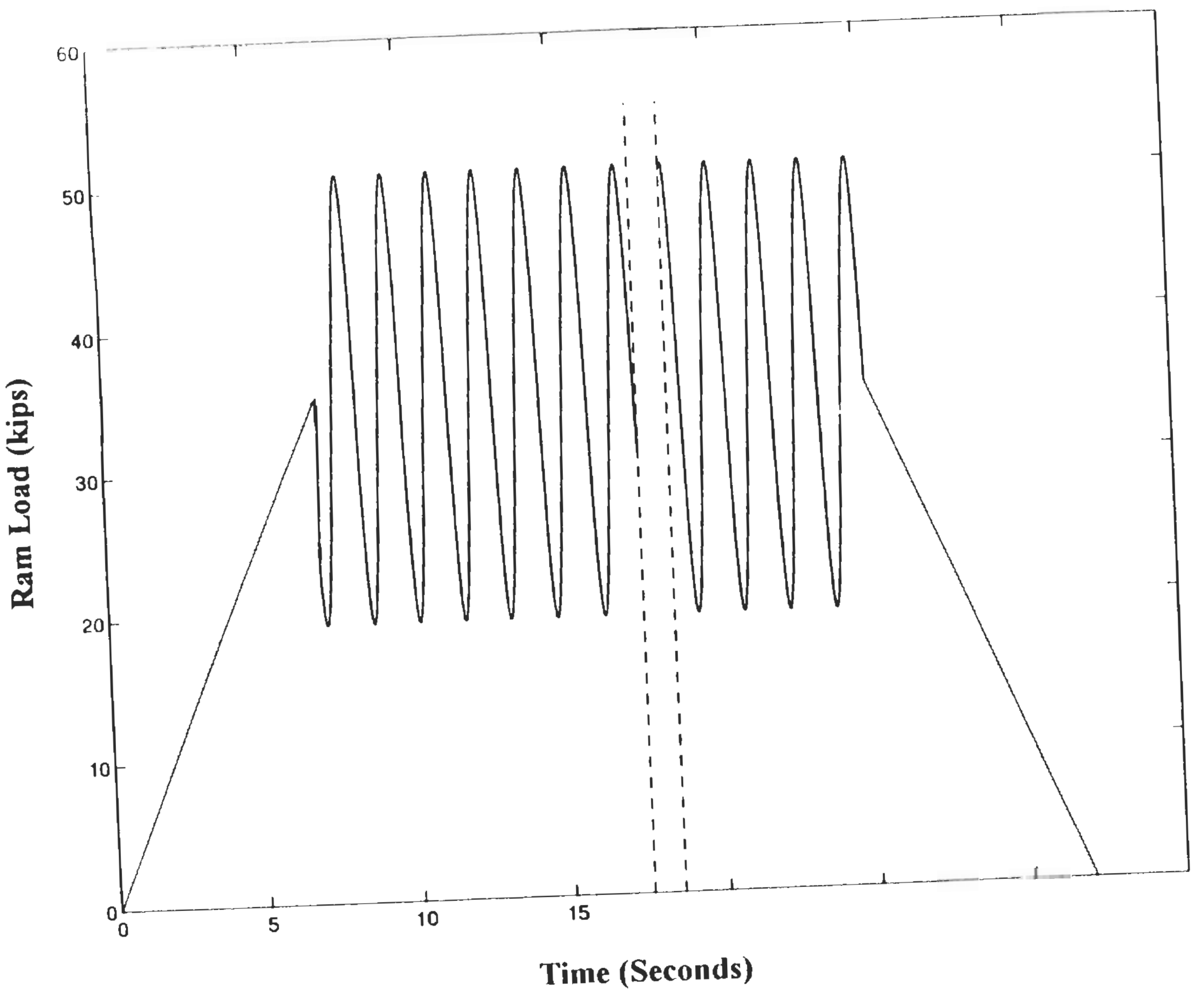

Figure 5.8 Fatigue Load Sequence for Beam 8

The beam was then loaded to 55 kips with strains being monitored during the loading. During the application of this load, the sound of one wire snapping was heard. The deflection now increased to 3.75 inches. An additional load of 1 kip was added which caused the breaking of two more wires and the deflection at this point was 4 inches. This marked the final stage of loading for this beam as it was obvious that further loading would result in the breaking of some more wires and a probable failure of the beam.

CHAPTER 6

RESULTS AND DISCUSSION

6.1 INTRODUCTION

The results of the tests on Beam10 and Beam8 were studied to compare and contrast differences in the trends in the deflection, strand stress, crack widths and other properties. Effects of fatigue loading and more particularly, effects of stress ranges chosen for cyclic loading were evident in the results obtained. Results of tests on both Beam10 and Beam8 shall be discussed. The pretest condition of the beams is described in Section 1.3.

Through out this chapter, the load magnitude will mean the load applied by the ram at the center of the beam. This load does not include the self-weight of the beam or the weight of the steel load spreader beam (identified as Beam D in Chapter 5). Therefore, the actual load applied at each point on the prestressed concrete beam is half of this load in addition to half the weight of the steel load spreader beam. All deflections are at the center of the beam with respect to the existing camber and not with respect to the absolute horizontal. All stresses are the resulting stresses in the strands due to all the loads acting on the beam at a particular stage including the prestress, the self weight, steel load spreader beam and the applied ram load.

6.2 GENERAL TEST RESULTS

Both beams during the first static tests behaved very close to the predicted response. The second static test exhibited the cracked behavior with steep increase in deflections, stresses and crack widths at the reopening of the cracks. The measured effective prestress for Beam10 was 159 ksi corresponding to a crack reopening load of 25.44 kips. This is the average of three different observers each taking three readings. The maximum and minimum readings differed by only 3.2 kips. The effective prestress for Beam8 was 164 ksi corresponding to a crack reopening load of 27.97 kips. These values were quite close to the value of 153 ksi determined in the previous research projects (31,32,33). All stresses calculated at different load stages were based on an effective prestress of 153 ksi.

Beam10, subjected to over 1.5 million cycles of loading between 20 and 41 kips performed very well and showed no serious signs of deterioration. On the other hand, Beam8 started showing signs of deterioration at 145,000 cycles. The first sound of a wire in a strand breaking in Beam8 was heard between 140,000 and 150,000 cycles. After 261,000 cycles, six more wires were heard failing and a total of 16 wires were heard breaking over the entire cycling. Testing continued even when no one was present to observe the beam. It is likely that more strands ruptured during that time.

6.3 LOAD DEFLECTION RESPONSE

6.3.1 Load-Deflection during initial static tests

The load-deflection responses of the beams were linear till the first cracking load and were very close to the predicted deflections at all load levels. The first cracks were noticed at a load level of 42 kips for Beam10 and at a load of 40 kips for Beam8 when the load-deflection curve showed a reduction in slope. The second static test was done immediately after the first static test before any fatigue loading was applied to see the influence of flexural cracks. The second load-deflection curve followed that of the first static test closely up to the stage when the cracks reopened, at about 25 kips. The curve became non-linear from about a load of 25 kips. Figure 6.1A and 6.1B show the load-deflection curves for the beams during different cycles. Those curves identified as '@ 1 cycle' and '@ 2 cycles' represent curves during the first and the second static test respectively.

6.3.2 Load-Deflection under fatigue

During intermediate static tests conducted after a certain number of cycles, deflections were checked during every load stage. The deflections got larger with additional fatigue load cycles for both beams. Beam10 during the first static test deflected 1.56 inches at a load of 50 kips. After an addition of 300,000 cycles, the load deflection curve still was close to the curve from the first static test and at a load of 50 kips Beam10 deflected 2.44 inches. At the end of 1,500,000 cycles, the residual deflection was 0.375 inches and the deflection at 50 kips was 2.62 inches, 1.06 inches larger than at the first static test. Between 100,000 cycles and 1,500,000 cycles, the response did not change much. Figure 6.1A shows the load-deflection curves of the beam under different cycles of loading (between 20 and 41 kips).

Beam8, subjected to a far more severe loading range (between 20 and 50 kips)

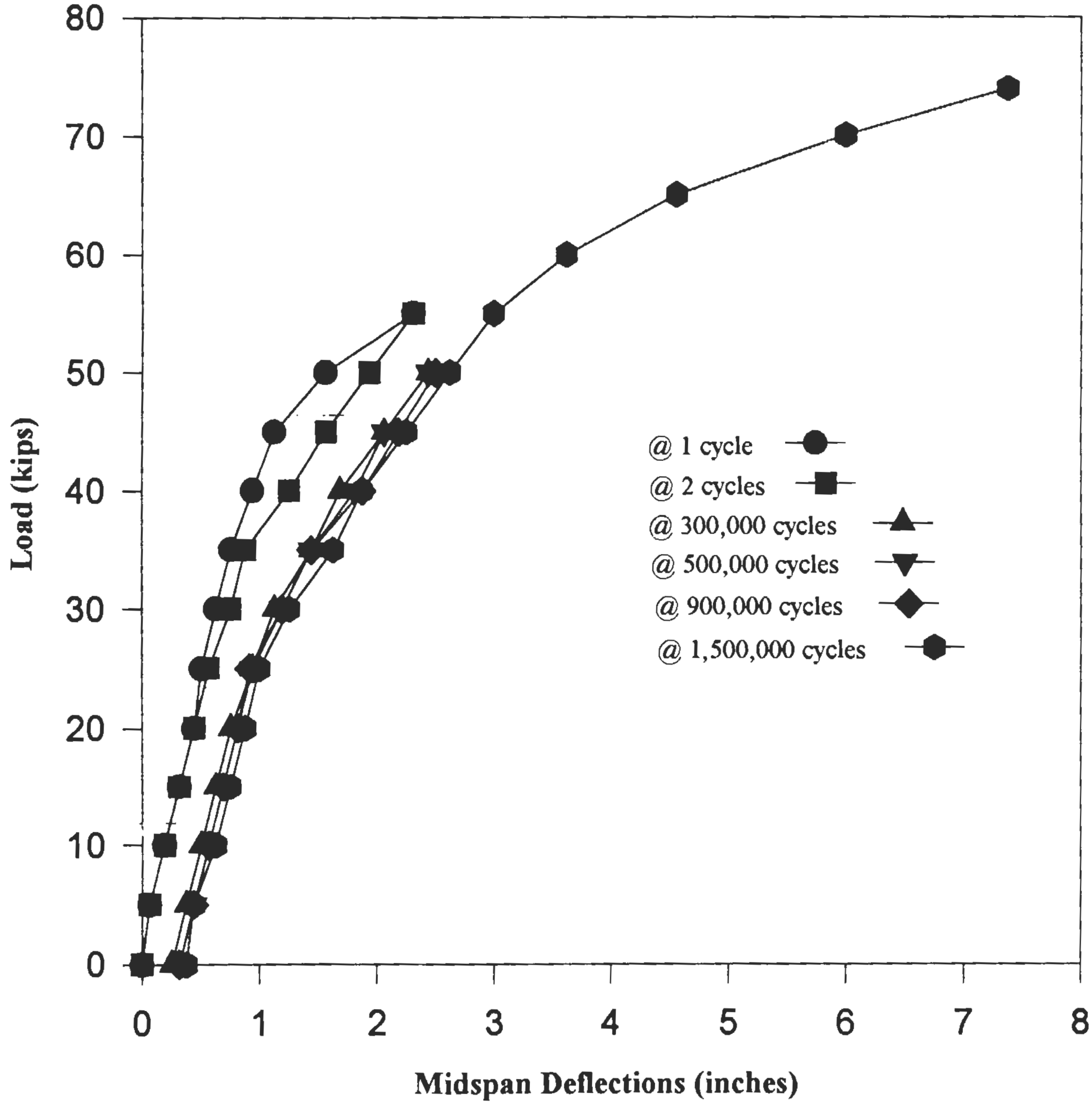

Figure 6.1A Load-Deflection Curve for Beam10

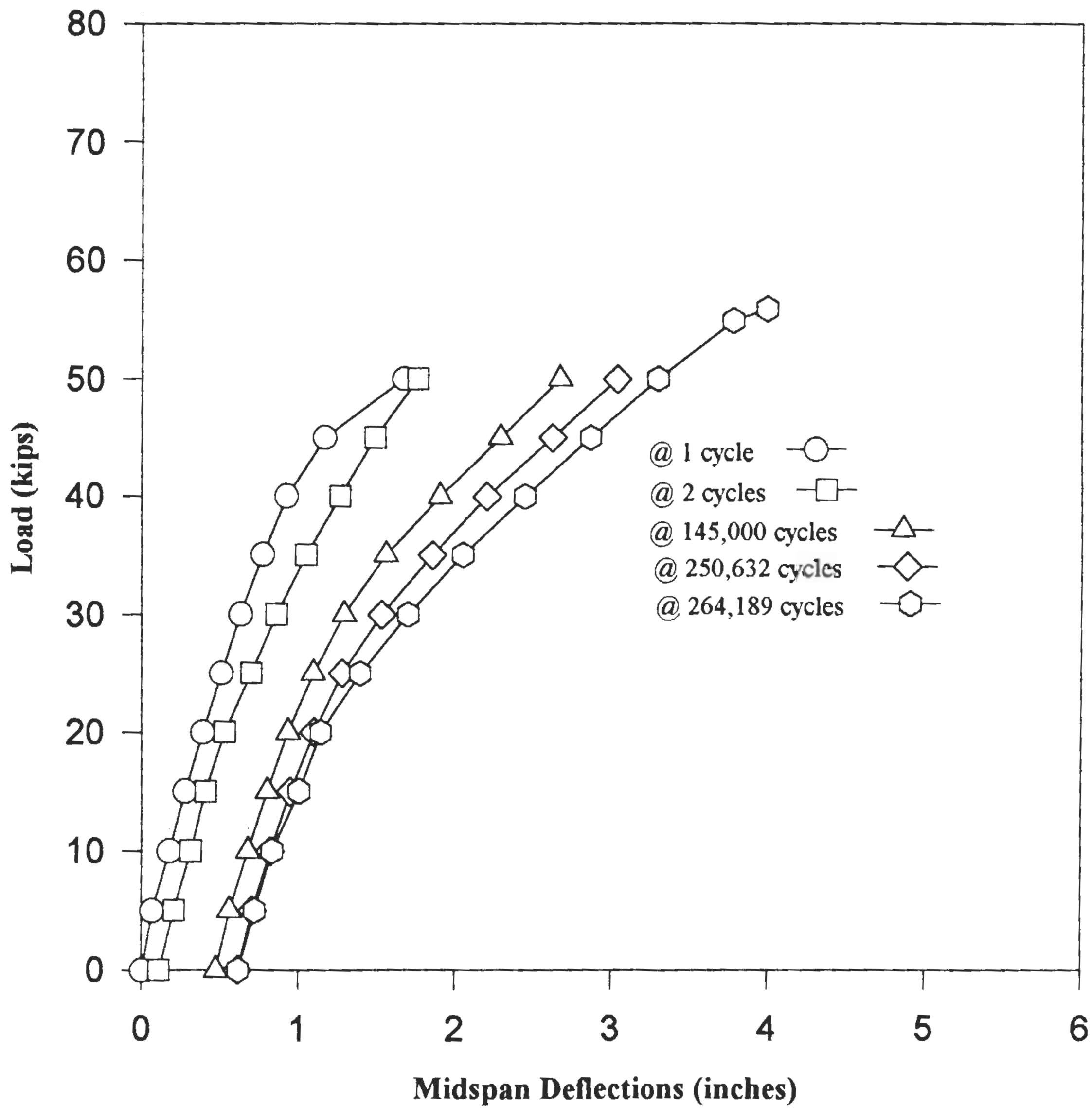

Figure 6.1B Load-Deflection Curve for Beam8

showed signs of distress after about 145,000 cycles of loading. The deflection at 50 kips during the first static test was 1.67 inches. At 145,000 cycles, the deflection at the same load level was 2.67 inches. By the end of 264,000 cycles, the residual deflection was 0.614 inches and at a load of 50 kips the beam deflected 3.30 inches. By this stage the beam had experienced a failure of at least 16 strands, say equivalent to two complete strands with respect to its steel and prestress capacities. Figure 6.1B shows the load-deflections trends in the beam at different cycles of loading.

Beam10 performed far better than Beam8. A comparison of the load-deflection curves of both beams, shown in Figure 6.1C, established that the response of Beam10 at the end of 1.5 million cycles was very close to the behavior of Beam8 at the end of 145,000 cycles. Beam10 showed ductile behavior during the last static tests. Beam8 certainly lost its resistance to large deflections. Figure 6.1D shows the deflections at particular load levels (20 kips, 30 kips, 40 kips and 50 kips) at different number of cycles for Beam10, and similarly in Figure 6.1E for Beam8. Figure 6.1F shows a comparison of the response of Beam10 and Beam8 at different number of cycles. Figure 6.1G shows the residual deflections retained by the beams at different cycles. The adversity of the effects of fatigue loads in the higher range is clearly seen.

6.3.3 Deflections during the ultimate tests

The ultimate tests were performed after the completion of over 1.5 million cycles of loading between 20 and 41 kips for Beam10 and over 264,000 cycles between 20 and 50 kips for

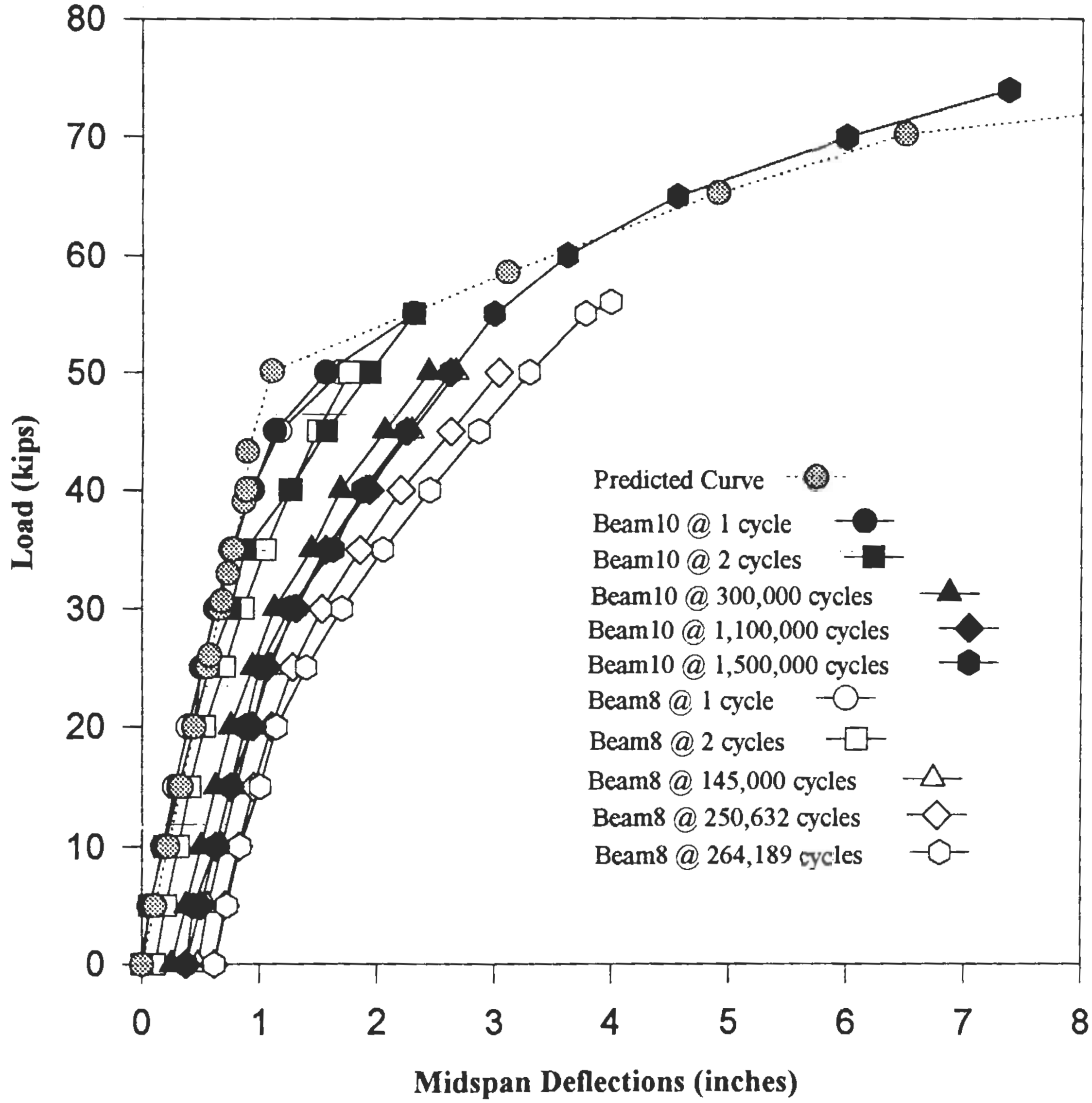

Figure 6.1C Load-Deflection Curve for both Beams

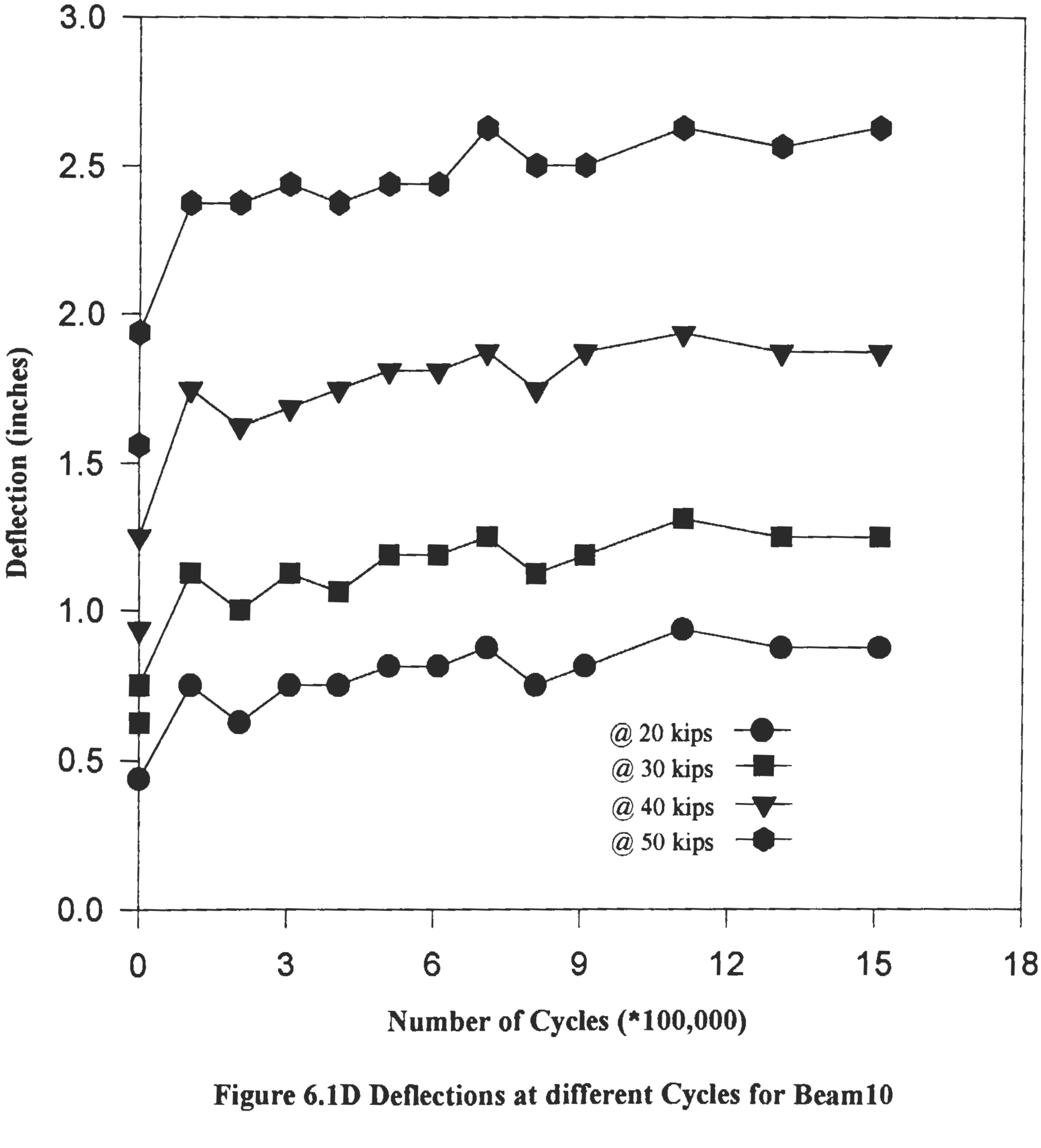

Figure 6.1D Deflections at different Cycles for Beam10

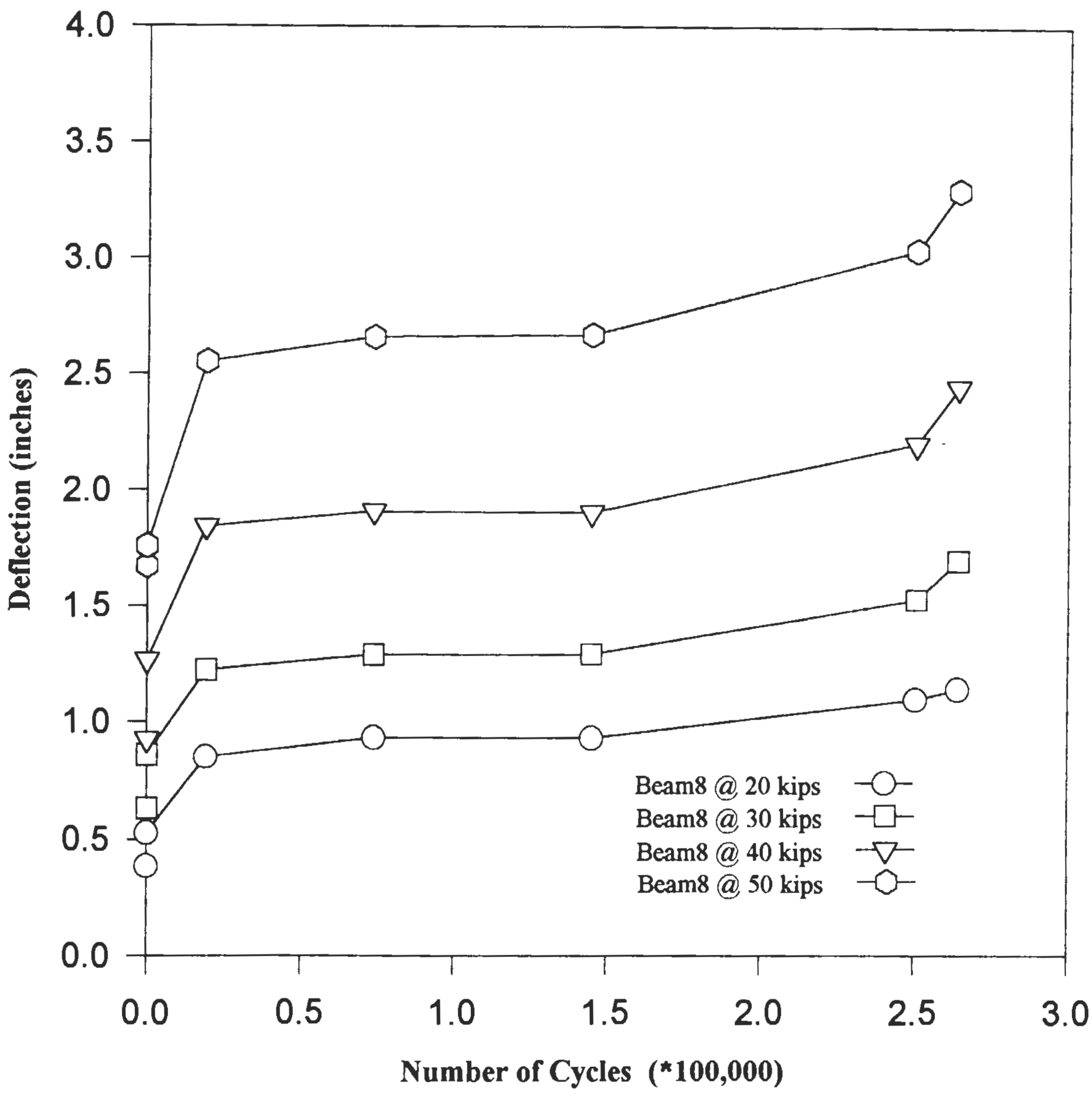

Figure 6.1E Deflections at different Cycles for Beam8

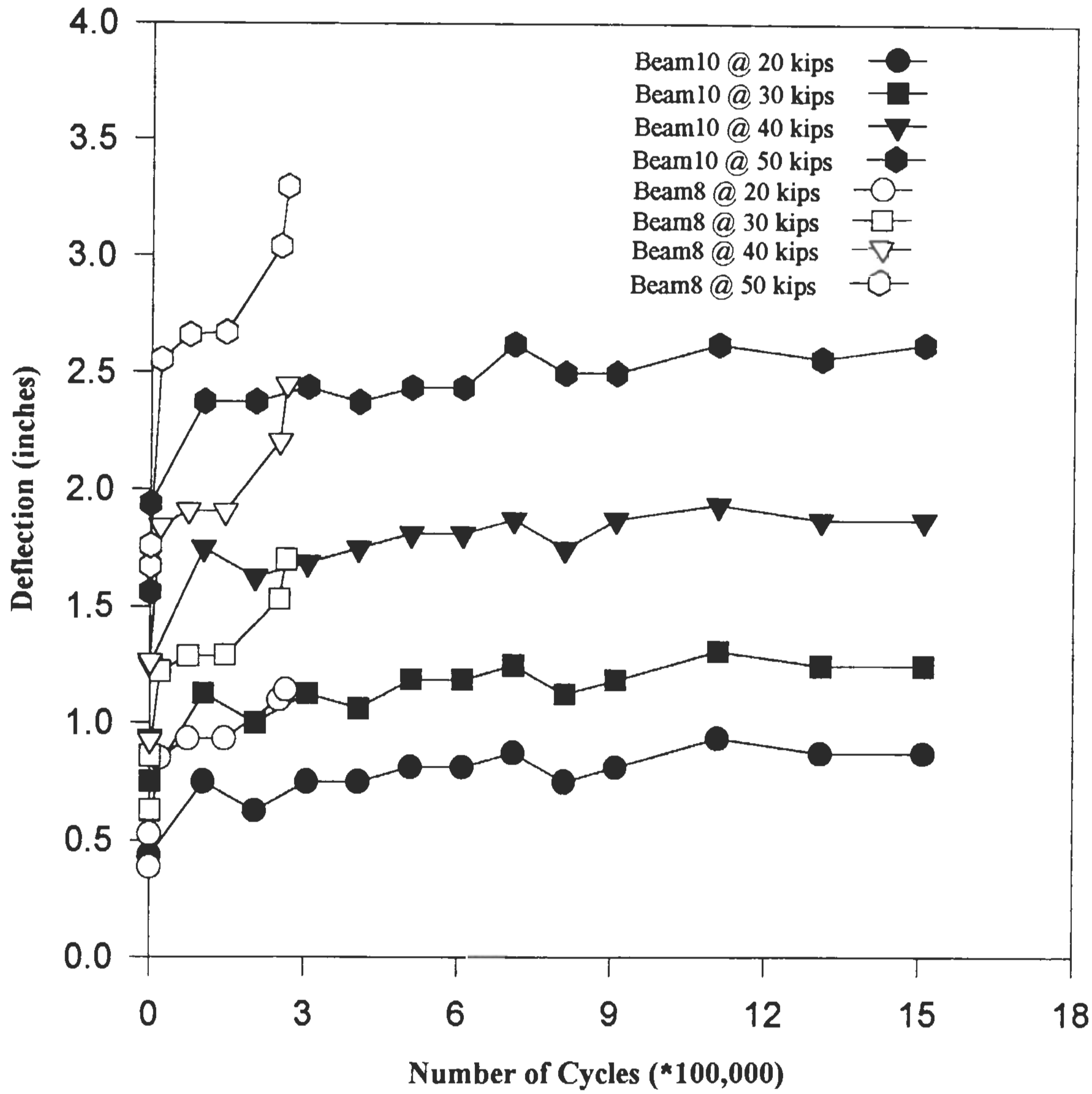

Figure 6.1F Deflections at different Cycles for the Beams

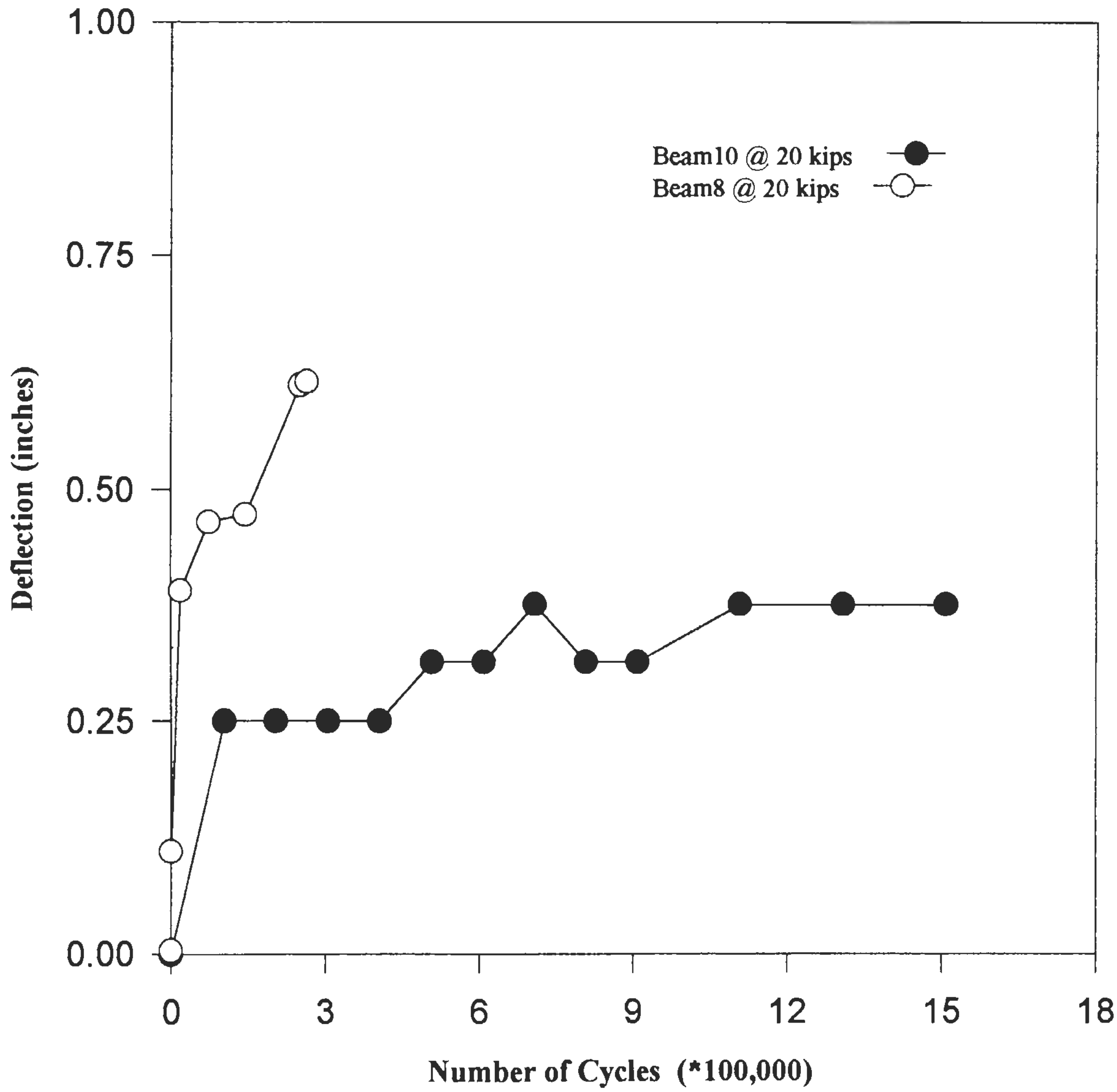

Figure 6.1G Residual Deflections for the Beams

Beam8. Beam8 had experienced failure of some wires in the strands before the ultimate test was performed.

Beam10 showed the same response to a load of 50 kips as the previous static tests did. The curve had a decreased slope after the crack reopening load of about 25 kips. The beam was loaded to 74 kips and deflected up to 7.375 inches. The beam did not show any signs of failure even at this stage and additional loads were not applied because of the stroke limitations of the ram. Figure 6.1H shows Beam10 deflected to 7.375 inches during the ultimate test. The predicted ultimate capacity was 79 kips at a deflection of 23.2 inches. It was concluded that Beam10 was extremely ductile as desired in bridge structures.

Beam8 followed a load-deflection response very different from its previous tests. At a load level of 50 kips, it deflected 3.3 inches and addition of further load caused further breaking of wires. At the maximum load of 56 kips, the largest deflection was 4 inches. Beam10 had reached the same deflection at between 60 and 65 kips. Figures 6.1A, 6.1B and 6.1C show the load deflection curves during their ultimate tests.

6.4 STRESSES IN PRESTRESSING STRANDS

Stresses in the strands were calculated from the strains measured in the strands. The stress in the strand due to the assumed effective prestress of 153 ksi, self weight and the weight of the steel beam was 156 ksi. This was the stress level at which the gages were tared and this corresponded to a strain level of 0.006283 in/in based on the measured stress strain curve of

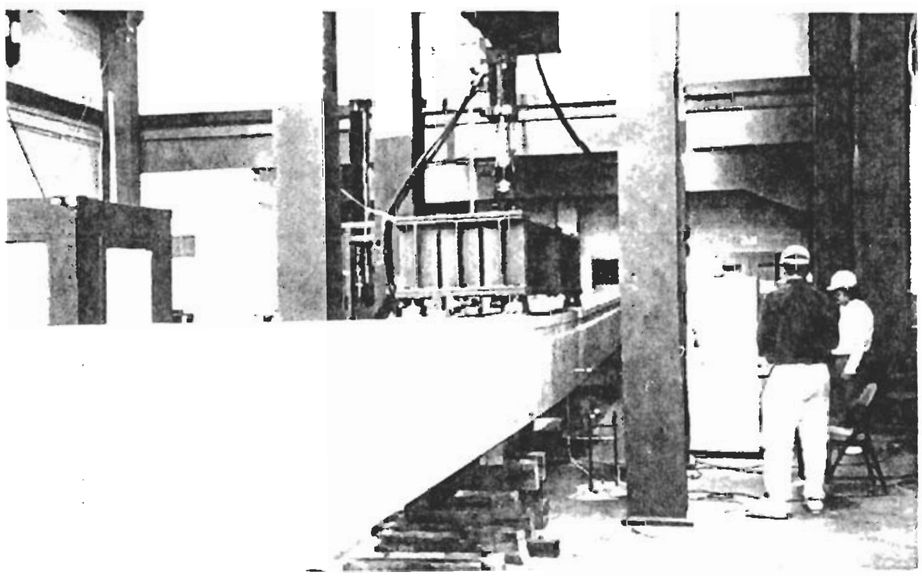

Figure 6.1H Beam10 During the Ultimate Test

the strands. Additional strains measured in the strands due to applied loads were added to this strain and the stresses were determined from the stress-strain curve for the strands shown in Figure 3.1. There might have been errors in reading the stresses accurately from the graph for a certain level of strain. Also, the cracks might not have occurred at same locations where the gages were attached. However, the difference in stresses would be very small especially at higher stress values and near ultimate load.

6.4.1 Stresses during the initial static tests

The stress response was linear up to the appearance of the first flexural cracks after which the rate of increase of stress in the strands increased as the load carried in tension by the concrete was transferred to the prestressing steel. The load vs. stress curves is shown in Figure 6.2A for Beam10 and in Figure 6.2B for Beam8. Beam10 was loaded to 55 kips and Beam8 to 50 kips. The beams were tested again under static conditions after the first static tests. The beams were now cracked and the stress response was non-linear beyond the crack reopening stage. This is very evident in the plots showing the response of the beams in the curves identified as '@ 2 cycles'. At a load of 50 kips, the stress in the strands were 182 ksi and 188 ksi for Beam10 and 189.42 ksi and 190.61 ksi for Beam8 during the first and second static tests respectively. The stresses were within the elastic limit of the strands.

6.4.2 Stresses under fatigue

The load-stress response of the beams were very similar to the load-deflection response as seen by comparing the plots. The stress in the strands increased with additional cycles. The

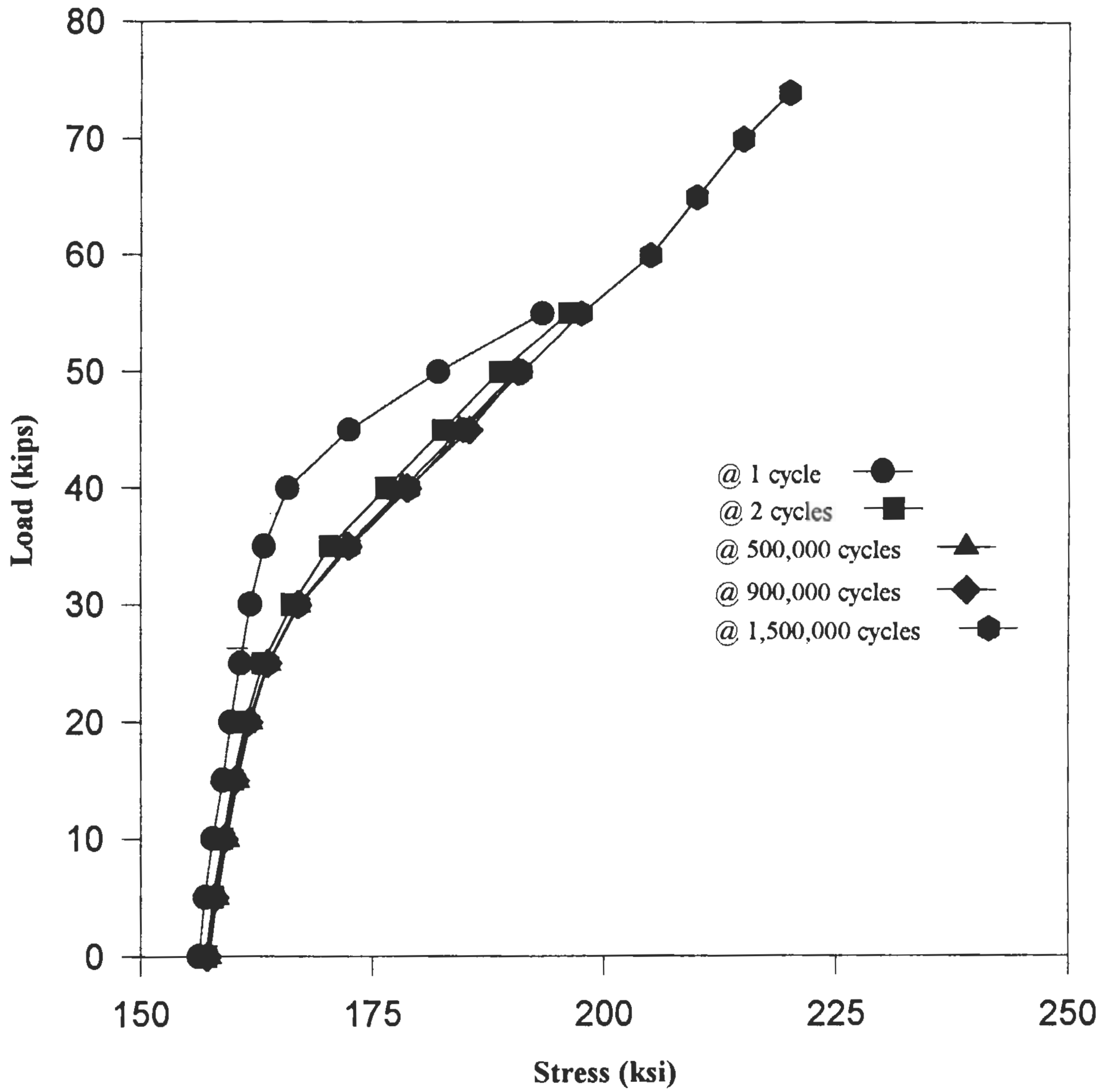

Figure 6.2A Stresses in Beam10

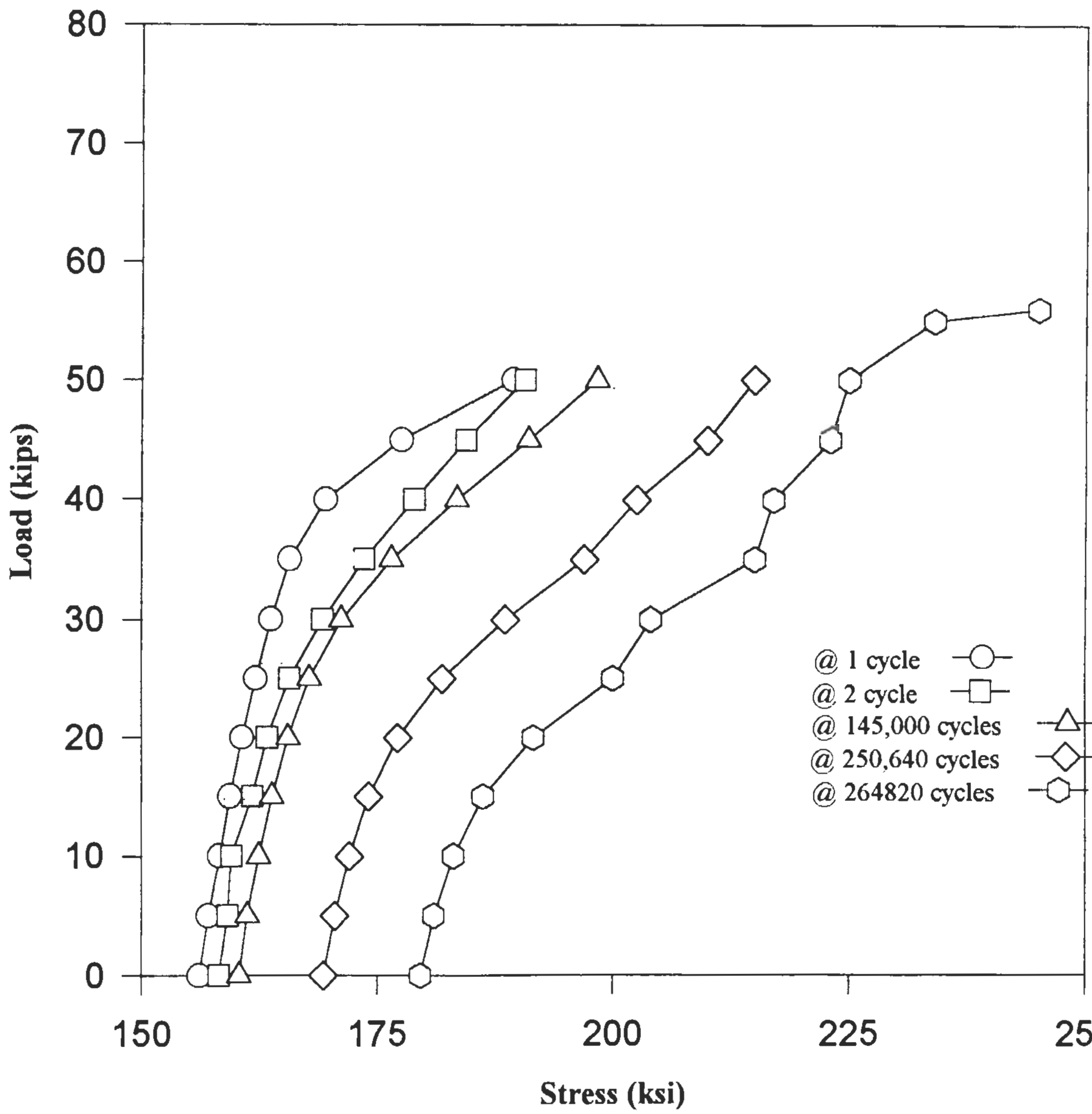

Figure 6.2B Stresses in Beam8

stresses did not experience large changes in Beam10 in a general sense. The stress at 50 kips at the end of 300,000 cycles was 190 ksi with a residual stress of 157 ksi, 0.72 ksi larger than when the first static test was done. At the end of 1.5 million cycles, the residual stress was still approximately 157 ksi and the stress at 50 kips was 191 ksi, 9 ksi larger than at the first static test. This amount of increase in stress levels can probably be considered normal, especially if the loading is equivalent to what a structure is expected to bear over its entire life.

Beam8 underwent very large changes in stress levels as a result of cycling. At a load of 50 kips, the stress level was 199 .6 ksi at the end of 20,000 cycles, 10.18 ksi more than during the first static test. At this stage the residual stress had increased to 160.46 ksi, an increase of over 3 ksi. By the end of 264,000 cycles, since a few strands were ruptured and the beam had actually failed, the stresses in the strands were in the non-linear range of the material at higher loads. The residual stress in the strands was 180 ksi and the stress at 50 kips was 225 ksi. The strands were in the non-linear range above a load of 25 kips. Figure 6.2C compares the stress response of both beams. Figure 6.2D shows the stress variations at 20, 30, 40 and 50 kips at different cycles for both beams. Figure 6.2E shows the residual stresses at zero applied load in the beams through out the tests.

6.4.3 Stresses in the Ultimate Tests

At the end of 1.5 million cycles, Beam10 showed the same response till a load level of 50 kips with a non-linear response above a load of about 25 kips. The beam was loaded at a slower rate from then on and the stresses increased at a sharp rate. The stress at the final load stage

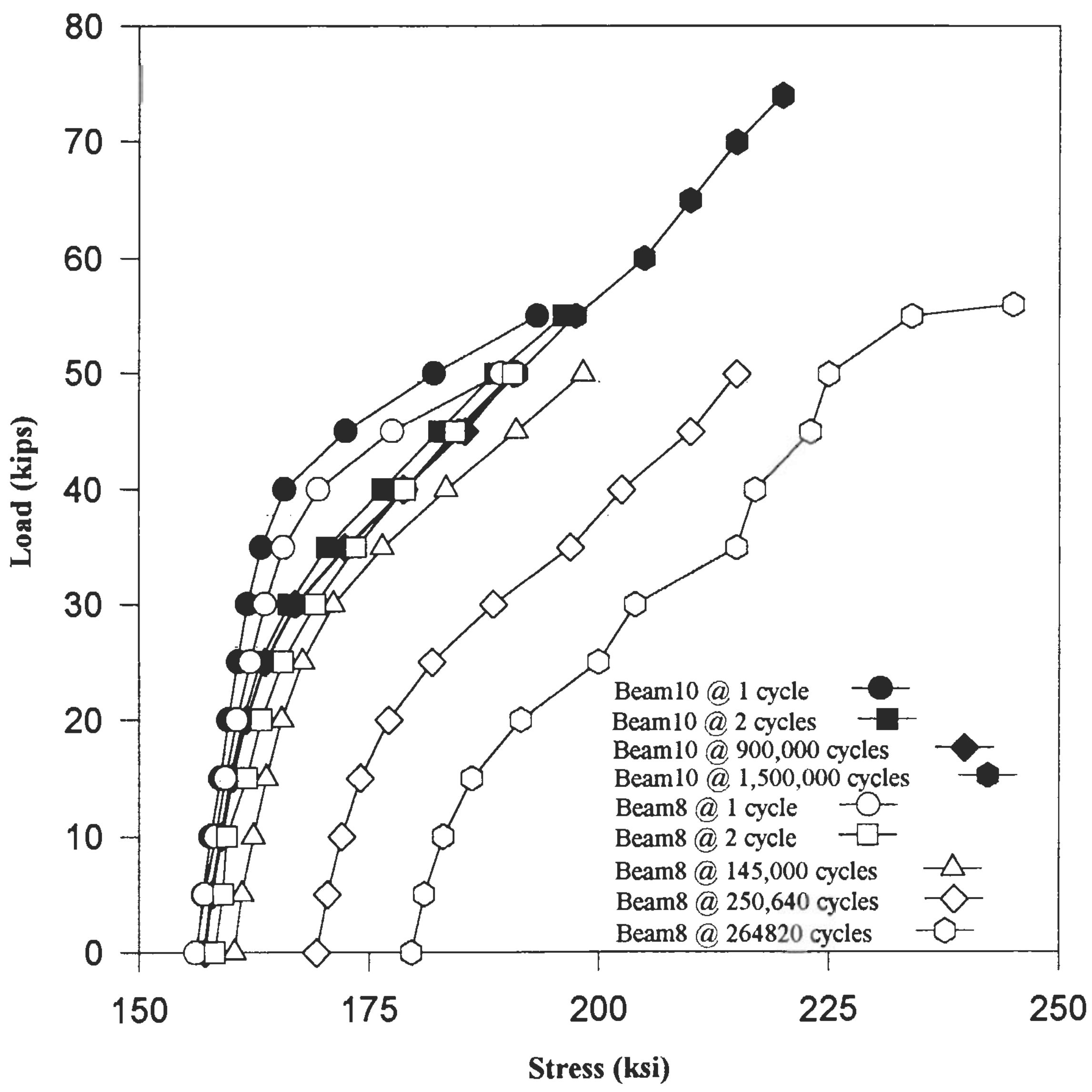

Figure 6.2C Stresses in Beams

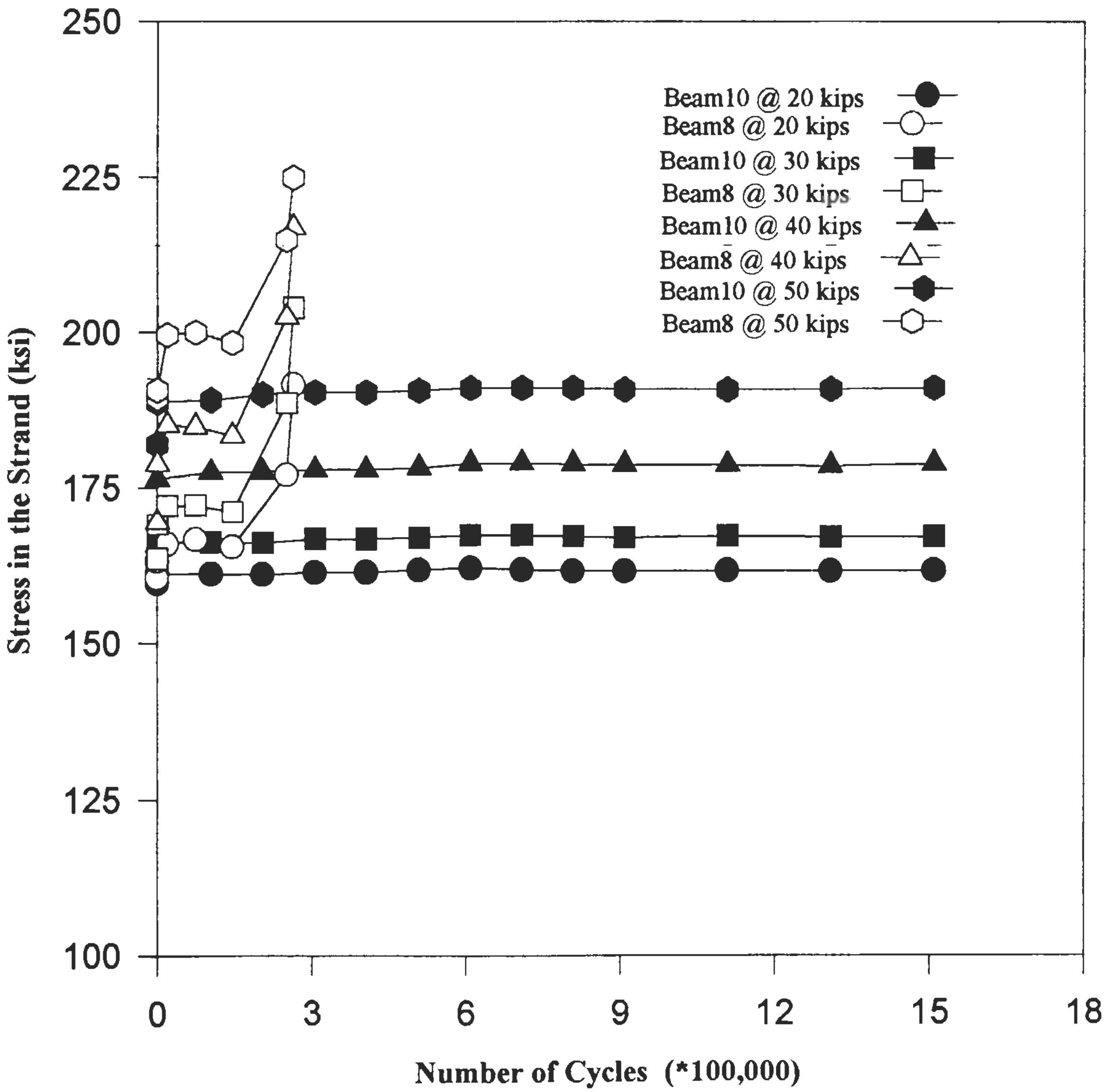

Figure 6.2D Stresses in Strands at different Cycles

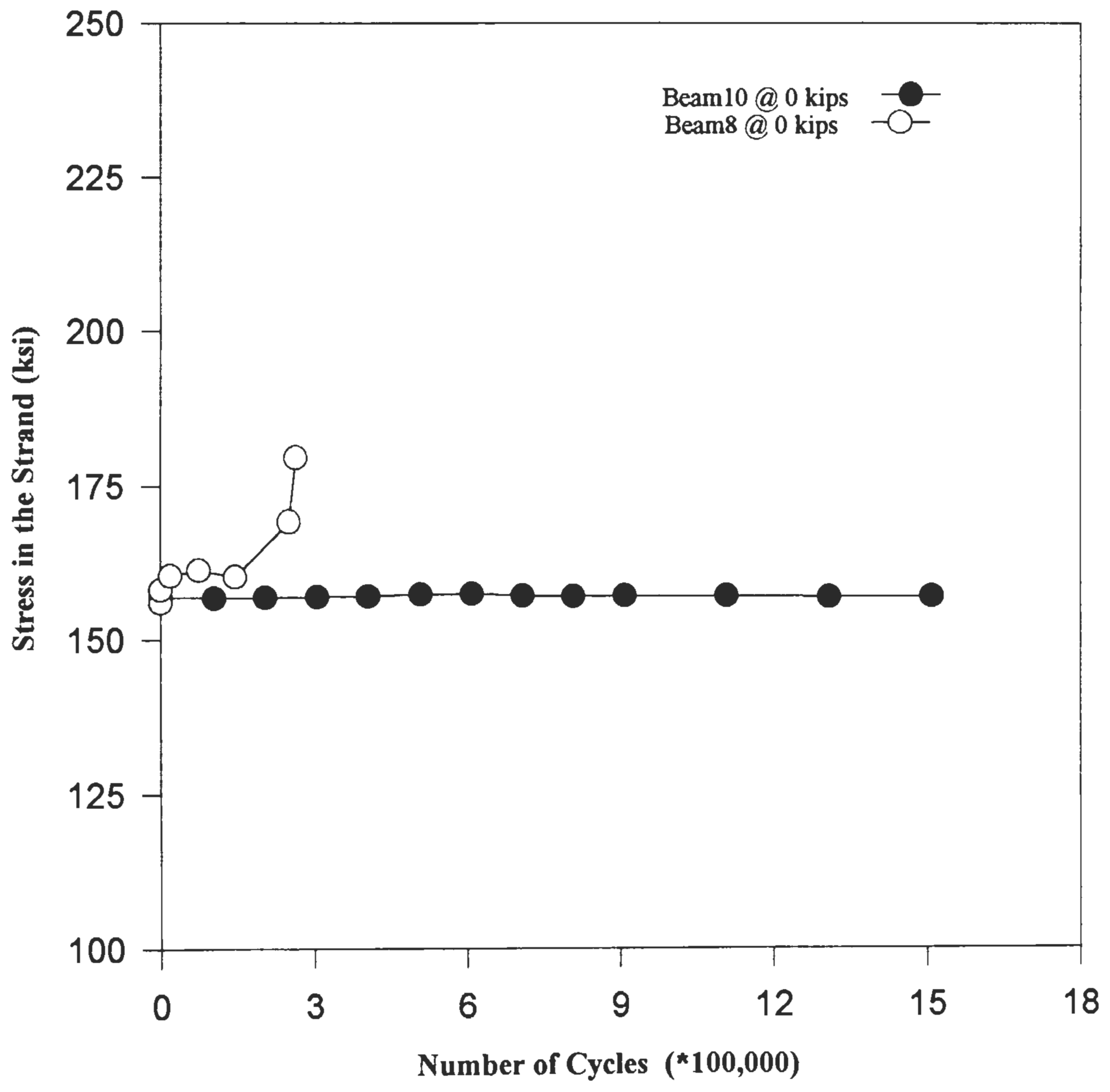

Figure 6.2E Residual Stresses in Strands

of 74 kips was 220 ksi. This level of stress is well below the breaking strength of 263 ksi based on the nominal strand area explaining why the beam had not failed even under the severe loading it was subjected to.

Several wires had ruptured during the tests in Beam8. The stresses became non-linear above a load of 15 kips and the stress level at a load of 45 kips was 223 ksi which was more than the stress in the strands at the ultimate load of 74 kips in Beam10. Strands were heard breaking more frequently beyond this stage. The beam was loaded to 56 kips and the stress at the final stage was 245 ksi, closer to the breaking strength of the strand. Figures 6.2A, 6.2B and 6.2C show the stress variations in the strands during the ultimate tests.

6.4.4 Stress Ranges

The stress ranges were expected to increase with the number of cycles. The stress ranges varied in the same manner that the deflections and stresses did; minor changes in Beam10 and drastic changes in Beam8. Beam10, loaded between 20 and 41 kips, had a stress range of 16.42 ksi, $0.062f_{pu}$ at the beginning of testing and by the end of 1.5 million cycles the range had only increased to 18.5 ksi on one of the gages. The measurements were very close to these values on the other gages too. The increase in stress range was about 2.08 ksi or $0.008f_{pu}$. Figure 6.2F shows the S-N curve for two typical strands in Beam10 when loaded between 20 and 41 kips.

The stress range in Beam8 when loaded between 20 and 50 kips was 28.81 ksi,

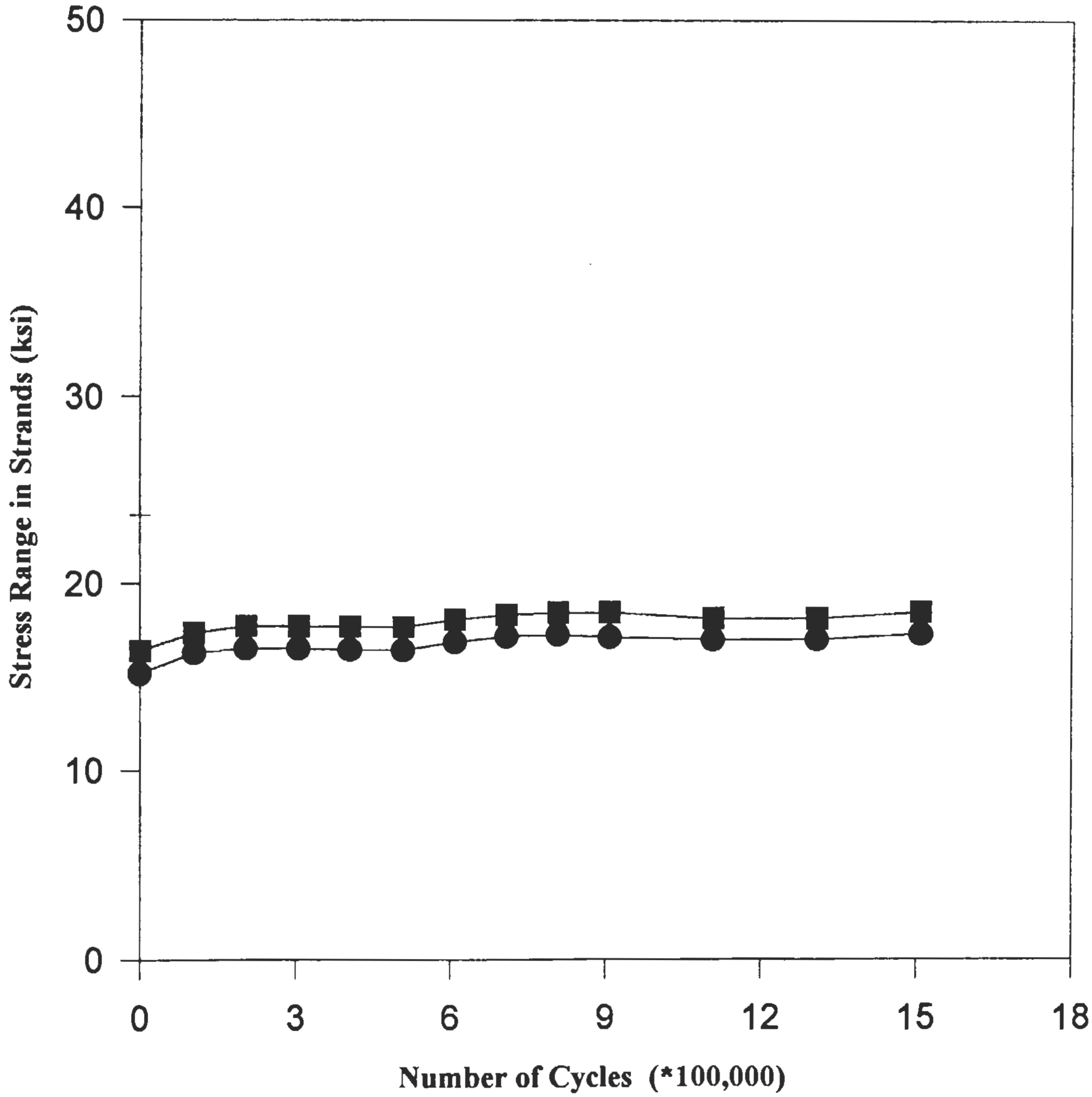

Figure 6.2F Typical Stress Ranges in Two Strands for Beam10

$0.11f_{pu}$ at the beginning of the test. At the end of the 264,000 cycles, the range had increased to 38 ksi, $0.144f_{pu}$ an increase of 32% or 9.29 ksi or $0.035f_{pu}$. An increase in the stress range of 4.89 ksi had occurred within the first 20,000 cycles and shows that the effects of loading to high stresses can be of significant detriment to a structure. Figure 6.2G shows the stress range in Beam8 through all the cycles when loaded between 20 and 50 kips. Figure 6.2H compares the stress ranges in both beams at different cycles. Notice that when comparing both beams at the same load range, 20-41 kips, the stress range for Beam8 is significantly higher than that for Beam10. Obviously, not too many cycles of overload are needed to cause significant increases in the stress range at normal load levels.

6.5 CRACK WIDTHS

6.5.1 Crack widths during initial static tests

When the first static tests were done, after a load of 30 kips, the beams were carefully observed for cracks in the maximum moment regions. The loading was done in small increments in order to determine the exact cracking load. The first flexural cracks were clearly seen through the microscope at a load of 42 kips in Beam10 and 40 kips for Beam8. Each load increment caused an increase in crack width or extension of the crack. The crack widths of several major cracks were read through out the tests.

On unloading, the cracks closed but did not appear to close completely. This can be attributed to the irregularities in the concrete. During the second static test, the cracks were observed to reopen between 25 and 30 kips when observed on the sides of the beams. When

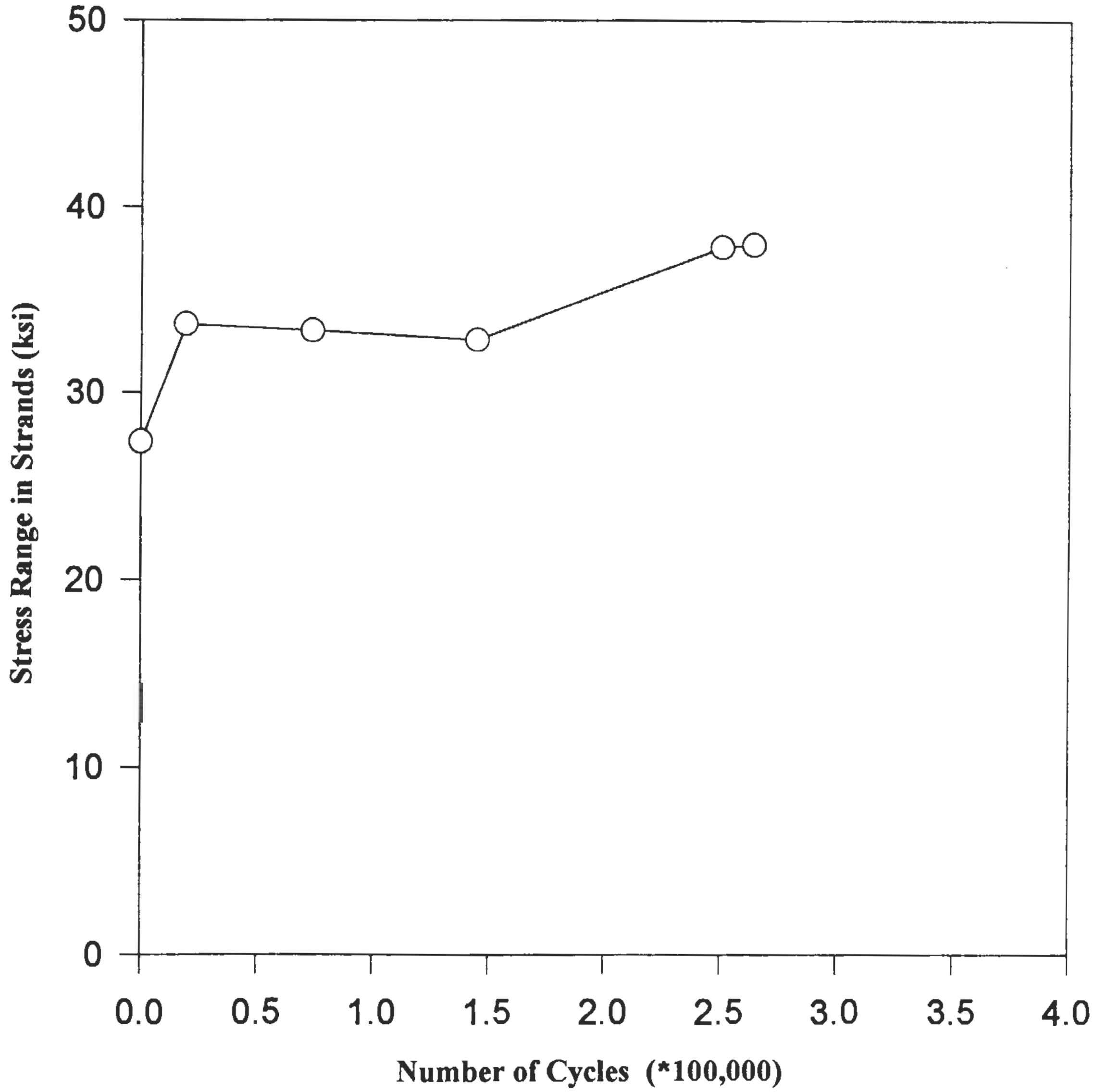

Figure 6.2G Typical Stress Ranges in Strands for Beam8

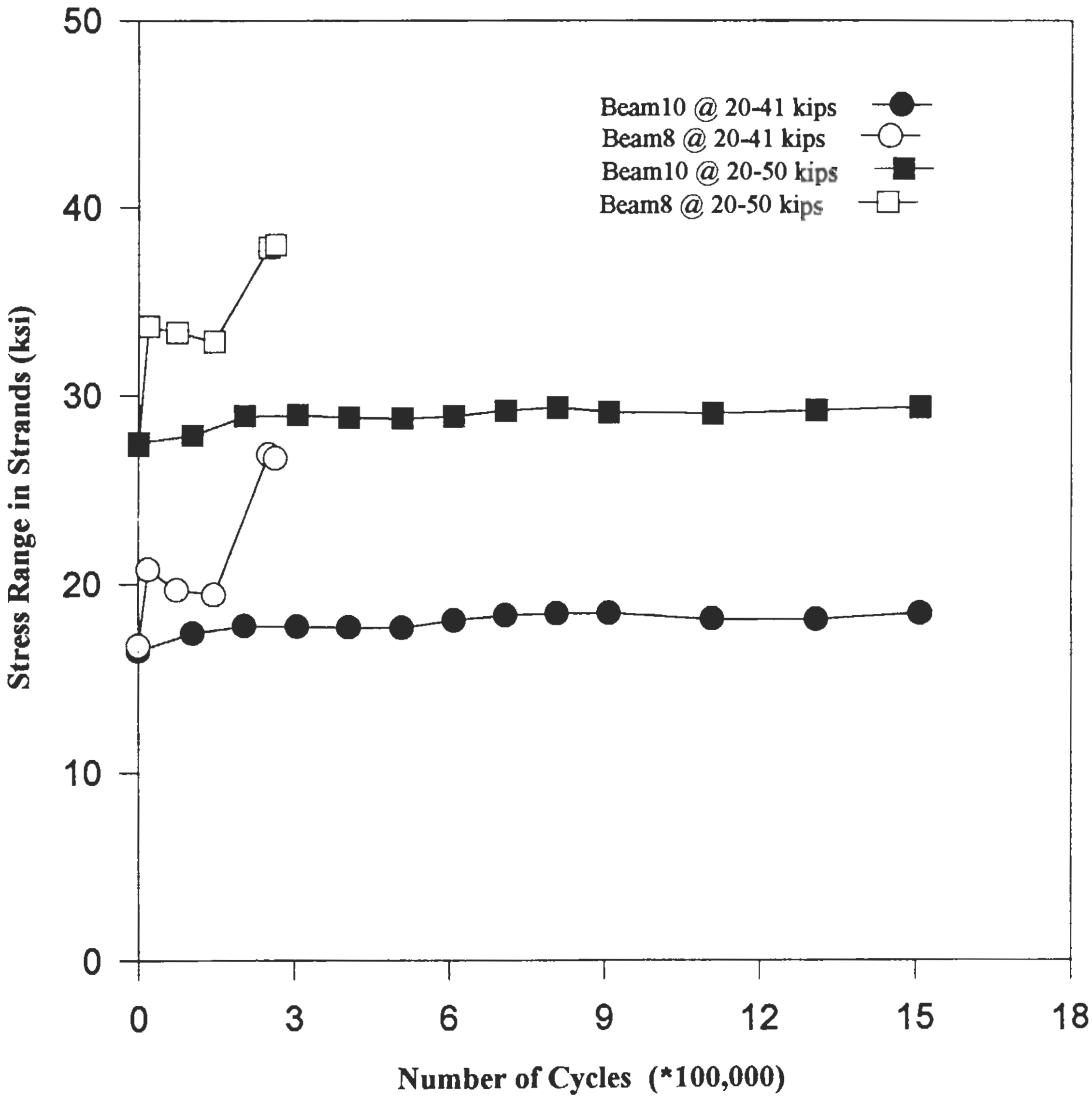

Figure 6.2H Comparision of Stress Ranges in Strands

observed on the bottom surface of the beam to determine the effective prestress, they could be seen to be reopening at slightly lower load levels.

6.5.2 Crack widths under fatigue

The crack widths increased due to the applied fatigue loads. In Beam10 the crack width at 50 kips increased from 0.009 inches during the first static test to 0.015 inches after the 1.5 million cycles of loading between 20 and 41 kips. Beam8 had larger cracks due to the greater effects of fatigue loads applied between 20 and 50 kips. The crack width at 50 kips during the first static test was 0.011 inches and at the end of 264,000 cycles, the width had increased to about 0.032 inches, an increase by nearly 300%. Figure 6.3A and 6.3B show the widths of two cracks, identified as CrackB and CrackE for Beam10. Figure 6.3C shows the crack widths for a crack Beam8. Figure 6.3D serves as a good comparison between the two beams and it can be inferred that the crack widths become undesirable under conditions that Beam8 was subjected to. Figure 6.3E shows the crack widths at different loads over the entire tests for the two beams. The crack widths were not measured at ultimate loads for safety reasons.

The cracks were monitored during the test. Cycling caused some extensions in cracks and some new cracks formed. No new cracks were found in the end regions as the moments in these regions remained below the cracking moment. Fatigue did not cause the cracks to become inclined nor cause shear failure. During the ultimate tests, the cracks were seen extending further into the top flange of the beam. Figures 6.4A and 6.4B show the crack patterns on the east and west sides of Beam10. Figure 6.4C shows a magnified view of the

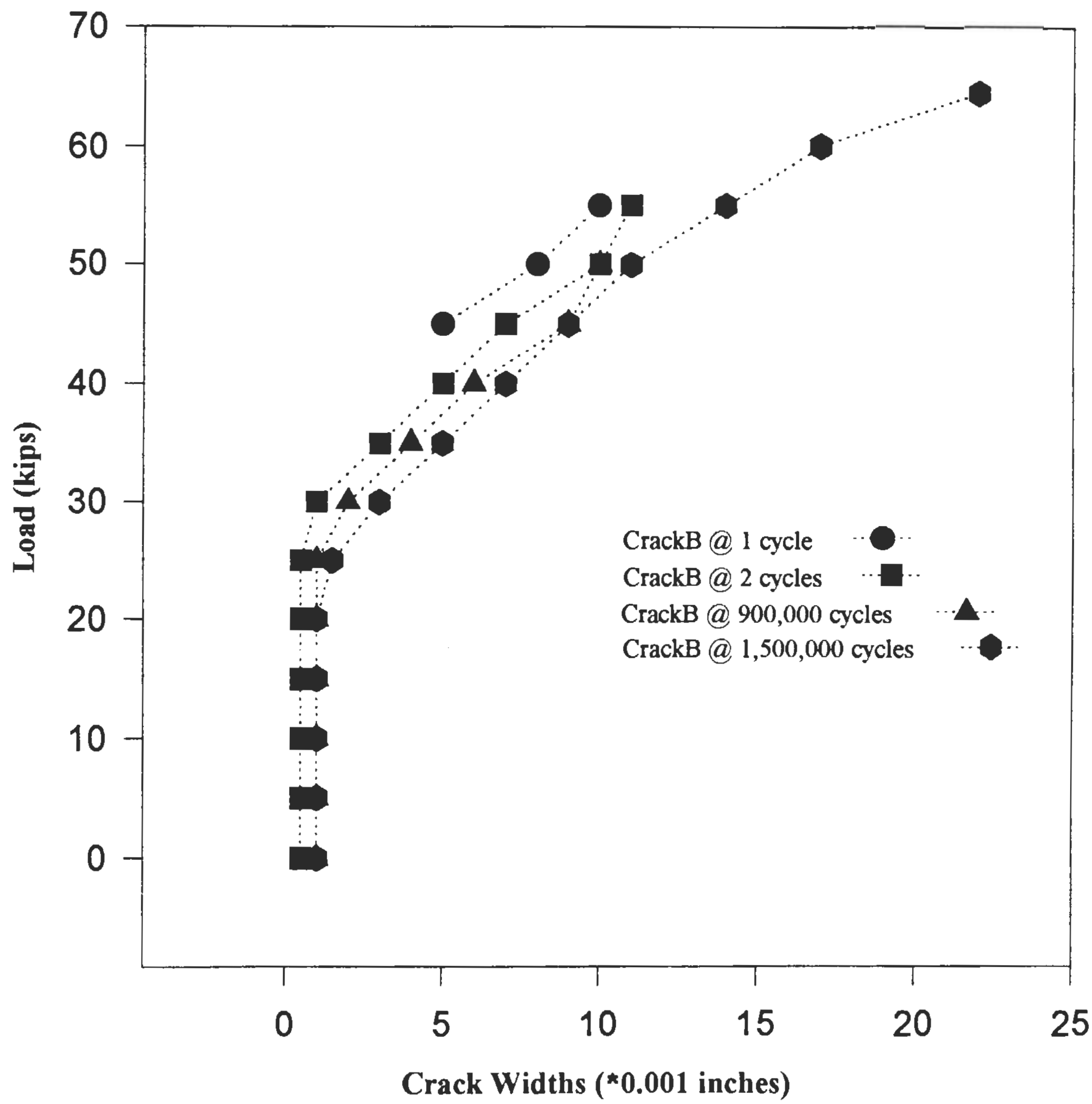

Figure 6.3A CrackB Widths for Beam10

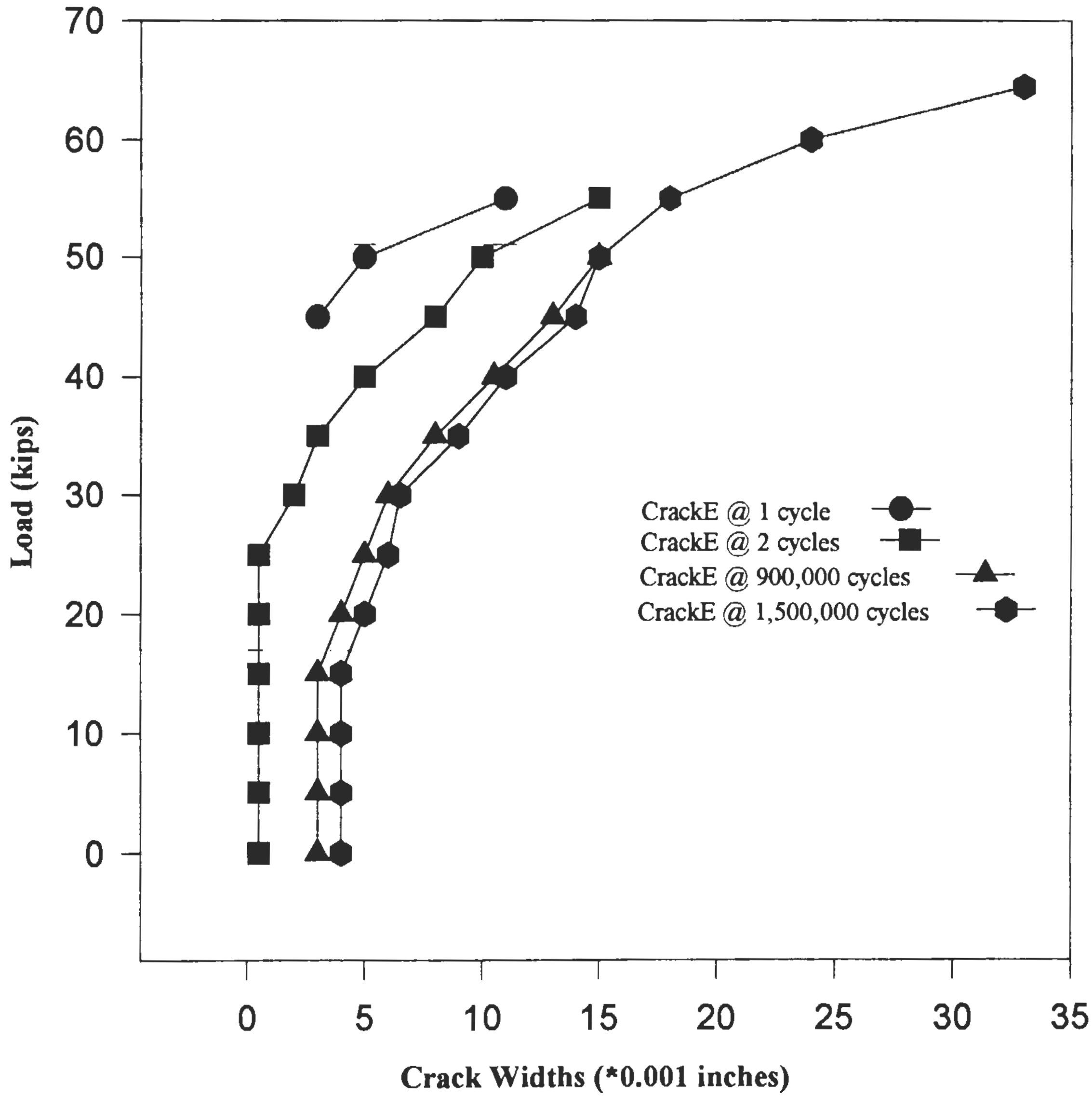

Figure 6.3B CrackE Widths for Beam10

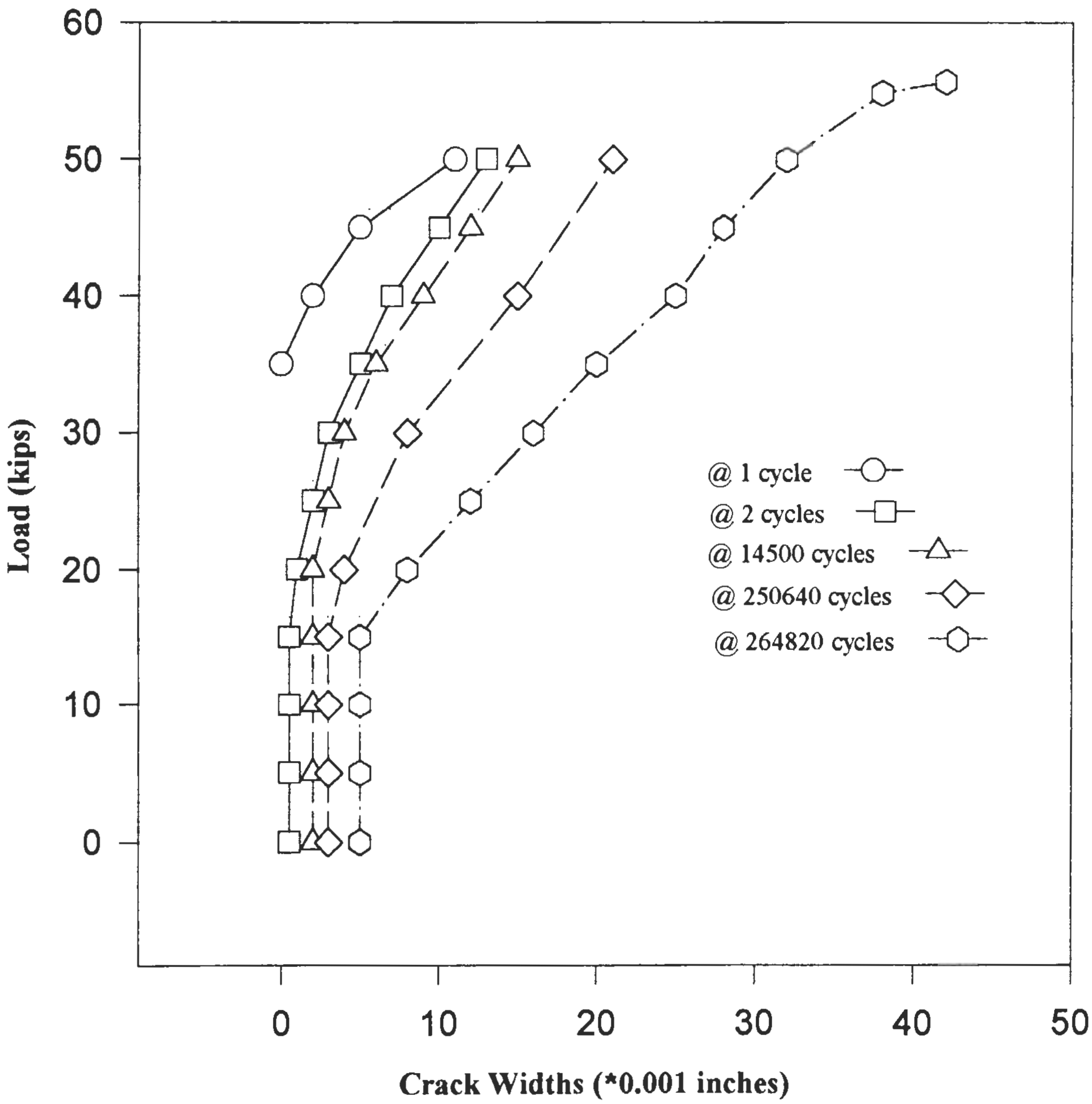

Figure 6.3C Typical Crack Widths for Beam8

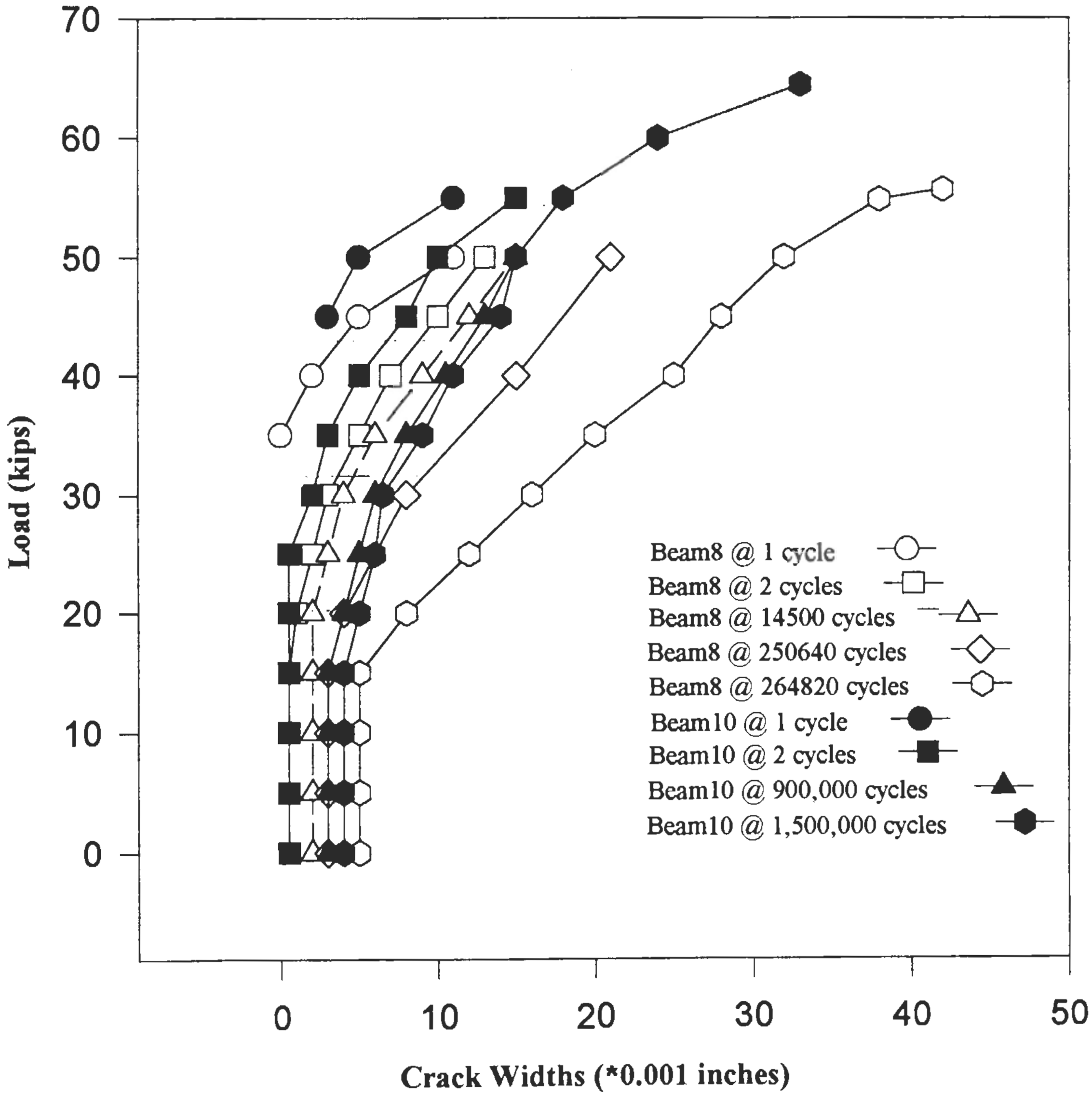

Figure 6.3D Crack Widths for Both Beams

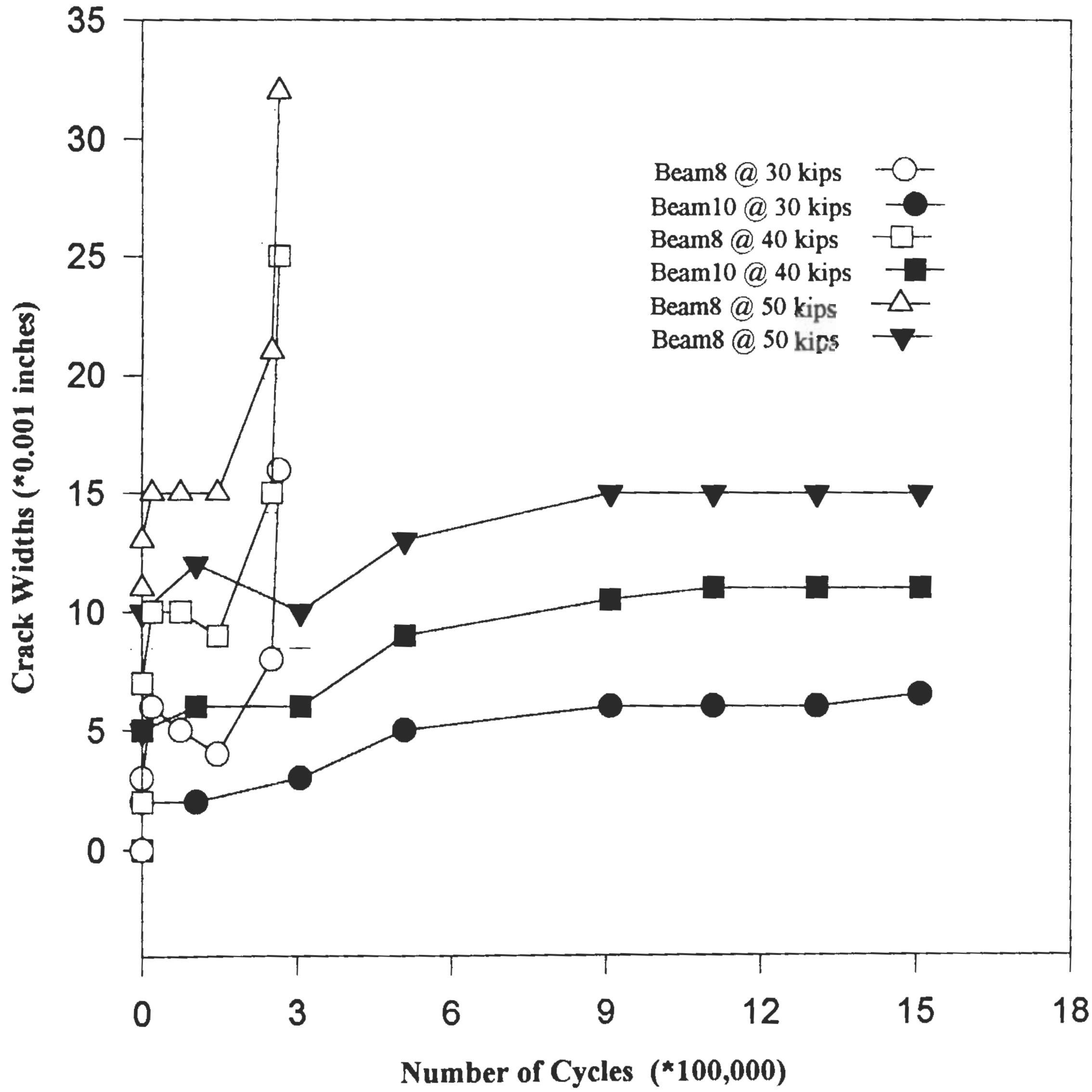

Figure 6.3E Comparision of Crack Widths for the Beams

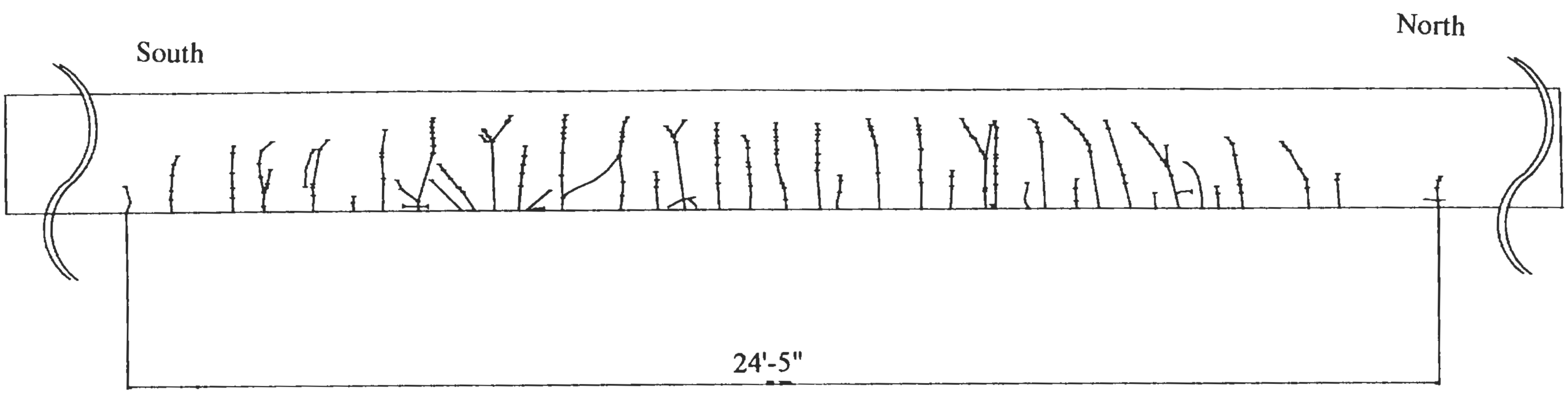

Figure 6.4A Cracks on the East side of Beam10

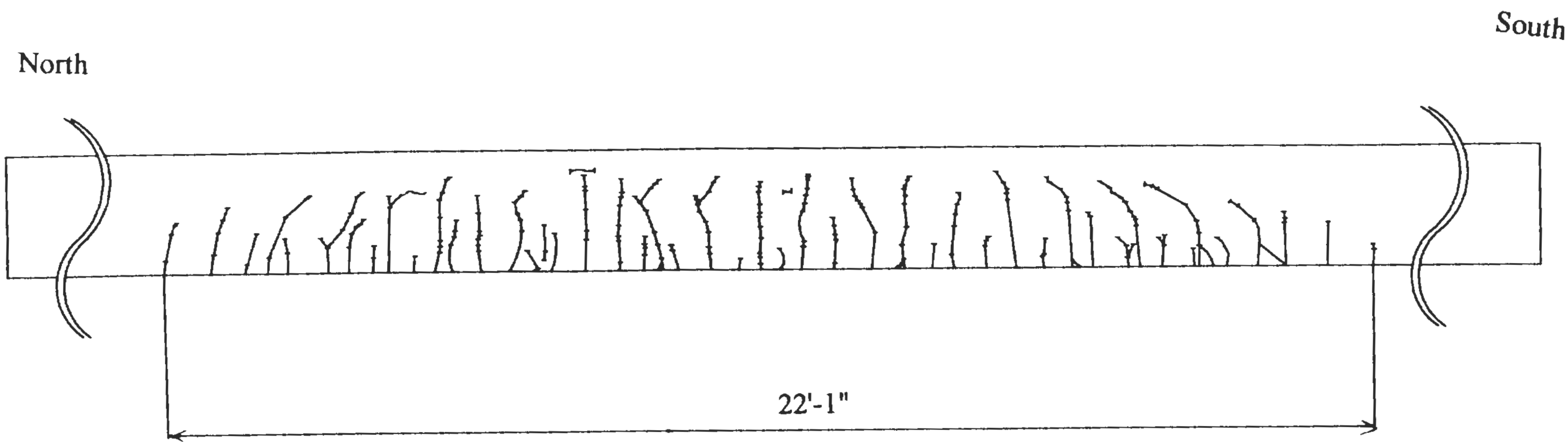

Figure 6.4B Cracks on the West side of Beam10

'A' Crack extent in Beam10 @ 1,500,000 cycles

'B' Crack extent in Beam8 @ 145,000 cycles

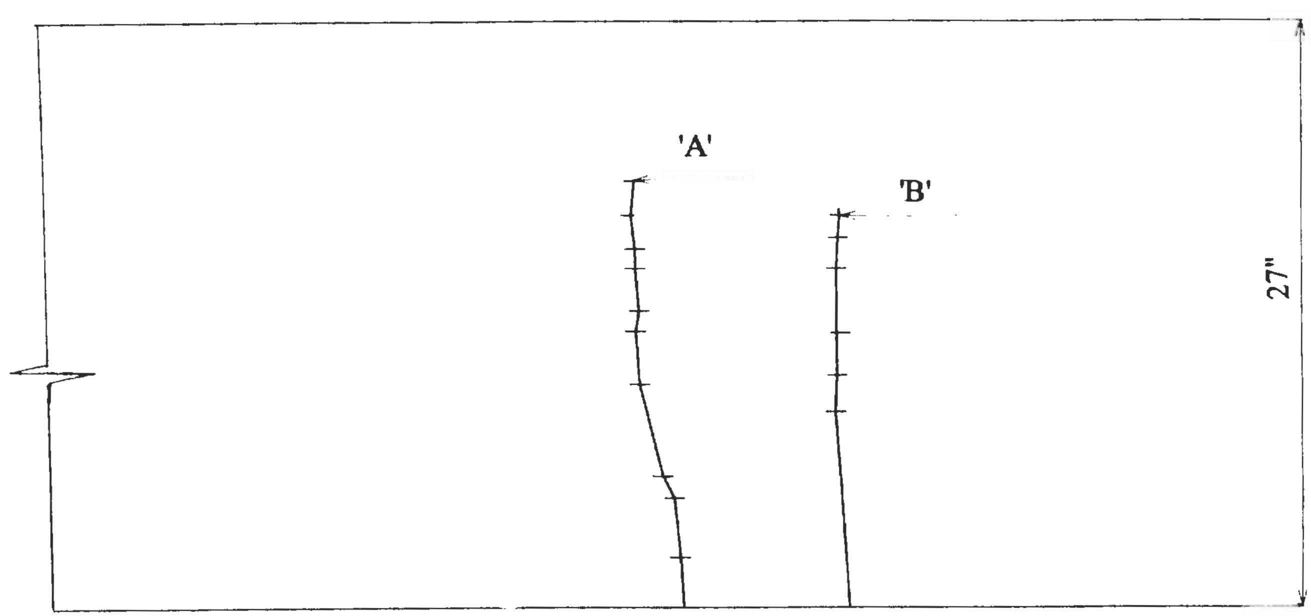

Figure 6.4C Comparision of Crack Extensions for Beam10 and Beam8

Note: This figure only compares the crack patterns on the two beams and the cracks are actually on two different beams.

typical crack patterns in Beams10 and Beam8 along the depth of the beam. It can be seen how far the cracks extended under smaller number of cycles for Beam8 in comparison to the extensions in Beam10 under higher number of cycles.

6.6 EFFECTS OF CORROSION

Prior to testing, on the east side of Beam10, a region in the midspan had at least one strand corroded since a horizontal crack along the strand was evident. This crack, identified as Crack 'H', seemed to be larger than all other cracks through out the test. A large piece of the concrete in this region fell off the beam in this region after about 650,000 cycles and two of the strands in the lower row were exposed. It was observed that the strands were corroded and a few wires had broken. All of the wires that were fractured at that time at that location showed no signs of recent fractures as the surface of the broken sections were rusted. It was concluded that they had not been induced by our tests. Figure 6.5A shows a picture of the strand with broken wires near CrackH.

This crack had extended up to 6 inches below the top of the beam by the end of the test. During the remaining fatigue loading, 2 more wires in this strand had fractured and this was very evidently due to the effects of fatigue as the broken sections of the wires were shiny and were certainly quite recent relative to the other wires that were rusted. These wires fractured at close to 1 million cycles of loading. Figure 6.5B shows the strand fractured due to fatigue loading.

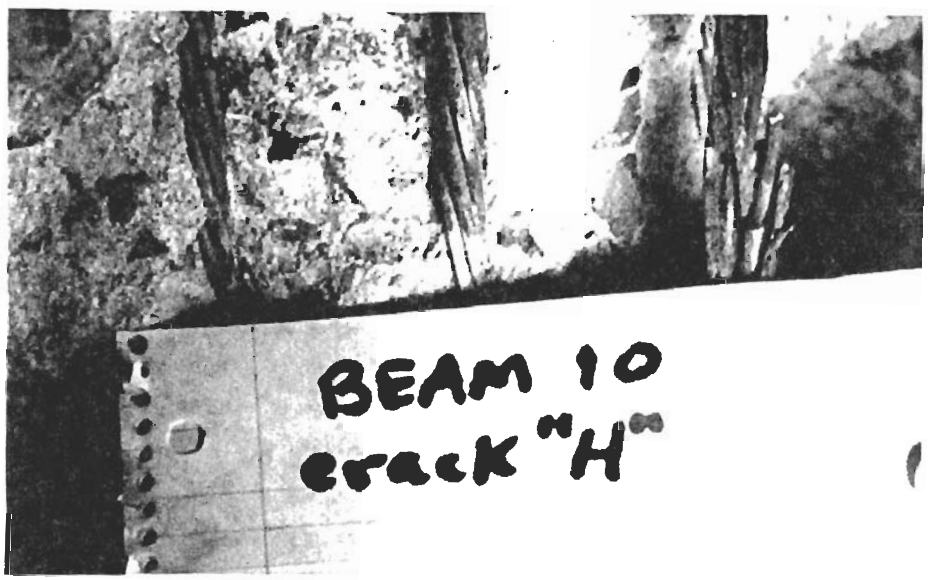

Figure 6.5A Fractures due to Corrosion

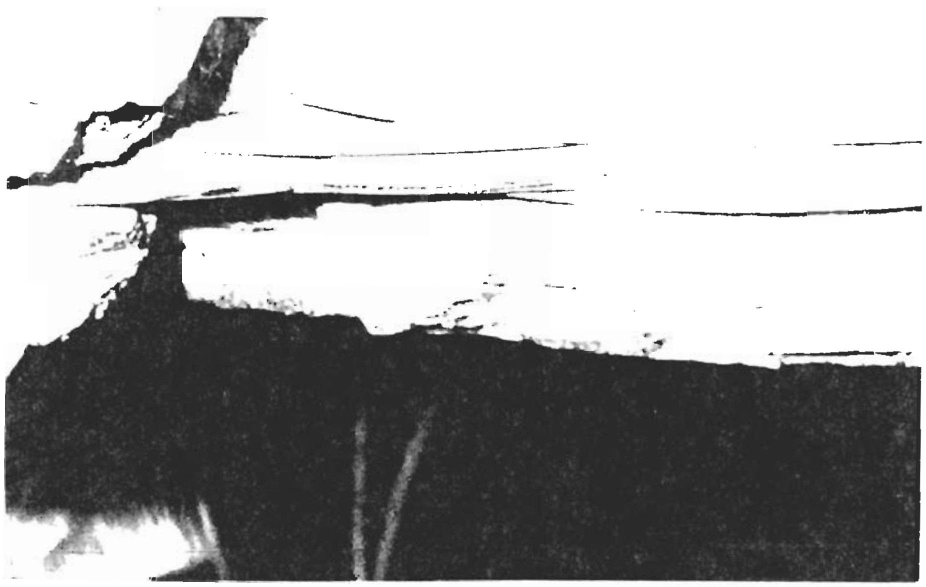

Figure 6.5B Fracture in a Strand due to Fatigue

After the completion of the test, more concrete was removed along the side and the bottom of the beam in the region where longitudinal cracking of concrete along the strands was observed. The first strand in the second row, immediately above the strand that had fractured, appeared fairly good but the second strand in the bottom row, immediately adjacent to the fractured strand had some rusting but little or no pitting. The clear cover to the strands were 2.75 inches on the sides and between 1.25 and 1.375 inches on the bottom. The stirrup near crackH had a cover of 2 inches to the side and 1.5 inches on the bottom. Some more concrete was removed further along the horizontal portion of CrackH. It was seen that 2 more wires were fractured earlier due to corrosion. The stirrup in this region was extremely rusted and the entire region of concrete appeared very loose. It was inferred that the corrosion in general was occurring first in the stirrups.

Towards the north end of the beam, on the east side, there was a longitudinal crack visible along the exterior first strand indicating rusting. Concrete was chipped off in this region to observe the strand and it appeared quite rusty. The stirrup here had a cover of only 1/2" to 3/4" and again it seemed like the rusting actually was beginning to occur at the stirrups. It could also be possible that this very small cover was the initiating cause of rusting.

6.7 OTHER RESULTS

6.7.1 Dial Gages

The readings on the slip dial gages were observed at regular intervals. There did not seem to be any significant change for Beam10. One of the strands in Beam8 that failed during the tests was the strand that was in the middle and the concrete in that region had spalled off. The dial gage attached to the end of this strand had moved by 0.005 inches, indicating that there may have been some loss in bond strength for that strand.

6.7.2 Chemical tests on the water samples

During testing, it was observed that water had become trapped inside of one end of Beam8 at some time during its life. Water samples collected from Beam8 were analyzed in the Environmental Research Laboratory. The sample was found to have a chloride ion content of 99.5 ppm. It was also tested for calcium, iron, magnesium and sodium ion contents. A large sodium ion concentration of 1839750 ppb was found to exist. This must be due to the deicer salts spread on the bridge decks. The possibility of these ions seeping into the bridge beams is high and can be a cause for further corrosion in bridge structures. It is therefore necessary to have a sufficient protective cover on the bridge decks.

CHAPTER 7

SUMMARY AND CONCLUSIONS

7.1 SUMMARY

Two beams from the Walnut Street Bridge built 1960 in East Hartford, CT, were tested for their fatigue strength. The beams served in the bridge for 27 years. They were Beam No. 8 and Beam No. 10 out of the 13 box beams that existed in the bridge. The beams were 56 feet long, 27 inches deep and 3 feet wide box beams. They contained 22 strands of 7/16 inch diameter with an effective prestress of 153 ksi. #4 stirrups were provided at a spacing of 14 inches. The sections had an ultimate capacity of 1117 kip-ft, equivalent to 79 kips of ram load.

Both beams were precracked before subjecting them to fatigue loads. Initial, intermediate and final static tests were conducted on both beams to see the effects of fatigue loads, if any. Beam10 was loaded between 20 and 41 kips, 41 kips being the maximum permitted design load as per AASHTO Specifications (8) causing a bottom fiber stress of $6\sqrt{f'_c}$ It was loaded to over 1.5 million cycles of load. The beam performed very well till the end of the tests and showed a very ductile behavior during the ultimate test. Beam8 was loaded between 20 kips and 50 kips, 50 kips being the load that caused a bottom fiber stress of $9\sqrt{f'_c}$. Beam8 was considered as failed due to fatigue at 264,000 cycles and further loading was discontinued because of fracture of several wires in the strands. Test results of Beam10 and Beam8 were studied and compared to draw conclusion regarding the effects of fatigue loading on bridge structures.

7.2 CONCLUSIONS

It should be noted that the beams tested had been in service for 27 years and that these tests subjected the beams to higher loads than they were designed for or were subjected to in actual service. These tests support the following conclusions.

1. Fatigue need not be a concern as long as the beam is uncracked. Although this was not directly determined by these tests, this result can be inferred due to the low observed stress range in the strands prior to cracking.

2. Beam10 proved to be resistant to severe fatigue problems when loaded to levels that caused the bottom fiber to reach the maximum permitted level of $6\sqrt{f'_c}$ as per the AASHTO guidelines. Its load-deflection and load-stress responses were satisfactory. It sustained over 1.5 million cycles of loads at this range.

3. Beam8, subjected to fatigue loads up to a load level causing a bottom fiber stress of $9\sqrt{f'_c}$, started failing after about 145,000 cycles. This level of loads is certainly to be avoided.

4. The limit of $0.06f_{pu}$ for the stress range in the strands, set by the ACI 215 Committee

report, proved to be consistent with our results. Beam10 with a stress range of $0.062f_{pu}$ performed well; Beam8 with a stress range of $0.110f_{pu}$ performed poorly.

5. Fatigue loading at high stress ranges can cause significant damage to the structure and the harmful effects occur in a very short time. At the end of 264000 cycles on Beam8, the deflections were 35% larger than those of Beam10 after 1.5 million cycles and at the same load. The losses in prestress and the residual stresses in the strands were relatively higher in Beam8. After not many cycles of overload, there were significant increases in the stress range even for normal service loads for Beam8.

6. Fatigue loading at high ranges had very adverse effects on the crack widths and crack extensions. The crack widths had increased by about 70% at the end of 1.5 million cycles of loading for Beam10. Crack widths in Beam8 had increased by 300% after 264000 cycles of loading and was about twice as wide as those in Beam10. The crack extensions at the end of 145000 cycles of overloads on Beam8 were similar to the crack extension patterns at the end of 1,500,000 cycles of loading within the permitted stress level.

7. It can be concluded that fatigue problems can occur with small increases in load range levels. Beam8 had only 13% greater total applied moment than Beam10 during the fatigue cycling. Beam10 at the end of 1.5 million cycles of loads between 20 and 41 kips performed better than Beam8 at a stage when it had undergone only 145,000

cycles of loads between 20 and 50 kips. The plots in Chapter 6 show the drastic increase in crack widths and stresses in Beam8 compared to Beam10.

8. Corrosion can be a serious problem when combined with fatigue. Beam10, though it performed very well in general, did experience propagation in failure and damages induced by corrosion. It is therefore absolutely necessary that sufficient protection against corrosion be provided in bridge structures.

9. The M-Φ method of analysis predicts the beam behavior with considerable accuracy.

10. The actual stress levels after the beam had cracked were very close to the predicted stress levels using the neutral axis depths determined from the M-Φ method of analysis.

11. As expected, due to their excess shear capacity, the beams were resistant to shear failures under both static and dynamic conditions.

12. These particular beams could be expected to serve longer satisfactorily in a bridge provided the bridge did not experience frequent overloads. Similar bridge girders can be evaluated to be in a good condition to resist fatigue if no corrosion is occurring. However, it is recommended that additional confirmation be sought to establish a correlation between structural soundness and degrees of deterioration.

REFERENCES

1. ACI Committee 215, "*Considerations for the Design of concrete Structures subjected to fatigue*" ACI Committee Report 215R1-R74, 1992.

2. ACI Committee 318, Building Code Requirements for Reinforced Concrete (ACI 318-92), American Concrete Institute.

3. ACI Committee 363, "State-of the Art Report on High-Strength Concrete", Journal of the American Concrete Institute 81:4 (July-Aug 1984).

4. ASTM C-39 *"Standard Test Method for Compressive Strength of Cylindrical Concrete Specimens" in Annual Book of ASTM Standards.*

5. ASTM C-42, *"Standard Test Method for Obtaining and Testing Drilled Cores and Sawed Beams of Concrete" in Annual Book of ASTM Standards.*

6. ASTM C-469, *"Standard Test Method for Static Modulus Of Elasticity and Poisson's Ratio of Concrete in Compression" in Annual Book of ASTM Standards.*

7. American Association Of State Highway officials (AASHO), *Standard Specifications for Highway Bridges*, 1957.

8. Standard merican Association Of State Highway & Transportation Officials (AASHTO), *Specifications for Highway Bridges*, 1992.

9. Abeles, P.W., Brown, E.I. II, Hu, C.H., "*Fatigue Resistance of Under-Reinforced Prestressed Beams subjected to different stress ranges; Miner's Hypothesis*", Abeles Symposium on fatigue of concrete, SP-41, American Concrete Institute, Detroit, 1974, pp. 237-277.

10. Bachman, P. M., Kreger, M.J. Breen, "*An exploratory investigation of Shear Fatigue Behavior of Prestressed Concrete Girders*" Final Research Report 465-1 by Center for Transportation Research, University of Texas at Austin, November 1984.

11. Collins, M.P. and Mitchell D., "*Prestressed Concrete Structures*" Prentice Hall, 1991.

12. Coggins, F.B., French, C.W., "*Material Properties and Corrosion Condition of a Twenty-Year-Old Prestressed Bridge Girder*" Final Report for Structural Engineering Report No. 92-02, Department Of Civil and Mineral Engineering, Institute of Technology, University Of Minnesota, May 1992.

13. *"Criteria for Prestressed Concrete Bridges"*, Bureau of Public Roads (1955)

14. Gaynor, R.D., "*Effect of Horizontal Reinforcing Steel on the Strength of Molded Cylinders*", ACI Journal, 837-840 (July 1965).

15. Heins, C.P. and Lawrie, R.A., "*Design of modern concrete Highway Bridges*", John Wiley & Sons, 1984.

16. Hognestad E., Hanson N.W. and McHenry D., "*Concrete Stress Distribution in Ultimate Strength Design*", ACI Journal , 455-77. (December 1955).

17. Knudsen, K.E. and Eney, W.J "*Endurance of a Full-Scale Pretensioned Concrete Beam*" Highway Research Board, Proceedings Of The Thirty-Sixth Annual Meeting Washington, D.C., January 7-11, 1957 Vol. 36.

18. Kripanarayanan, Koladi M. and Branson, Dan E. "*Short-Time Deflections of Beams Under Single and Repeated Load Cycles*", Jan-Feb 1972, pp110-117.

19. Leon, R.T., French, Catherine W., Olson, S.A. and Coggins, F.B., "*Reusability Of 20 year old Prestressed Bridge Girders*", in Proceedings of the Conference on Bridge Research in Progress. Iowa State University, Ames, Iowa 353 (September 1988).

20. Libby, J.R., "*Modern Prestressed Concrete - Design Principles and Construction Methods*", Van Nostrand Reinhold, 4th Edition.

21. Lin, T.Y. and Burns, Ned H., "*Design Of Prestressed Concrete Structures*", John Wiley & Sons, 3rd Edition (1981).

22. Murray, V.E. and Frantz, G.C., "*Chloride Testing Of 27-Year Old Prestressed Bridge Beams*", PCI Journal, V.37 No.5 pp 68-79.

23. Murray, V.E. and Frantz, G.C., "*Tests on Prestressed Concrete Bridge Beams, Part-II - Chloride Penetration in the Bridge Beams*", JHRAC Project Report, Department Of Civil Engineering, University Of Connecticut, Storrs, CT, January 1991, 143 pp.

24. Naaman, A.E. "*Fatigue in Partially-Prestressed Concrete Beams*", ACI SP-75, American Concrete Istitute, Detroit, Mich, 25-46.

25. Nilson, A.H., "*Design of Prestressed Concrete*", John Wiley & Sons, 2nd Edition (1981).

26. Overman T.R., Breen J.E., Frank K.H. "*Fatigue Strength of Prestressed Concrete Girders*" Final Research Report by Center for Transportation Research, Bureau of

Engineering Research, The University of Texas at Austin, November 1984.

27. PCI Design Handbook, 3rd Edition.

28. Preston, H.K., Osborn, A.E.N. and Roach, C.E., "*Restoration of Strength in Adjacent Prestressed Concrete Box Beams*" Final Report for Research Project No. 84-21, Wiss Janey, Elstner Associates, Princeton Junction, New Jersey, May 1987.

29. Rabbat, B.G., Kaar P.H., Russell H.G. and Bruce R.N. Jr., "*Fatigue Tests of Pretensioned Girders With Blanketed and Draped Strands*" (at PCA, Skokie, IL) PCI Journal , July-August 1979, pp 88-114.

30. Russell B.W. and Burns, N.H., "*Static and Fatigue Behavior of pretensioned composite bridge girders made with High-Strength Concrete*", PCI Journal, May-June 1993, pp. 116-128.

31. Shenoy, C.V. and Frantz G.C., "*A Simple Method of Gripping Prestressing Strands for Tension Tests*", PCI Journal, V.36, No.4, July-August 1991, pp. 58-65.

32. Shenoy, C.V. and Frantz G.C. "*Structural Tests of 27-Year-Old Prestressed Concrete Bridge Beams*", PCI Journal, Sep-Oct 1991, V. 36 No. 5, pp 80-90.

33. Shenoy, ChanduV. and Frantz, Gregory C., "*Tests on Prestressed Concrete Bridge Beams. Part I - Structural Tests of the Bridge Beams*" JHRAC Project Report, Department Of Civil Engineering, University Of Connecticut, Storrs, CT, January 1991, 120 pp.

34. Tabatabai, H and Dickson, T.J., "*Comprehensive Strength and Durability Evaluation of 34-Year-Old-Post-tensioned Concrete Bridge Girder*", Research Report, Construction Technology Laboratories, Inc., Skokie, IL, Oct. 1992.

35. *Tentative Recommendations for Prestressed Concrete* ACI-ASCE Joint Committee 323-1958.

36. Zumbrunnen, L.G., Russell, B.W. and Burns, N.H. "*Behavior Of Statically Loaded Pretensioned Concrete Beams with 0.5-inch Diameter Debonded Strands*" Research Report Number 1210-4, Center for Transportation Research, Bureau of Engineering Research, The University of Texas at Austin, January 1992.

37. Rao, C. "*Fatigue Tests of Prestressed Concrete Bridge Beams*," unpublished MS Thesis, The University of Connecticut, Storrs, CT, December, 1995.

APPENDIX A

BOX BEAM DESIGN

CALCULATIONS BASED ON 1992 AASHTO SPECIFICATIONS:

The calculations for the design of the box-beam in a bridge if designed today would be based on the recommendations of the 1992 AASHTO specifications for Highway Bridges (8) and shall be as follows. Calculations are made for interior box beams only.

1. Design Conditions

Span length = L = 54'-0" center to center of bearings

Width of the bridge = 39'-0"

Width of roadway between curbs = 29'-0"

Live Load = HS20-44 truck + impact

2. Materials Used

Concrete: Normal Weight = 152 pcf

Concrete strength @ 28 days = f'_c = 5 ksi (assumed)

Concrete strength @ release = f'_{ci} = 3.5 ksi (assumed)

Prestressing steel: 7/16" diameter 250 ksi prestressing strands

Total Area of prestressing steel = A_{ps} = 2.38 in^2

3. Section Properties

Area of concrete cross section = A_c = 560.5 in^2

Moment of inertia = I = 50,334 in^4

Distance from bottom fiber to center of gravity of section = C_b = 13.35 in

Section modulus w.r.t. bottom fiber of cross section = S_b = 3770 in^3

Section modulus w.r.t. top fiber of cross section = S_t = 3687 in^3

4. Design Loads and Moments

4(a). Dead Load

Self weight of the beam = 592 plf

Moment due to weight of girder = M_G = 213 kip-ft.

4(b). Superimposed Dead Load per Beam

1. Asphalt wearing surface (2 inches thick) = 0.73 k-ft

   Weight per beam = 0.73/11 = 0.0067 kip-ft

2. Sidewalk = 0.9 kip/ft

   Weight per beam = 0.08 kip/ft

3. Diaphragm = 275 pounds @ midspan

Moment due to superimposed load = 57 kip-ft

Moment due to total dead load = M_D = 213 + 57 = 270 kip-ft

4 (c). Live Load

Live Load Distribution (AASHTO 3.23.4):

$$LoadFraction = \frac{S}{D}$$

where S is width of the precast member = 3 feet

D = (5.75-0.5NL) + 0.7NL(1-0.2C)$^{1/2}$

when C $\leq$ 5

$$C = K(\frac{W}{L})$$

$$C = 1(\frac{33}{27})$$

NL = Number of traffic lanes = 2

$D = 5.97$

$$\text{Load Fraction} = \frac{S}{D} = \frac{3}{5.97} = 0.5$$

Live Load moment $= M_L$

$$M_L = 699.3 \frac{\text{Kip} - \text{ft}}{\text{Lane}} \left(\frac{\text{Wheel Loads} * 0.5 * 1.28}{2} \right)$$

$M_L = 224$ kip-ft

<u>5. Flexural Strength</u>

Using Group I loading combination

Maximum Factored moment $= M_u$

$$M_u = 1.3\,(M_D + 1.67\,M_L)$$

$$M_u = 1.3\,(270 + 1.67 * 224) = 837.3 \text{ kip-ft}$$

Average stress in prestressing steel at ultimate load $= f_{su}$

$$f^{*}_{su} = f_s'\left(1 - \frac{0.5\rho^{*} f'_s}{f'_c}\right)$$

where f'_s is the ultimate strength of prestressing steel and f'_c is the compressive strength of concrete at 28 days and ρ is the ratio of area of prestressing steel to the area of concrete.

$$\rho = \frac{Aps}{bd} = \frac{(22 * 0.108)}{(36 * 24.36)} = 0.0027$$

$$f^{*}_{su} = 250\left(1 - \left(0.5 * 0.0027 * \frac{250}{5}\right)\right) = 233 \text{ Ksi}$$

Moment of Ultimate resistance $= \phi M_n$

$$\Phi\, Mn = \Phi \quad Aps * \quad \Phi \quad \Phi\left[\; Aps * f^{*}su \; * d\left(1 - \frac{0.6\rho * f^{*}su}{f'_c}\right)\right]$$

$$\phi\, M_n = 1038.9 \text{ kip-ft} > 837.3 \text{ kip-ft}$$

Note: For factory produced precast prestressed concrete members $\phi = 1.0$

6. Check Maximum and Minimum Steel Percentages

6(a) Maximum Steel Percentage

$$\text{Reinforcement Index} \quad = \quad \rho \frac{f^{*}su}{f'c}$$

$$= \quad 0.0027 \frac{233}{5}$$

$$= 0.12582.$$

As per AASHTO 9.18.1, maximum reinforcement index for a rectangular section is 0.3.

7(b). Minimum Steel Reinforcement

As per AASHTO 9.18.2, the total amount of prestessed reinforcement must be adequate to satisfy

$$\phi M_n \geq 1.2\, M_{cr}$$

where M_{cr} is the moment causing flexural cracking at a section due to externally applied loads.

Cracking stress for normal weight concrete as per AASHTO $= f_{cr} = 7.5$ □f_c psi

$f_{cr} = 530$ psi

$$M_{cr} \quad = \quad S_b \left(\frac{P_{sc}}{Ac} + \frac{P_{sc}}{S_b} + f_{cr} \right)$$

where $P_{se} = 0.8(0.7*250*2.376) = 334.6$ kips

$M_{cr} = 649.8$ kip-ft

$$\frac{\Phi Mn}{Mcr} = \frac{1038.9}{649.8} = 1.6 > 1.2$$

O.K.

Reference (15) has a detailed procedure for the analysis and design methods for prestressed concrete bridges.

APPENDIX B

MTS CONFIGURATION FOR THE STATIC TEST

Configuration file	:c:\Desktop\MTS-TSII\staticPC1.tcc

Input Signal Display Section

STROKE

Signal Source	: Slot1
Type	: AC Conditioner
Sensor name	: DISP_5"
Sensor Full Scale	: -5.00000 in to 5.00000 in
Sensor Range	: 5.00000 in
Upper Limit	: 1.00000 in Ret to Orig Position
Lower Limit	: -2.80000 in Ret to Orig Position
Zero offset	: 0.00000 % Unlock

LOAD

Signal Source	: Slot2
Type	: DC Conditioner
Sensor name	: FORCE_100 kip
Sensor Full Scale	: -100.000 in to 100.000 in
Sensor Range	: 100.000 in
Upper Limit	: 53 kip Ramp to Zero Load
Lower Limit	: -4 kip Ramp to Zero Load
Zero offset	: 5.81665 % Unlock

Output Signal Display Section

Output 2

Type	: Readout
Device	: STROKE
Scale	: 0.50000 in
Offset	: 0.00000 V

Output 1

Type	: Readout
Device	: LOAD
Scale	: 10.0000 kip
Offset	: 0.00000 V

Control Channel Display Section

CONTROL CHANNEL 1

Channel		: Control Channel 1
Drive Type		: Dual 252 Valve
Valve Driver		
	Type	: Dual 252 Valve
	Polarity	: Inverted
	Valve Balance A	: 0.05000
	Valve Balance B	: 0.05000
	Dither Amplitude	: 0.10000
	Dither Frequency	: 791.504
Underpeak Detectors		
	Input Signal:	: Undefined
Error Actions		
	Maximum Error Action	: Disabled
	Minimum Error Action	: Disabled

Control Modes

STROKE POD

Mode		: Control Mode 1
Mode Type		: PIDF
Command		: Pod
Feedback		: STROKE
Gain		
	P	: 10.0000
	I	: 0.10000
	D	: 0.00000
	F	: 0.00000
Error Detectors		
	Minimum Error	: 0.78740
	Maximum Error	: 0.78740

STROKE SG

Mode	: Control Mode 2
Mode Type	: PIDF
Command	: Segment Generator

Feedback		: STROKE
Gain		
	P	: 13.5000
	I	: 0.13500
	D	: 0.00000
	F	: 0.00000
Error Detectors		
	Minimum Error	: 0.78740
	Maximum Error	: 0.78740

LOAD POD

Mode		: Control Mode 3
Mode Type		: PIDF
Command		: Pod
Feedback		: LOAD
Gain		
	P	: 1.00000
	I	: 0.10000
	D	: 0.00000
	F	: 0.00000
Error Detectors		
	Minimum Error	: 4.49618
	Maximum Error	: 4.49618

LOAD SG

Mode		: Control Mode 4
Mode Type		: PIDF
Command		: Segment Generator
Feedback		: LOAD
Gain		
	P	: 1.75000
	I	: 0.17500
	D	: 0.00000
	F	: 0.00000
Error Detectors		
	Minimum Error	: 4.49618
	Maximum Error	: 4.49618

STROKE/LOAD LIMITED

Mode		: Control Mode 5
Mode Type		: Channel Limited Channel
Command		: Pod
Feedback		: STROKE
Limit Feedback		: LOAD
Gain		
	Master P	: 10.0000
	Limit P	: 4.00000
	Upper Limit	: 0.20000 kip
	Lower Limit	: -0.0000 kip

APPENDIX C

MTS CONFIGURATION FOR THE FATIGUE TEST

Configuration file :c:\Desktop\MTS-TSII\dynamicPC1.tcc

Input Signal Display Section

STROKE

Signal Source	: Slot1
Type	: AC Conditioner
Sensor name	: DISP_5"
Sensor Full Scale	: -5.00000 in to 5.00000 in
Sensor Range	: 5.00000 in
Upper Limit	: 1.000 in Ret to Orig Position @-1.5"
Lower Limit	: -1.80 in Ret to Orig Position @-1.5"
Zero offset	: 0.00000 % Unlock

LOAD

Signal Source	: Slot2
Type	: DC Conditioner
Sensor name	: FORCE_100 kip
Sensor Full Scale	: -100.000 kip to 100.000 kip
Sensor Range	: 100.000 in
Upper Limit	: 53 kip Ramp to Zero Load
Lower Limit	: -1 kip Ramp to Zero Load
Zero offset	: 4.07104 % Unlock

Output Signal Display Section

Output 2

Type	: Readout
Device	: STROKE
Scale	: 0.50000 in
Offset	: 0.00000 V

Output 1

Type	: Readout
Device	: LOAD
Scale	: 10.0000 kip
Offset	: 0.00000 V

Control Channel Display Section

CONTROL CHANNEL 1

Channel	: Control Channel 1
Drive Type	: Dual 252 Valve
Valve Driver	
Type	: Dual 252 Valve
Polarity	: Inverted
Valve Balance A	: 0.05000
Valve Balance B	: 0.05000
Dither Amplitude	: 0.10000
Dither Frequency	: 791.504

Underpeak Detectors	
Input Signal:	: Load
Maximum	: 41 kip
Minimum	: 3.00000 kip
Sensitivity	: 2.00000 kip
Action	: Disabled

Error Actions	
Maximum Error Action	: Disabled
Minimum Error Action	: Disabled

Control Modes

STROKE POD

Mode	: Control Mode 1
Mode Type	: PIDF
Command	: Pod
Feedback	: STROKE

Gain	
P	: 10.0000
I	: 0.10000
D	: 0.00000
F	: 0.00000
Error Detectors	
Minimum Error	: 0.78740
Maximum Error	: 0.78740

STROKE SG

Mode	: Control Mode 2
Mode Type	: PIDF
Command	: Segment Generator
Feedback	: STROKE
Gain	
P	: 13.5000
I	: 0.13500
D	: 0.00000
F	: 0.00000
Error Detectors	
Minimum Error	: 0.78740
Maximum Error	: 0.78740

LOAD POD

Mode	: Control Mode 3
Mode Type	: PIDF
Command	: Pod
Feedback	: LOAD
Gain	
P	: 1.00000
I	: 0.10000
D	: 0.00000
F	: 0.00000
Error Detectors	
Minimum Error	: 4.49618
Maximum Error	: 4.49618

LOAD SG

Mode	: Control Mode 4
Mode Type	: PIDF
Command	: Segment Generator
Feedback	: LOAD
Gain	
P	: 1.75000
I	: 0.17500
D	: 0.00000
F	: 0.00000

Error Detectors		
	Minimum Error	: 4.49618
	Maximum Error	: 4.49618

STROKE/LOAD LIMITED

Mode		: Control Mode 5
Mode Type		: Channel Limited Channel
Command		: Pod
Feedback		: STROKE
Limit Feedback		: LOAD
Gain		
	Master P	: 10.0000
	Limit P	: 4.00000
	Upper Limit	: 0.20000 kip
	Lower LImit	: -0.10000 kip

APPENDIX D

CONFIGURATION FILE FOR THE DATA ACQUISITION UNIT

Meas Prog-Setting
Set of data Periodic Measurement
Cycletime 0 ms
Time per Period 2 min
Cycles per Period 100
Periods 1
Time Statistic No
Autom. Print No
Autom. Store No
Autom. Structure Storage No
Autom. Measurement Yes
Device 1
First Channel 11
Last Channel 20

Devicesetting
Tare is active
Printer D20A ON
Autocalibration ON
Datatransfer: binary
Power frequency 60 Hz

Channelsetting
Device Channel Transducer Type Thermocouple Cablelength
Unit Amplifier UPM100-Zero Zero Value K.Factor Br.Factor
Integr.-Time Single Int.Time Total Int. Time
1 1 3251G(IND1/2) ---------- 50m
mm 5kHz 10mV/V Yes 4.41830 159.432 4.000
1.00ms 1ms 100ms
1 2 3251A(SG1/4) ---------- 50m
μm/m 600Hz 5V Yes -0.8481 2.000 1.000
16.66ms 1.66ms 100ms
1 3 3251A(SG1/4) ---------- 50m
μm/m 600Hz 5V Yes -0.22610 2.000 1.000
16.66ms 1.66ms 100ms
1 4 3251A(SG1/4) ---------- 50m

µm/m	600Hz 5V		Yes	-0.16890	2.000	1.000
16.66ms		1.66ms	100ms			
1	5		3251A(SG1/4)	----------		50m
µm/m	600Hz 5V		Yes	-0.32040	2.000	1.000
16.66ms		1.66ms	100ms			
1	6		3251H(SG4/4)	----------		50m
µm/m	DC 5V		Yes	0.16350	2.000	4.000
16.66ms		1.66ms	100ms			
1	7		3251A(SG1/4)	----------		50m
µm/m	DC 5V		Yes	-0.13950	2.000	1.000
16.66ms		1.66ms	100ms			
1	8		3251H(SG4/4)	----------		50m
µm/m	DC 5V		Yes	-4.75970	1.980	4.000
16.66ms		1.66ms	100ms			
1	9		3251B(SG1/4)	----------		50m
µm/m	DC 5V		Yes	-0.37460	2.0	1.000
16.66ms		1.66ms	100ms			
1	10		3251H(SG4/4)	----------		50m
µm/m	DC 5V		Yes	9.09020	3.92	4.000
16.66ms		1.66ms	100ms			
1	11		3251B(SG1/4)	----------		50m
µm/m	DC 5V		Yes	0.00000	2.06	1.000
500.0ms		1ms	1ms			
1	12		3251B(SG1/4)	----------		50m
µm/m	DC 5V		Yes	-0.18300	2.06	1.000
500.0ms		1ms	1ms			
1	13		3251B(SG1/4)	----------		50m
µm/m	DC 5V		Yes	-0.35220	2.06	1.000
500.0ms		1ms	1ms			
1	14		3251B(SG1/4)	----------		50m
µm/m	DC 5V		Yes	-0.16430	2.06	1.000
500.0ms		1ms	1ms			
1	15		3251B(SG1/4)	----------		50m
µm/m	DC 5V		Yes	-0.14340	2.06	1.000
500.0ms		1ms	1ms			
1	16		3251B(SG1/4)	----------		50m
µm/m	DC 5V		Yes	-0.23440	2.06	1.000
500.0ms		1ms	1ms			
1	17		3251B(SG1/4)	----------		50m
µm/m	DC 5V		Yes	-0.13950	2.06	1.000
500.0ms		1ms	1ms			
1	18		3251B(SG1/4)	----------		50m

μm/m	DC 5V		Yes	-0.39880	2.06	1.000
500.0ms		1ms	1ms			
1	19		3251B(SG1/4)	----------		50m
μm/m	DC 5V		Yes	-0.12360	2.06	1.000
500.0ms		1ms	1ms			
1	20		3251G(SG1/2)	----------		50m
MM	5KhZ 10MV/V		Yes	4.44330	159.432	4.000
500.0ms		1ms	1ms			

APPENDIX E

A SAMPLE TEST FILE FOR BEAM 10

Procedure Detail   Time: 113.2346

Procedure Name = TESTE Default Procedure
File Specification = C:\TS2\TWSX\TESTE.000

Data File Options
File Format = Excel Text File
Log Events = Yes
Include Procedure Description = Yes

Recovery Options
Autosave enabled.
On step done
At least every = 10 Min

Ramp to 30.5kips mean load : Step
Step Done Trigger 1 = Ramp to 30.5K mean

Ramp to 30.5K mean : Monotonic Command
Start Trigger = Step Start
End Trigger = <none>
Segment Shape = Ramp
Rate = 5000 (lbf/Sec)
CONTROL CHANNEL 1
Control Mode = LOAD SG
Endlevel = 30500 (lbf)

Cycle b/n 20K & 41K : Step
Step Done Trigger 1 = Cycle b/n 20 & 41k

Cycle b/n 20 & 41k : Cyclic Command
Start Trigger = Step Start

End Trigger = <none>
Segment Shape = Haversine
Frequency = 1 (Hz)
Repeats = 100000 cycles
Amplitude/Mean Control = On
CONTROL CHANNEL 1
Control Mode = LOAD SG
Endlevel 1 = 20000 (lbf)
Endlevel 2 = 41000 (lbf)

Ramp to Zero load : Step
Step Done Trigger 1 = Ramp to Zero load

Ramp to Zero load : Monotonic Command
Start Trigger = Step Start
End Trigger = <none>
Segment Shape = Ramp
Rate = 5000 (lbf/Sec)
CONTROL CHANNEL 1
Control Mode = LOAD SG
Endlevel = 0 (lbf)

Test Control Started Time: 0.022599999
Calendar Time: 11-30-1994 05:08:16 PM
File Name: C:\TS2\TWSX\TESTE.000
Procedure Name: TESTE Default Procedure
Operator: MTS
Teststar Config: C:\Desktop\MTS-TSII\dynamicPC1.tcc

Test Control Done Time: 100014.74
Calendar Time: 12-01-1994 08:55:10 PM
Loop Counters:
Total Counters:
Axial 200002

APPENDIX F

A SAMPLE TEST FILE FOR BEAM 8

Procedure Detail   Time: 20715.676

Procedure Name = TESTCC Default Procedure (modified)
File Specification = C:\TS2\TWSX\TESTCC.000

Data File Options
  File Format = Excel Text File
  Log Events = Yes
  Include Procedure Description = Yes

Recovery Options
  Autosave enabled.
    On step done
    At least every = 10 Min

Ramp to 35kips mean load : Step
  Step Done Trigger 1 = Ramp to 35 K mean

  Ramp to 35 K mean : Monotonic Command
    Start Trigger = Step Start
    End Trigger = <none>
    Segment Shape = Ramp
    Rate = 5000 (lbf/Sec)
    CONTROL CHANNEL 1
      Control Mode = LOAD SG
      Endlevel = 35000 (lbf)

Cycle b/n 20K & 50K : Step
  Step Done Trigger 1 = 300times, 0.66Hz

  300times, 0.66Hz : Cyclic Command
    Start Trigger = Step Start
    End Trigger = <none>
    Segment Shape = Haversine
    Frequency = 0.66 (Hz)

Repeats = 187350 cycles
Amplitude/Mean Control = On
CONTROL CHANNEL 1
Control Mode = LOAD SG
Endlevel 1 = 20000 (lbf)
Endlevel 2 = 50000 (lbf)

Ramp to Zero load : Step
Step Done Trigger 1 = Ramp to Zero load

Ramp to Zero load : Monotonic Command
Start Trigger = Step Start
End Trigger = <none>
Segment Shape = Ramp
Rate = 5000 (lbf/Sec)
CONTROL CHANNEL 1
Control Mode = LOAD SG
Endlevel = 0 (lbf)

Test Control Started Time: 0.021799998
Calendar Time: 03-06-1995 04:30:31 PM
File Name: C:\TS2\TWSX\TESTCC.000
Procedure Name: TESTCC Default Procedure
Operator: MTS
Teststar Config: C:\Desktop\MTS-TSII\dynamicPC2.tcc

Test Control Stopped Time: 80418.992
Calendar Time: 03-07-1995 02:50:49 PM
Loop Counters:
Total Counters:
Axial 106144

Test Control Reset Time: 80533.711
Calendar Time: 03-07-1995 02:52:44 PM
Loop Counters:
Total Counters:
Axial 0